Analysis of Experiments on the Scattering of Protons by Protons

G. BREIT, H. M. THAXTON AND L. EISENBUD*
University of Wisconsin, Madison, Wisconsin
(Received April 19, 1939)

The new observations of Herb, Kerst, Parkinson and Plain and of Heydenburg, Hafstad and Tuve are analyzed. No definite indication of a p wave anomaly or higher phase shifts is found. The s wave anomaly is the major effect observed. The phase shift K_0 responsible for it is compared with theoretical expectation using potentials which are constant (except for their Coulombian part) within distances 0.75, 1, 1.25 in units $e^2/mc^2=2.81\times10^{-13}$ cm. The first of these gives a too rapid and the last a too slow variation of K_0 with energy. The interaction radius e^2/mc^2 agrees with experiment much better than the others. The potential energy giving the best agreement with experiment, when superposed on the Coulomb energy within this distance, is determined within a few tenths of a percent and is 11.3 Mev. The Gauss error potential $Ae^{-\alpha r^2}$ with $\alpha=16$ and with 9×10^{-13} cm as the unit of length gives a too slow variation of K_0 with E. Experiment agrees decidedly better with $\alpha\sim20$. An over-all fit can be obtained with $\alpha=21.6$, $A=51.4\ mc^2$. The shortening of the range of force is about the same as that previously suggested by Rarita and Present from calculations on the binding energy of H^3. This is surprising since the discovery of the electric quadrupole moment of H^2 necessitates a revision of binding energy calculations. Conclusions about the range of force derivable from proton-proton scattering experiments are shown to be sensitive to a possible velocity dependence of the nuclear potential. The proton-proton and proton-neutron forces in ^1S states are compared and it is found that for both types of potentials the proton-proton interaction is less by approximately two percent. This difference is definitely outside the probable errors in the scattering experiments and is not very sensitive to velocity dependence.

The absence of p wave anomalies in the data from 1830 to 2400 kev is not sufficiently clear cut to claim a definite disagreement with Feenberg's inequality derived from saturation requirements with exchange forces. The effects expected are close to the consistency of the measurements.

The paper includes formulas and tables for the calculation of anomalies due to phase shifts, discussions of geometrical corrections and of some of the effects of experimental errors on the conclusions. Some of the features that may be learned by extensions to higher and lower energies are pointed out. An outline is given in the introduction.

I. INTRODUCTION

OBSERVATIONS on the anomalous scattering of protons by protons have been made by Wells,[1] White,[2] by Tuve, Heydenburg and Hafstad,[3] by Hafstad, Heydenburg and Tuve,[4] by Herb, Kerst, Parkinson and Plain[5] and by Heydenburg, Hafstad and Tuve.[6] The present paper concerns itself with the interpretation of the experiments paying special attention to the results obtained in the two recent papers just mentioned. The data of Herb *et al.* extend the knowledge of the scattering to an energy of 2.4 Mev for the incident protons. These observations as well as the new measurements of Heydenburg, Hafstad and Tuve have been made with improvements in technique which resulted in a high degree of internal consistency. The analysis of the observations made below indicates a high accuracy in the values of the phase shift K_0 responsible for the s wave scattering anomaly recorded in Tables XI, XII and plotted in Figs. 6 and 7. The values obtained in the two laboratories join smoothly at the energy 860 kev for the data of Herb *et al.* and 867 kev for the data of Tuve *et al.*

The extension of the energy region to 2400 kev made by Herb and collaborators enables one to determine an average range for the nuclear force responsible for the s wave anomaly. An over-all fit between 800 and 2400 kev makes an accuracy of ~5 percent seem possible. A "square well" potential with a width e^2/mc^2 and a depth $D=10.52$ Mev represents this region quite well. For the Gauss error potential an over-all fit from 670 kev to 2392 kev is obtained for $Ae^{-\alpha r^2}$ with $A=51.44$, $\alpha=21.59$ in nuclear units. Fits made with the Gauss error potential to different parts of the experimental curve vary by amounts

* Now at Princeton University.
[1] W. H. Wells, Phys. Rev. **47**, 591 (1935).
[2] M. G. White, Phys. Rev. **47**, 573 (1935).
[3] M. A. Tuve, N. P. Heydenburg and L. R. Hafstad, Phys. Rev. **49**, 402 (1936); **50**, 806 (1936).
[4] L. R. Hafstad, N. P. Heydenburg and M. A. Tuve, Phys. Rev. **51**, 1023 (1937); **53**, 239 (1938).
[5] R. G. Herb, D. W. Kerst, D. B. Parkinson and G. J. Plain, Phys. Rev. **55**, 603(A) (1939). Also paper in this issue. Referred to as HKPP in text.
[6] N. P. Heydenburg, L. R. Hafstad and M. A. Tuve, Phys. Rev. **55**, 603(A) (1939). Referred to as HHT in text.

illustrated in Table XIX which indicate 20 as the lower limit and 24 as the upper limit for α. Rarita and Present[7] have found it necessary to use a range corresponding to about $\alpha=20$ in order to account for the binding energy of H^3. They pointed out that with such a range the mass of He^4 should be expected to be smaller than the experimental value. The work of Margenau and Warren and Margenau and Tyrrell[7] has made it doubtful to what extent a shorter range is called for by the binding energy of H^3 since the difficulty according to them can be partly removed by suitable adjustments of the parameter g entering into the expression for nuclear forces. The new proton-proton scattering experiments show, however, that the range of force cannot be supposed to correspond to $\alpha=16$ as long as the interaction potential is supposed to be independent of velocity. It is surprising that the value obtained for α is so close to that obtained by Rarita and Present[7] from the binding energy of H^3 since this value gives a too small mass of He^4. The discovery of the electric quadrupole moment of H^2 recently made by Rabi and coworkers[8] makes the meaning of these binding energy calculations rather doubtful since the ^3S states are mixed with $^3D_1$. The effect of couplings of the $(\sigma_1\mathbf{r})(\sigma_2\mathbf{r})$ type which are demonstrated by the quadrupole moment has been already considered for the position of the ^3S and ^1S terms in the deuteron[9] and even for the relatively small magnitudes expected from relativistic considerations appreciable effects have been obtained. Larger effects should follow from the mesotron theory[10] and the connection of the range of force with binding energies is decidedly an open one. On the other hand, the ^1S state remains uncoupled to the others[11] so that this interaction can be investigated independently with the proton-proton and with the slow neutron-proton scattering experiments.

On the other hand, the scattering experiments do not give a unique answer to the question of range because of the possibility of velocity dependence.[12] It will be seen at the end of the paper that changes of the order of 1.6 percent of the depth of the potential well through an energy region of 2.4 Mev for incident protons would account for the observations using an old fashioned range of $\alpha=16$. The mesotron theories of nuclear forces in their usual form involve the arbitrary feature of "cutting off" which presumably introduces errors regarding velocity dependence since the relative importance of long and short wave-lengths is different for collisions with different energies of relative motion. This point is doubtless speculative and controversial but it was thought of interest to see in a purely empirical manner to what extent conclusions about range are affected by the introduction of a velocity dependence.

The saturation and stability arguments with exchange forces have led Feenberg[13] to the establishment of a lower limit for the repulsion in the ^3P state which should cause a small scattering anomaly to appear at two Mev. Here again the existence of the electric quadrupole of the deuteron changes the situation. The assumption regarding the possibility of representing nuclear

[7] W. Rarita and R. D. Present, Phys. Rev. **51**, 788 (1937); H. Margenau and D. T. Warren, Phys. Rev. **52**, 790 (1937); **52**, 1027 (1937); W. A. Tyrrell, Jr., and H. Margenau, Phys. Rev. **53**, 939(A) (1938); H. Margenau and W. A. Tyrrell, Phys. Rev. **54**, 422 (1938); W. Rarita and Z. I. Slawsky, Phys. Rev. **54**, 1053 (1938).

[8] I. I. Rabi, J. R. Zacharias, N. F. Ramsey, Jr., and J. M. B. Kellogg **55**, 595(A) (1939); J. M. B. Kellogg, I. I. Rabi, N. F. Ramsey, Jr., and J. R. Zacharias, Phys. Rev. **55**, 318 (1939).

[9] S. S. Share and G. Breit, Phys. Rev. **52**, 546 (1937); G. Breit, Phys. Rev. **51**, 248 (1937); **54**, 153 (1938). First *a priori* introduction of $(\sigma_1\mathbf{r})(\sigma_2\mathbf{r})$ terms for nuclear forces apart from magnetic effects was made by Wheeler, Phys. Rev. **50**, 643 (1936). See also E. Wigner Phys. Rev. **51**, 106 (1937). The existence of the quadrupole moment as an effect of these terms and other interesting effects have been discussed by J. Schwinger, Phys. Rev. **55**, 235 (1939). Chicago meeting American Physical Society, November 25, 1938.

[10] H. Yukawa, Proc. Phys. Math. Soc. Japan **17**, 48 (1935); H. Yukawa and S. Sakata, Proc. Phys. Math. Soc. Japan **19**, 1084 (1937); H. Yukawa, S. Sakata and M. Taketani, Proc. Phys. Math. Soc. Japan **20**, 319 (1938); H. Yukawa, S. Sakata, M. Kobayasi and M. Taketani, Proc. Phys. Math. Soc. Japan **20**, 720 (1938); N. Kemmer, Proc. Roy. Soc. **34**, 354 (1938); N. Kemmer, Proc. Camb. Phil. Soc. **34**, 354 (1938); H. Fröhlich, W. Heitler and N. Kemmer, Proc. Roy. Soc. **A166**, 154 (1938); H. J. Bhabha, Proc. Roy. Soc. **A166**, 501 (1938); W. Heitler, Proc. Roy. Soc. **A166**, 529 (1938).

[11] G. Breit, Rev. Sci. Inst. **9**, 63 (1938). See end of first column on p. 74. The ^1S term remains uncoupled to all other terms for two particles of spin $\frac{1}{2}$.

[12] J. A. Wheeler, Phys. Rev. **50**, 643 (1936). Here the possibility of velocity dependence for nuclear force is introduced.

[13] E. Feenberg, Phys. Rev. **52**, 667 (1937); See also G. Breit and E. Wigner, Phys. Rev. **53**, 998 (1938) for feasible upper limit on the repulsion.

forces as a mixture of Wigner, Heisenberg, Majorana and Bartlett interactions cannot be maintained any longer and this assumption was made in deriving the inequality. It appears unlikely, however, that the experiment could have concealed a negative phase shift of $-0.25°$ which is approximately the amount expected using the old fashioned theory with $\alpha=16$. Unfortunately the effect looked for is at the limit of experimental accuracy and a definite claim for the absence of such a phase shift cannot be made. A discussion of the evidence is given under "Possibilities at low and high energies and higher phase shifts" as well as in connection with Table XIV and Figs. 3, 4 and 5.

The paper is divided into two longer sections. The first is concerned with the handling of experimental material up to the point of obtaining the phase shifts and is called "Determination of Phase Shift from Experimental Data." The second is concerned with the interpretation of the phase shifts in terms of interaction potentials and is called "Calculation of the Potentials." The first part is less speculative than the second. In the first part the subdivisions are as follows.

1. Coefficients for the calculation of the scattering anomaly. Here tables and formulas are given for the calculation of the s wave anomaly in sufficient detail to make the analysis of experimental material easy in the future.

2. Effect of error consisting of a constant factor. Here the effect introduced into the value of the s wave phase shift K_0 due to an error consisting of a constant factor is calculated.

3. Effect of error in voltage. This is similar to 2.

4. Estimate of spread of beam due to collisions. The checks made by Herb *et al.* on the performance of the apparatus using argon and krypton scattering showed the presence of an effect of pressure. The spread of the beam due to collisions is estimated and is seen to be of the right order of magnitude. Multiple scattering is discussed.

5. Values of phase shift derived from experiment. (*a*) Explanation of tables. The experimental results are tabulated and the comparison of theoretical expectation is compared in this section with experiment. (*b*) Corrections due to geometry of apparatus. For low angle scattering corrections for geometry enter. They are of importance for conclusions regarding higher phase shifts. (*c*) Possible presence of p and d wave anomalies. Upper limits for their effect on K_0.

The second section contains the following subdivisions.

1. The proton-neutron interaction. (*a*) Square wells. Eqs. (8.2) and (8.3) for calculation of depth and Eq. (8.4) for scattering cross section of ^3S. Eqs. (8.5) and (8.6) for relation between depth and scattering cross section for ^1S. Connection with virtual level treatment in Eq. (8.8). (*b*) Expansions for wells of any shape. Eqs. (9.1) for Taylor expansion of logarithmic derivative in several parameters. (*c*) Formulas for neutron-proton potential for the Gauss error type interaction. Eqs. (10.1), (10.4), (10.6), (10.7), (10.8) and (10.9) for calculation of depth of proton-neutron potential corresponding to given scattering. Effect of neglecting tail of Gauss error potential in Eq. (10.91). (*d*) Intercomparison of numerical integrations used for proton-proton and proton-neutron potentials.

2. Coulomb effect for square wells. Calculations of phase shifts for proton-proton scattering are made with least trouble using "square wells" without Coulomb potential inside. Corrections for the Coulomb potential inside the well are made here. See Eq. (11.2) for effect of Coulomb potential on depth. Necessary quantities collected in Table XVI. Eq. (11.5) and Table XVII for calculation of phase shift with fixed depth superposed on Coulomb potential.

3. Adjustment of range and values obtained from experiment.

4. Comparison of proton-proton and proton-neutron interaction. See Tables XX, XXI.

5. Possibilities at lower and higher energies and evidence regarding p scattering. Some of the points which may be learned by extending experiments to lower and higher energies are discussed and the evidence regarding p scattering available at present is reviewed.

A table of Coulomb functions for $L=0$ is given in the appendix.

Notation

M = mass of proton; M_H = mass of hydrogen atom.

$\mu = M/2$ = reduced mass in the collision of two protons.
v = relative velocity of the two protons before the collision.
r = distance between protons.
E = kinetic energy of the incident proton.
E' = energy in frame of center of gravity = $E/2$.
$\Lambda = \hbar/\mu v$.
$k = 2\pi/\Lambda$, $\eta = e^2/\hbar v$, $\rho = kr$.
$L\hbar$ = angular momentum of colliding particles around common center of gravity.
P_L = Legendre function.
θ = scattering angle in the reference system of center of gravity.
$\Theta = \theta/2$ = scattering angle in the laboratory reference system.
F_L = regular solution of the differential equation for r times the radial wave function in a Coulomb field normalized so as to be asymptotic to a sine wave of unit amplitude at ∞.
K_L = phase shift defined by the asymptotic form of $\mathfrak{F}_L = r$ times the radial function in the actual field. The phase of $\mathfrak{F}_L$ minus that of F_L at large r is K_L.
G_L = irregular solution of the same equation as F_L having $K_L = \pi/2$.
σ = scattering cross section per unit solid angle in the laboratory system.
$\mathbf{P}$ = scattering cross section per unit solid angle in the center of gravity system.
$(\Delta\mathbf{P})_0$ = change in $\mathbf{P}$ due to the s scattering anomaly.
$(\Delta\mathbf{P})_1$ = change in $\mathbf{P}$ due to the p scattering anomaly.
$(\Delta\mathbf{P})_2$ = change in $\mathbf{P}$ due to the d scattering anomaly including interference terms with K_0.
$\mathbf{P}_M$ = value of $\mathbf{P}$ using Mott's formula.
$\mathbf{X}$, $\mathbf{Y}$ defined by Eq. (1).
Y = yield of scattered protons, per microcoulomb, per mm oil pressure.
$\mathfrak{M} = (2\mu v^2/e^2)^2\mathbf{P}_M$ = quantity tabulated in Table I of BCP.
ρ_H = density of hydrogen in scattering chamber.
$2b$ = width of slit in analyzing system.
A = area of hole in analyzing system. Same symbol as depth of Gauss error potential.
R_0 = distance from hole to beam if beam is very narrow.
$\check{r}$ = distance from hole to center of beam if beam is wide.
$\underline{h}$ = distance from hole to slit.
$\mathfrak{R} = \mathbf{P}/\mathbf{P}_M$ = ratio of scattering to that expected by Mott's formula.
$\dot{\rho}$ = radius of circular beam.
$\sigma_{\pi\nu}$ = scattering cross section of neutron having zero energy with a free proton.
$\sigma_{th} = 4\sigma_{\pi\nu}$.
$F = r$ times radial function for proton-neutron collision.
$E_3 = -$energy of deuteron in normal state.
D_1, D_3 = depths of square wells representing, respectively, proton neutron interaction in the singlet and triplet states.
χ defined by Eq. (8.3).
r_0 = radius of square well.
a_1, a_3 = intercepts on axis of r of tangents to F for zero energy neutrons for singlet and triplet states.
$y = dF/Fdx$ or $d\mathfrak{F}/\mathfrak{F}dx$.
A, α = constants for Gauss error potential $Ae^{-\alpha r^2}$.
$\lambda = A/\alpha$.
$C = 0.577216$ = Euler's constant.
$C_0 = [2\pi\eta/(e^{2\pi\eta}-1)]^{\frac{1}{2}}$.
$C_L = [1/1.3\cdots(2L+1)][1+\eta^2/L^2]^{\frac{1}{2}}\cdots \times[1+\eta^2/1^2]^{\frac{1}{2}}C_0$.

II. Determination of Phase Shift from Experimental Data

1. Coefficients for the calculation of the scattering anomaly

The values of the coefficients of $\sin K_0 \cos K_0$ and $\sin^2 K_0$ in $\mathbf{P}/\mathbf{P}_M$ as given by Breit, Condon and Present[14] are not quite accurate enough for the discussion of the newer improved data. The relation between η and the energy in Mev as used there is slightly inaccurate because of the use of old values of e, h, m, M, c and it is difficult

[14] G. Breit, E. U. Condon and R. D. Present, Phys. Rev. **50**, 825 (1936). Referred to as BCP in text. See references to previous theoretical work in BCP. A more accurate comparison of the proton-proton and proton-neutron interactions was made by G. Breit and J. R. Stehn, Phys. Rev. **52**, 396 (1937). This paper is referred to as BS in the text.

to interpolate from the tables with sufficient accuracy. Values of the coefficients obtained by improved and more systematic calculations are listed below in Table I. It was found at times more convenient to interpolate from tables of the quantities $\mathbf{X}$, $2\mathbf{Y}/\eta$ defined by

$$\mathbf{X}=\mathbf{s}^{-2}\cos\alpha_0+\mathbf{c}^{-2}\cos\beta_0;$$
$$\mathbf{Y}=\mathbf{s}^{-2}\sin\alpha_0+\mathbf{c}^{-2}\sin\beta_0; \quad (1)$$
$$\alpha_0=\eta\ln\mathbf{s}^2;\quad \beta_0=\eta\ln\mathbf{c}^2$$

in the notation of BCP. The quantities $\mathbf{X}$, $2\mathbf{Y}/\eta$ are, therefore, also listed in the tables. The relations are

$$\boldsymbol{\sigma}=4\mathbf{cP}, \quad (2)$$

$$(2\mu v^2/e^2)^2(\Delta\mathbf{P})_0=-\frac{2\mathbf{X}}{\eta}\sin K_0\cos K_0+\left(\frac{4}{\eta^2}+\frac{2\mathbf{Y}}{\eta}\right)\sin^2 K_0\cdots, \quad (2.1)$$

$$\mathfrak{M}=(2\mu v^2/e^2)^2\mathbf{P}_M=\mathbf{s}^{-4}+\mathbf{c}^{-4}-\mathbf{s}^{-2}\mathbf{c}^{-2}\cos\eta\ln\mathbf{s}^2\mathbf{c}^{-2}, \quad (2.2)$$

$$\mathbf{P}=\mathbf{P}_M+(\Delta\mathbf{P})_0 \quad (2.3)$$

where $\boldsymbol{\sigma}$ is the collision cross section per unit solid angle for scattered as well as recoil protons. The values of $\mathfrak{M}$ are also tabulated. The quantities $-2\mathbf{X}/\eta\mathfrak{M}$, $4/\eta^2\mathfrak{M}+2\mathbf{Y}/\eta\mathfrak{M}$ can be used directly for the calculation of $\mathbf{P}/\mathbf{P}_M$. The relation of η to E as used in Tables I, II, III, IV, V is $\eta=0.15818(E/\text{Mev})^{-\frac{1}{2}}$. The conversion factor 0.15818 is not known with an accuracy corresponding to the number of figures used above. If, in future applications, it should be desired to correct the inaccuracy present in the conversion factors it is sufficient to attribute the values of the quantities given in the tables to the values of E that correspond to the tabulated values of η.

The conversion factors as used in the present paper correspond to the following values of the fundamental physical constants: $e/mc=1.7575\times10^7$, $e=4.8036\times10^{-10}$, $c=2.9986\times10^{10}$. C.g.s. electrostatic units are used here and below. The value of c, as used, is slightly incorrect. The more accurate value is 2.99796×10^{10}. This inaccuracy is of no practical consequence in the present work. From the above numbers one obtains $m=0.9115\times10^{-27}$. Using $R_\infty=109{,}737$ cm^{-1} for the Rydberg constant for infinite mass one obtains $h=6.628\times10^{-27}$, $\hbar=1.0549\times10^{-27}$, $e^2/\hbar c=1/137.08$. The quotient 1 Mev/mc^2 is determined by the above constants as $10^6(e/mc)/c^2=1/0.511(61)$. For the computation of η one needs besides the ratio M_H/m where M_H is the mass of the hydrogen atom. The Faraday constant $9648.9=e/Mc$ where M is the mass of the oxygen atom divided by 16. Using $M_H=1.0081\,M$ one obtains $M_H/m=1836.2$. It was assumed that it should be good enough to compute η by $\eta=(e^2/\hbar c)(c/v)=(e^2/\hbar c)c(M_H/2m)^{\frac{1}{2}}(mc^2/Ve)^{\frac{1}{2}}$ where V is the electrostatic difference of potential through which the protons have been accelerated. This gives $\eta=0.15810(E/\text{Mev})^{-\frac{1}{2}}$, $1/\eta=6.3251(E/\text{Mev})^{\frac{1}{2}}$. There is some question as to whether one should use the mass of the hydrogen atom or the mass of the proton in these calculations. The influence of extranuclear electrons is presumably negligible in the collision process itself but it has not been sufficiently investigated to be quite sure of this point. The incident particles must be practically entirely protons which do not have electrons permanently attached to them. From this point of view it would have been better to use M_H-m rather than M_H as the mass of the particles. On the other hand, there is spectroscopic evidence for M_H/m being close to 1838 which corresponds to $(M_H-m)/m=1837$. It appeared safest, therefore, to use $(M_H-m)/m=1836.2$ since this is close to the mean of 1835.2 and 1838. The remaining uncertainty in this number is probably of no importance for the present purpose particularly since it enters to the $\frac{1}{2}$ power. If the ratio of the mean mass of the oxygen atom and the mass of O^{16} is taken into account the ratio 1836.2 changes to 1835.7. The effect of the corresponding change in η is not taken into account in the tables.

For most work one can use Tables I and II to give by interpolation the values of the coefficients of $\sin K_0\cos K_0$ and $\sin^2 K_0$ for $\mathbf{P}/\mathbf{P}_M$. For better accuracy, particularly with graphs, Tables III and IV for $\mathbf{X}$ and $-2\mathbf{Y}/\eta$ are to be preferred. For the lowest energies in Table III the interval is not small enough to secure on interpolation a better accuracy in $\mathbf{X}$ than about two percent at $\Theta=15°$. It is unnecessary to have a better accuracy in this region since $\mathbf{P}/\mathbf{P}_M$ is nearly 1. For higher scattering angles Θ the

TABLE I.* *Values of* $2\mathbf{X}/\eta\mathfrak{M}$ *as functions of* E *and of scattering angle* Θ.

$\Theta=15°$	20°	25°	30°	35°	40°	42.5°	45°	E (KEV)	η
0.1764	0.4773	0.984	1.775	2.892	4.113	4.544	4.704	150	0.40822
.2555	.6190	1.218	2.139	3.426	4.820	5.307	5.488	200	.35353
.3224	.7396	1.417	2.453	3.889	5.435	5.974	6.174	250	.31621
.3811	.8459	1.595	2.733	4.305	5.988	6.574	6.791	300	.28865
.4336	.9418	1.755	2.987	4.684	6.494	7.124	7.356	350	.26724
.4814	1.0297	1.903	3.222	5.034	6.964	7.634	7.881	400	.24998
.5258	1.1112	2.041	3.441	5.356	7.404	8.112	8.373	450	.23569
.5662	1.197	2.170	3.648	5.672	7.820	8.563	8.838	500	.22359
.6423	1.328	2.408	4.029	6.245	8.591	9.402	9.701	600	.20411
.7105	1.455	2.625	4.378	6.769	9.298	10.172	10.493	700	.18897
.7730	1.572	2.826	4.701	7.257	9.956	10.887	11.230	800	.17676
.8311	1.682	3.013	5.003	7.715	10.572	11.558	11.921	900	.16666
.8856	1.785	3.190	5.289	8.144	11.155	12.192	12.574	1000	.15810
.820	1.660	2.977	4.945	7.623	10.45	11.43	11.79	880	.16854
.991	1.983	3.533	5.843	8.982	12.29	13.43	13.84	1210	.14373
1.077	2.148	3.816	6.302	9.676	13.23	14.45	14.90	1400	.13362
1.161	2.308	4.094	6.753	10.361	14.15	15.46	15.94	1600	.12499
1.251	2.480	4.391	7.237	11.094	15.15	16.54	17.05	1830	.11687
1.314	2.600	4.598	7.573	11.606	15.84	17.30	17.83	2000	.11179
1.349	2.668	4.716	7.764	11.897	16.24	17.73	18.28	2100	.10910
1.450	2.862	5.054	8.313	12.728	17.37	18.96	19.55	2400	.10205
1.634	3.216	5.669	9.313	14.24	19.43	21.21	21.87	3000	.091279
1.773	3.483	6.134	10.071	15.40	21.00	22.92	23.63	3500	.084508
1.902	3.732	6.566	10.78	16.47	22.45	24.51	25.26	4000	.079050
2.022	3.965	6.972	11.44	17.475	23.82	26.00	26.80	4500	.074529
2.136	4.185	7.356	12.06	18.43	25.115	27.41	28.25	5000	.070704

* The values of η given in the last column of this table were used also for the succeeding tables. The quantities calculated are functions of η directly rather than E.

accuracy of interpolation increases rapidly and similarly for higher energies.

The coefficients for the computation of effects of higher phase shifts K_1, K_2, $\cdots$ are given sufficiently accurately in BCP. The indications of the presence of such phase shifts are as yet not definite enough to make it necessary to have more accurate calculations.

At the end of Tables III, IV, V are given numerical formulas which express the values of $\mathbf{X}$, $-2\mathbf{Y}/\eta$, $\mathfrak{M}$ in terms of the energy E measured in Mev. These formulas are usually sufficiently accurate from 1000 kv on to $E=\infty$. They are obtained from the expansions

$$\begin{aligned}\mathbf{X}&=\mathbf{s}^{-2}+\mathbf{c}^{-2}-\frac{\eta^2}{2}[\mathbf{s}^{-2}(\ln \mathbf{s}^2)^2+\mathbf{c}^{-2}(\ln \mathbf{c}^2)^2]\\&\quad+\frac{\eta^4}{24}[\mathbf{s}^{-2}(\ln \mathbf{s}^2)^4+\mathbf{c}^{-2}(\ln \mathbf{c}^2)^4]-\cdots\\&=\mathbf{s}^{-2}+\mathbf{c}^{-2}-\frac{0.01250}{E}[\mathbf{s}^{-2}(\ln \mathbf{s}^2)^2+\mathbf{c}^{-2}(\ln \mathbf{c}^2)^2]\\&\quad+\frac{0.00002603}{E^2}[\mathbf{s}^{-2}(\ln \mathbf{s}^2)^4+\mathbf{c}^{-2}(\ln \mathbf{c}^2)^4]-\cdots,\end{aligned}\tag{3.1}$$

$$\begin{aligned}\frac{2\mathbf{Y}}{\eta}&=2[\mathbf{s}^{-2}\ln \mathbf{s}^2+\mathbf{c}^{-2}\ln \mathbf{c}^2]\\&\quad-\frac{\eta^2}{3}[\mathbf{s}^{-2}(\ln \mathbf{s}^2)^3+\mathbf{c}^{-2}(\ln \mathbf{c}^2)^3]\\&\quad+\frac{\eta^4}{60}[\mathbf{s}^{-2}(\ln \mathbf{s}^2)^5+\mathbf{c}^{-2}(\ln \mathbf{c}^2)^5]+\cdots\\&=2[\mathbf{s}^{-2}\ln s^2+\mathbf{c}^{-2}\ln c^2]\\&\quad-\frac{0.008332}{E}[\mathbf{s}^{-2}(\ln \mathbf{s}^2)^3+\mathbf{c}^{-2}(\ln \mathbf{c}^2)^3]\\&\quad+\frac{0.00001041}{E^2}[\mathbf{s}^{-2}(\ln \mathbf{s}^2)^5+\mathbf{c}^{-2}(\ln \mathbf{c}^2)^5]+\cdots,\end{aligned}\tag{3.2}$$

$$\begin{aligned}\mathfrak{M}&=\mathbf{s}^{-4}+\mathbf{c}^{-4}-\mathbf{s}^{-2}\mathbf{c}^{-2}\\&\quad+(\eta^2/2)\mathbf{s}^{-2}\mathbf{c}^{-2}(\ln(\mathbf{s}^2\mathbf{c}^{-2}))^2\\&\quad-(\eta^4/24)\mathbf{s}^{-2}\mathbf{c}^{-2}(\ln(\mathbf{s}^2\mathbf{c}^{-2}))^4+\cdots\\&=\mathbf{s}^{-4}+\mathbf{c}^{-4}-\mathbf{s}^{-2}\mathbf{c}^{-2}\\&\quad+(0.01250/E)\mathbf{s}^{-2}\mathbf{c}^{-2}(\ln(\mathbf{s}^2\mathbf{c}^{-2}))^2\\&\quad-(0.00002603/E^2)\mathbf{s}^{-2}\mathbf{c}^{-2}(\ln(s^2c^{-2}))^4+\cdots.\end{aligned}\tag{3.3}$$

TABLE II. *Values of* $4/\eta^2\mathfrak{M}+2\mathbf{Y}/\eta\mathfrak{M}$ *as function of* E *and of scattering angle* Θ.

$\Theta=15°$	20°	25°	30°	35°	40°	42.5°	45°	E (KEV)
−0.1916	−0.1247	0.2120	0.981	2.288	3.849	4.419	4.633	150
− .1731	− .0230	.4969	1.603	3.426	5.565	6.340	6.629	200
− .1472	.0869	.790	2.233	4.571	7.286	8.262	8.626	250
− .1171	.2012	1.089	2.868	5.719	9.009	10.187	10.625	300
− .0850	.3182	1.389	3.504	6.869	10.731	12.111	12.624	350
− .0514	.437	1.692	4.142	8.020	12.455	14.04	14.62	400
− .0165	.556	1.995	4.781	9.16	14.179	15.96	16.62	450
+ .0189	.677	2.300	5.421	10.32	15.90	17.89	18.62	500
.0911	.919	2.910	6.702	12.63	19.35	21.74	22.62	600
.1648	1.163	3.521	7.985	14.94	22.80	25.59	26.62	700
.2393	1.408	4.134	9.27	17.24	26.25	29.44	30.62	800
.3143	1.653	4.747	10.55	19.55	29.70	33.29	34.62	900
.3897	1.899	5.360	11.84	21.86	33.15	37.14	38.62	1000
.2994	1.604	4.624	10.30	19.09	29.01	32.52	33.82	880
.5489	2.416	6.65	14.53	26.71	40.40	45.23	47.02	1210
.693	2.884	7.82	16.98	31.09	46.95	52.55	54.62	1400
.846	3.378	9.05	19.55	35.71	53.86	60.26	62.62	1600
1.022	3.946	10.46	22.51	41.02	61.79	69.12	71.82	1830
1.152	4.365	11.50	24.69	44.95	67.66	75.66	78.63	2000
1.229	4.613	12.12	25.97	47.26	71.11	79.52	82.63	2100
1.459	5.353	13.96	29.83	54.18	81.46	91.07	94.63	2400
1.919	6.84	17.65	37.54	68.03	102.2	114.2	118.63	3000
2.303	8.07	20.73	43.98	79.58	119.4	133.4	138.64	3500
2.687	9.31	23.80	50.40	91.12	136.7	152.7	158.64	4000
3.072	10.55	26.88	56.84	102.67	153.9	172.0	178.65	4500
3.456	11.78	29.95	63.26	114.21	171.2	191.2	198.64	5000

TABLE III. *Values of* $\mathbf{X}$ *as function of* E *and of scattering angle* Θ. *In expansion* E *is in Mev.*

$\Theta=15°$	20°	25°	30°	35°	40°	42.5°	45°	E (KEV)
7.79	6.60	5.484	4.700	4.203	3.928	3.863	3.841	150
9.69	7.34	5.807	4.856	4.283	3.978	3.904	3.881	200
10.87	7.79	6.004	4.950	4.332	4.006	3.929	3.904	250
11.68	8.09	6.136	5.013	4.365	4.026	3.946	3.920	300
12.27	8.31	6.232	5.058	4.388	4.040	3.958	3.932	350
12.72	8.48	6.304	5.092	4.406	4.050	3.967	3.940	400
13.07	8.61	6.360	5.119	4.418	4.059	3.974	3.947	450
13.35	8.71	6.405	5.140	4.431	4.065	3.980	3.952	500
13.78	8.87	6.473	5.172	4.447	4.075	3.988	3.960	600
14.09	8.99	6.521	5.195	4.459	4.082	3.994	3.966	700
14.33	9.07	6.560	5.212	4.468	4.087	3.999	3.970	800
14.66	9.19	6.609	5.236	4.480	4.095	4.005	3.976	1000
14.48	9.13	6.582	5.223	4.473	4.090	4.002	3.973	880
14.89	9.28	6.645	5.253	4.489	4.100	4.010	3.980	1210
15.16	9.38	6.687	5.273	4.499	4.105	4.014	3.986	1600
15.32	9.44	6.712	5.285	4.505	4.109	4.018	3.988	2000
15.36	9.45	6.717	5.287	4.506	4.110	4.019	3.988	2100
15.44	9.48	6.730	5.293	4.509	4.112	4.020	3.990	2400
15.55	9.52	6.747	5.301	4.513	4.115	4.022	3.992	3000
15.66	9.56	6.764	5.309	4.517	4.117	4.024	3.994	4000
15.73	9.58	6.775	5.314	4.520	4.118	4.026	3.995	5000
16.00	9.68	6.816	5.333	4.530	4.124	4.031	4.000	
$-1.364/E$	$-0.492/E$	$\frac{-0.2083}{E}$	$\frac{-0.0975}{E}$	$\frac{-0.0500}{E}$	$\frac{-0.0297}{E}$	$\frac{-0.0254}{E}$	$\frac{-0.0240}{E}$	Expansion at $E=\infty$. In expansion E is in Mev.
$\frac{+0.02075}{E^2}$	$\frac{+0.00472}{E^2}$	$\frac{+0.00128}{E^2}$	$\frac{0.00038}{E^2}$	$\frac{+0.00012}{E^2}$	$\frac{+0.00004}{E^2}$	$\frac{+0.00003}{E^2}$	$\frac{+0.000024}{E^2}$	

TABLE IV. *Values of $-2\mathfrak{Y}/\eta$ as function of E and of scattering angle Θ. In expansion E is in Mev.*

$\Theta=15°$	20°	25°	30°	35°	40°	42.5°	45°	E (KEV)	$4/\eta^2$
65.46	32.45	18.22	11.27	7.71	5.991	5.600	5.472	150	24.003
69.12	33.55	18.60	11.42	7.77	6.021	5.619	5.488	200	32.005
71.39	34.22	18.83	11.51	7.81	6.032	5.633	5.501	250	40.006
72.89	34.67	18.98	11.56	7.83	6.041	5.639	5.506	300	48.007
74.02	34.99	19.09	11.61	7.84	6.050	5.646	5.512	350	56.008
74.88	35.23	19.18	11.63	7.86	6.06	5.65	5.519	400	64.009
75.50	35.42	19.24	11.66	7.87	6.06	5.66	5.52	450	72.01
76.03	35.59	19.29	11.68	7.88	6.06	5.66	5.52	500	80.01
76.85	35.81	19.37	11.71	7.89	6.07	5.66	5.53	600	96.01
77.42	35.97	19.43	11.73	7.90	6.07	5.66	5.53	700	112.02
77.84	36.09	19.47	11.74	7.90	6.08	5.66	5.53	800	128.02
78.42	36.26	19.53	11.77	7.91	6.08	5.68	5.53	1000	160.02
78.08	36.18	19.49	11.76	7.90	6.08	5.67	5.53	880	140.82
78.84	36.39	19.56	11.79	7.92	6.08	5.67	5.54	1210	193.63
79.27	36.53	19.62	11.81	7.92	6.08	5.67	5.54	1600	256.04
79.63	36.61	19.65	11.82	7.93	6.09	5.68	5.54	2000	320.05
79.71	36.62	19.66	11.82	7.94	6.09	5.68	5.54	2100	336.05
79.84	36.69	19.66	11.82	7.94	6.09	5.68	5.54	2400	384.05
80.00	36.74	19.68	11.82	7.94	6.09	5.68	5.54	3000	480.08
80.25	36.79	19.71	11.84	7.94	6.09	5.68	5.54	4000	640.11
80.35	36.83	19.72	11.84	7.94	6.09	5.68	5.54	5000	800.13
80.86	36.97	19.77	11.86	7.95	6.094	5.680	5.545		
$\frac{-2.457}{E}$	$\frac{-0.704}{E}$	$\frac{-0.238}{E}$	$\frac{-0.0891}{E}$	$\frac{-0.0356}{E}$	$\frac{-0.0161}{E}$	$\frac{-0.0123}{E}$	$\frac{-0.01110}{E}$	Expansion at $E=\infty$. In expansion E is in Mev.	
$\frac{+0.0224}{E^2}$	$\frac{+0.00405}{E^2}$	$\frac{+0.00088}{E^2}$	$\frac{+0.00021}{E^2}$	$\frac{+0.000054}{E^2}$	$\frac{+0.000014}{E^2}$	$\frac{+0.000008}{E^2}$	$\frac{+0.000006}{E^2}$		

TABLE V. *Values of $\mathfrak{M}$ as function of E and of scattering angle Θ. In expansion E is in Mev.*

$\Theta=15°$	20°	25°	30°	35°	40°	42.5°	45°	E (KEV)
216.4	67.79	27.29	12.97	7.121	4.679	4.164	4.000	150
214.4	67.05	26.98	12.84	7.073	4.669	4.162	4.000	200
213.2	66.59	26.79	12.76	7.045	4.663	4.160	4.000	250
212.4	66.28	26.66	12.71	7.026	4.658	4.159	4.000	300
211.8	66.06	26.57	12.67	7.012	4.655	4.158	4.000	350
211.3	65.89	26.50	12.64	7.002	4.653	4.158	4.000	400
211.0	65.76	26.45	12.62	6.999	4.651	4.157	4.000	450
211.0	65.65	26.41	12.60	6.988	4.650	4.157	4.000	500
210.2	65.49	26.34	12.58	6.978	4.648	4.157	4.000	600
209.9	65.38	26.29	12.56	6.971	4.646	4.156	4.000	700
209.7	65.29	26.26	12.54	6.966	4.645	4.156	4.000	800
209.4	65.17	26.21	12.52	6.959	4.644	4.156	4.000	1000
209.5	65.24	26.24	12.54	6.963	4.644	4.156	4.000	880
209.1	65.09	26.18	12.51	6.954	4.642	4.155	4.000	1210
208.7	64.93	26.11	12.48	6.944	4.640	4.155	4.000	2000
208.6	64.88	26.10	12.48	6.942	4.640	4.155	4.000	2400
208.4	64.84	26.08	12.47	6.940	4.639	4.155	4.000	3000
208.3	64.78	26.05	12.46	6.936	4.639	4.155	4.000	5000
208.0	64.68	26.01	12.44	6.930	4.638	4.154	4.000	
$\frac{+1.387}{E}$	$\frac{+0.494}{E}$	$\frac{+0.198}{E}$	$\frac{+0.0803}{E}$	$\frac{+0.0288}{E}$	$\frac{+0.00635}{E}$	$\frac{+0.00153}{E}$		Expansion at $E=\infty$. In expansion E is in Mev	
$\frac{-0.0200}{E^2}$	$\frac{-0.00421}{E^2}$	$\frac{-0.00096}{E^2}$	$\frac{-0.00020}{E^2}$	$\frac{-0.000030}{E^2}$	$\frac{-0.000002}{E^2}$				

In these expansions E is in Mev and $\eta E^{\frac{1}{2}}$ was taken to be 0.1581.

The number of counts expected according to Mott's formula is practically independent of the choice of fundamental constants. It can be expressed in terms of the Faraday constant, the velocity of light and the density of hydrogen in the scattering volume. In addition there enters $\mathfrak{M}$ of Eq. (3.3) which is 4 for $\Theta=45°$ at all energies and depends only little on the energy at other angles. For one microcoulomb of incident protons the yield of scattered protons is:

$$Y=10^{-35}\rho_{\mathrm{H}}\left(\frac{e}{M_{\mathrm{H}}c}\right)c^4\frac{2bA}{R_0\mathfrak{h}}\mathfrak{M}(10^{-6}V_{\mathrm{abs}})^{-2}\cot\Theta.$$

Here the absolute coulomb and absolute volt are used as units, ρ_{H}=density of hydrogen, c=velocity of light, M_{H}=mass of neutral hydrogen atom. The quantities A, $2b$, R_0, $\mathfrak{h}$ refer to the detector system for counting protons. The notation is A=area of hole, $2b$=width of slit, R_0=distance from hole to beam, $\mathfrak{h}$=distance from hole to slit. Using $e/Mc=9648.9$ abs.-e.m.u. g-equiv.$^{-1}$, $c=2.99796\times10^{10}$ cm sec.$^{-1}$ and computing ρ_{H} for one mm of oil having density 0.864 with hydrogen at 0°C one obtains

$$Y_{\mathrm{abs}}=581.0\frac{2bA}{R_0\mathfrak{h}}\mathfrak{M}(10^{-6}V_{\mathrm{abs}})^{-2}\cot\Theta.$$

Here M is taken to be the mass of the average oxygen atom. Supposing that average hydrogen contains 0.04 percent of O_{17} and 0.20 percent O_{18} one has $M=(\frac{1}{16})\times1.000275\times$mass of O_{16} atom $=(1.000275/1.00813)M_{\mathrm{H}}$. The density of hydrogen at 0°C and normal atmospheric pressure was taken as 8.988×10^{-5} g/cm^3; the presence of deuterium was neglected. Boyle's law was assumed, and normal atmospheric pressure was used as the pressure due to 760 mm of mercury having density 13.5951 with the acceleration due to gravity having the value 980.665 cm sec.$^{-2}$. The deviation of the acceleration of gravity in Madison (980.365 cm sec.$^{-2}$) from the standard was taken into account. In international volts and coulombs (International volt=1.00045 abs. volt; International coulomb=0.99993 abs. coulomb)

$$Y_{\mathrm{intern}}=580.5\frac{2bA}{R_0\mathfrak{h}}\mathfrak{M}(10^{-6}V_{\mathrm{intern}})^{-2}\cot\Theta. \quad (3.4)$$

This is the Mott yield per international microcoulomb of incident protons neglecting the geometrical corrections which will be discussed later. The final adjustments to the reduction of data from both laboratories have been made from the above formula.

The assumption of the validity of Boyle's law and the compressibility of Apiezon oil B (the latter has been pointed out by Mr. L. E. Hoisington) introduce small errors in the above constant. The compressibility of oil presumably makes it necessary to decrease the above number by about 0.01 percent. Assuming the equation between volume and pressure for hydrogen to be $pv=0.99938+0.00062p$, with p in atmospheres, one has for small v; $1/v=1.00062p$. The above result should be increased therefore by 0.06 percent on account of the inaccuracy of Boyle's law. Both of these corrections were omitted as insignificant.

2. Effect of error consisting of constant factor

Because of an error in the measurement of the slit system through which the protons are admitted to the ionization chamber there may be present in the measurements an error consisting of a factor which does not depend on the scattering angle. Errors in the operation of the scale-of-ten counter that do not depend on the pulse size entering the amplifier are independent of scattering angle. Similarly some of the errors in the calibration of the Faraday cage used for measuring the primary current enter in the same way for angles and errors in the operation of the Faraday cage during the scattering measurements may depend on the primary energy but should be independent of the scattering angle. Similarly an error in the measurement of the pressure comes under the present head. An effect of an error in the measurement of the energy of the incident particles is also mainly of the nature of a constant factor for all angles but is slightly more complicated. It will be treated as a separate error in another section.

It is found on calculation that in the range 1400–2400 kev a factor independent of angle does not introduce an apparent presence of a p wave to an important degree. If the scattering is due to an s wave anomaly alone then a reasonably small error of this sort produces very nearly

the same error in K_0 at all scattering angles that are used in the experiments for determining K_0. This condition can be expected to persist at the higher energies because the Coulomb scattering becomes increasingly less important. Spherical symmetry in the system of the center of gravity which is characteristic of s scattering cannot be destroyed by an error which is independent of scattering angle and, therefore, a p wave anomaly cannot be introduced by such an error. On the other hand, in the lower energy region 600–900 kev, the Coulomb scattering becomes more important. The spherical symmetry of the scattering in the center of gravity system is then destroyed. A factor constant at all angles produces in this energy range effects on K_0 which depend on the scattering angle used. An apparent p wave anomaly can be introduced at these energies by such an error. Since one may expect theoretically that p and d anomalies increase with energy this circumstance is fortunate for judging experimental data as to presence in it of errors of this nature. For if the data indicate at the higher energies that the anomaly is due to s scattering alone then, even though the value of K_0 obtained from the data may be incorrect, there is no p scattering and, therefore, there should be no p scattering at the lower energies either. If, in addition, the 600–900-kev range shows no p scattering, then the absolute values in this voltage range must be right because otherwise a constant factor at all angles would introduce p scattering. There is at present no indication of a p wave in the 1400–2400-kev range and the above criterion can be used. Errors which are represented by a factor which depends on the scattering angle are, of course, not taken care of by the above type of test.

Let $\mathfrak{R}=\mathbf{P}/\mathbf{P}_M=$ then

$$\frac{\partial \mathfrak{R}}{\partial K_0}=-\frac{2\mathbf{X}}{\eta \mathfrak{M}}\cos 2K_0+\left(\frac{4}{\eta^2 \mathfrak{M}}+\frac{2\mathbf{Y}}{\eta \mathfrak{M}}\right)\sin 2K_0 \quad (4)$$

gives the sensitivity of $\mathfrak{R}$ to K_0 and

$$a_\Theta=(57.3°/100)/(\partial \mathfrak{R}/\mathfrak{R}\partial K_0);\ (\mathfrak{R}\rightarrow 1.01\mathfrak{R}) \quad (4.1)$$

represents the error in K_0 due to one percent error in $\mathfrak{R}$. In Table VI values of this error are listed for different scattering angles, energies and phase shifts. The latter were obtained from theoretical calculations with an interaction potential having a constant value through a distance e^2/mc^2. The negative of the potential energy (depth of well $=D$) within this distance in Mev is given in the last column. Outside the distance e^2/mc^2 the Coulomb field e^2/r was assumed to represent the potential energy. The phase shifts used correspond approximately to the experimental values. For $D=11$ Mev the phase shifts in this table were obtained by extrapolation from $D=10.0$ and $D=10.5$ Mev.

It is seen from the table that at $\Theta=15°$ and 20° the accuracy for determining K_0 is frequently poorer than at other scattering angles. For $K_0=34.8°$, $E=880$ kev, $\Theta=15°$ the accuracy is especially poor. This is because close to this energy the ratio $\mathfrak{R}$ is practically independent of K_0. At all energies the optimum range of angles for determining K_0 is around $\Theta=45°$. It should be pointed out again that at the higher energies the same percentage error in $\mathfrak{R}$ gives practically the same error in K_0 except at $\Theta=15°$ while from 1600 kev down there is a noticeable change in δK_0 with Θ.

The changes of sign in δK_0 which occur in Table VI are somewhat confusing, and it is at times better to express the results in terms of the percentage by which the apparent $\mathfrak{R}$ differs from the $\mathfrak{R}$ that is theoretically expected using the apparent K_0 as derived from the data at $\Theta=45°$. If the correct $\mathfrak{R}$ is changed at all angles into $(1+\epsilon)\mathfrak{R}=\mathfrak{R}'$, then the value of K_0 using $\Theta=\pi/4$ is $K_0+(\delta K_0)_{\pi/4}$ where

$$(\delta K_0)_{\pi/4}=\epsilon\left[\mathfrak{R}/(\partial \mathfrak{R}/\partial K_0)\right]_{\pi/4}.$$

From this phase shift the expected $\mathfrak{R}$ at other Θ is $\mathfrak{R}+(\partial \mathfrak{R}/\partial K_0)(\delta K_0)_{\pi/4}$. One has

$$\begin{aligned}\mathfrak{R}'/[\mathfrak{R}+(\partial \mathfrak{R}/\partial K_0)(\delta K_0)_{\pi/4}] &=1+(\epsilon/\delta K_0)[\delta K_0-(\delta K_0)_{\pi/4}]\\ &=1+(\epsilon/a_\Theta)(a_\Theta-a_{\pi/4}). \quad (4.2)\end{aligned}$$

The quantity $(a_\Theta-a_{\pi/4})/a_\Theta$ is thus the ratio of the apparent percentage deviation of $\mathfrak{R}$ from the value to be expected at scattering angle Θ from the apparent K_0 at $\Theta=45°$ to the percentage error in $\mathfrak{R}$. Values of this ratio are given in Table VII.

TABLE VI. *Values of error in phase shift K_0 in degrees due to one percent error in measured scattering.*

$\Theta=15°$	20°	25°	30°	35°	40°	42.5°	45°	E (KEV)	K_0	D (MEV)
−2.3	−0.97	−0.51	−0.28	−0.16	−0.10	−0.087	−0.082	175	5.5°	10.395
−1.4	− .71	− .40	− .23	− .12	− .061	− .045	− .039	275	9.6°	10.395
−1.2	− .64	− .42	− .29	− .19	− .091	− .038	− .013	375	13.7°	10.395
−1.1	− .67	− .55	− .85	+ .34	+ .049	+ .023	+ .017	450	16.4°	10.395
−1.1	− .85	−3.1	+ .29	+ .088	+ .047	+ .041	+ .039	550	19.8°	10.395
−1.2	−2.2	0.50	.14	.083	.068	.065	.064	650	23.8°	10.500
−1.5	+3.1	.27	.12	.094	.085	.084	.083	750	26.6°	10.500
−2.2	+0.85	.21	.12	.11	.102	.101	.101	850	29.2°	10.500
−2.7	.70	.20	.13	.11	.11	.11	.11	880	30.0°	10.500
1.8	.30	.18	.16	.15	.15	.15	.15	1210	36.2°	10.500
0.94	.26	.19	.17	.17	.17	.17	.17	1400	39.0°	10.500
.66	.25	.20	.19	.19	.19	.19	.20	1600	41.4°	10.500
.51	.25	.21	.21	.21	.22	.22	.22	1830	43.8°	10.500
.46	.25	.22	.22	.22	.23	.23	.23	2000	45.1°	10.500
.43	.25	.23	.23	.23	.23	.24	.24	2100	45.7°	10.500
.39	.26	.24	.25	.25	.26	.26	.26	2400	47.6°	10.500

3. Effect of error in voltage

If the experiment is performed at an energy E and if there is only an s wave anomaly the ratio $\mathfrak{R}=\mathbf{P}/\mathbf{P}_M$ is given by Eqs. (2) with a suitable K_0. If the energy at the scattering volume is incorrectly judged to be

$$E'=E+\delta E$$

one obtains an apparent experimental value $\mathfrak{R}'$ for that ratio at the energy E'. This value corresponds to an apparent phase shift K_0' if Eqs. (2) are used. In this section

$$\delta K_0=K_0'-K_0$$

will be called the error in the phase shift. This nomenclature is not the best because it takes no account of the fact that at the energy E' the correct phase shift differs from K_0. This circumstance will be discussed later in connection with the variation of K_0 with E and the effect of a possible error in voltage on the magnitude of the interaction potential. It will then be seen that only a fraction of K_0 matters for conclusions drawn from experiments at the higher energies.

It is seen in Table V that $\mathfrak{M}$ changes very slowly with energy. It is thus sufficiently accurate to consider $\mathbf{P}_M$ as being proportional to E^{-2}. The apparent value of $\mathfrak{R}$ at energy E' is then

$$\mathfrak{R}'=(E'/E)^2\mathfrak{R}\cong(1+2\delta E/E)\mathfrak{R}.$$

This may be equated to

$$\mathfrak{R}+(\partial\mathfrak{R}/\partial E)\delta E+(\partial\mathfrak{R}/\partial K_0)\delta_{E,\Theta}K_0.$$

One obtains thus

$$\delta_{E,\Theta}K_0=(2\mathfrak{R}/E-\partial\mathfrak{R}/\partial E)\delta E/(\partial\mathfrak{R}/\partial K_0)\cdots. \quad (5)$$

Treating again $\mathfrak{M}$ as independent of the energy one has

$$\frac{\partial\mathfrak{R}}{\partial E}=-\frac{\sin K_0\cos K_0}{E\eta\mathfrak{M}}\left(\mathbf{X}-\eta\frac{\partial\mathbf{X}}{\partial\eta}\right)+\frac{\sin^2 K_0}{E\mathfrak{M}}\left(\frac{4}{\eta^2}+\frac{\mathbf{Y}}{\eta}-\frac{\partial\mathbf{Y}}{\partial\eta}\right). \quad (5.1)$$

TABLE VII. *Percentage by which apparent ratio to Mott is higher than value calculated from apparent phase shift K_0 determined at $\Theta=45°$ if at all angles the measured yields are too high by one percent and if the anomaly is due only to s scattering. Quantity tabulated is $(a_\Theta-a_{\pi/4})/a_\Theta$. Values of K_0 correspond to $r_0=e^2/mc^2$, $D=10.5$ Mev.*

$\Theta=15°$	20°	25°	30°	35°	40°	42.5°	E (KEV)	K_0
1.04	0.85	0.46	0.164	0.043	0.008	0.002	880	30.0°
.92	.50	.14	.02	−.003	−.002	−.001	1210	36.2°
.81	.34	.064	−.0004	−.009	−.003	−.000	1400	39.0°
.70	.22	.015	−.019	−.013	−.004	−.001	1600	41.4°
.58	.12	.019	−.028	−.015	−.004	−.001	1830	43.8°
.50	.07	−.032	−.032	−.016	−.004	−.002	2000	45.1°
.46	.051	−.038	−.033	−.016	−.004	−.001	2100	45.7°
.34	−.001	−.052	−.037	−.017	−.003	−.001	2400	47.6°

TABLE VIII. *Values of error in phase shift K_0 in degrees due to one percent error in voltage of scattering volume.*

$\Theta=15°$	20°	25°	30°	35°	40°	42.5°	45°	E (KEV)	K_0	D (MEV)
−4.6	−2.0	−1.05	−0.60	−0.36	−0.23	−0.20	−0.19	175	5.5°	10.395
−2.9	−1.5	−0.86	− .51	− .30	− .17	− .14	− .13	275	9.6°	10.395
−2.4	−1.4	− .91	− .65	− .46	− .26	− .15	− .10	375	13.7°	10.395
−2.3	−1.5	−1.19	−1.8	+ .63	+ .027	− .031	− .045	450	16.4°	10.395
−2.3	−1.8	−0.65	+0.51	+ .081	− .004	− .014	− .018	550	19.8°	10.395
−2.6	−4.6	+ .90	.17	.049	.018	.013	.012	650	23.8°	10.500
−3.2	+6.1	.41	.12	.055	.038	.035	.034	750	26.6°	10.500
−4.7	+1.6	.27	.10	.067	.056	.055	.055	850	29.2°	10.500
−5.7	1.26	.25	.10	.071	.063	.061	.061	880	30.0°	10.500
+3.6	0.43	.17	.12	.114	.113	.113	.114	1210	36.2°	10.500
1.7	.33	.17	.14	.14	.14	.14	.14	1400	39.0°	10.500
1.1	.29	.18	.16	.16	.16	.16	.16	1600	41.4°	10.500
0.83	.27	.19	.18	.18	.18	.19	.19	1830	43.8°	10.500
.71	.26	.20	.19	.19	.20	.20	.20	2000	45.1°	10.500
.66	.26	.20	.20	.20	.21	.21	.21	2100	45.7°	10.500
.56	.26	.22	.22	.22	.23	.23	.23	2400	47.6°	10.500

Computing this one obtains the numbers in Table VIII.

The phase shifts, energies and depths of well in Table VIII correspond to those in Table VI. The effect of an error in voltage is seen to become nearly independent of the angle at the higher energies. In this respect the effect of an error in voltage is very similar to that of an error due to a factor independent of angle.

The effect of an error in voltage is somewhat simpler when it is expressed in terms of the percentage by which the observed scattering at an angle Θ differs from the scattering to be expected, when only an s scattering anomaly is assumed and when the observed scattering at $\Theta=45°$ is used. This can be done using the numbers tabulated in Tables VI and VIII. The quantity recorded in the latter table is

$$b_\Theta=0.573E\delta_{E,\,\Theta}K_0/\delta E. \tag{5.2}$$

The quantity $\mathfrak{R}$ is a function of K_0 and E and in the absence of exact knowledge of the voltage the value of $\mathfrak{R}$ theoretically expected at the angle Θ and the apparent energy E' using observations at $\Theta=\pi/4$ is

$$\mathfrak{R}(K_0+\delta_{E,\,\pi/4}K_0,\,E+\delta E)$$
$$=\mathfrak{R}+(\partial\mathfrak{R}/\partial K_0)\delta_{E,\,\pi/4}K_0+(\partial\mathfrak{R}/\partial E)\delta E=\mathfrak{R}''.$$

The ratio of the apparent value $\mathfrak{R}'$ to this expected value $\mathfrak{R}''$ is then

$$\mathfrak{R}'/\mathfrak{R}''=1+(\partial\mathfrak{R}/\mathfrak{R}\partial K_0)(\delta_{E,\,\Theta}K_0-\delta_{E,\,\pi/4}K_0)$$
$$=1+(\delta E/E)(b_\Theta-b_{\pi/4})/a_\Theta. \tag{5.3}$$

By means of Eq. (5.3) and Tables VI and VIII one can obtain the ratio $\mathfrak{R}'/\mathfrak{R}''$. The percentage by which the observed value at scattering angle Θ should differ from the value to be expected on the basis of measurements made at $\Theta=45°$ is seen to be the percentage of error in the voltage multiplied by

$$(b_\Theta-b_{\pi/4})/a_\Theta.$$

Values obtained in this way are tabulated in Table IX.

4. Estimate of spread of beam due to collisions. Discussion of pressure effects in argon and krypton. Multiple scattering

As the beam goes through the scattering chamber it becomes spread on account of the many small collisions that each bombarding particle makes with the hydrogen atoms of the gas. The purpose of the present section is to make estimates of the order of magnitude of the additions to the width of the beam due to this cause. The diameter of the beam must be kept somewhat smaller than the diameter of the foil used to admit the protons into the evacuated Faraday cylinder connected to the current integrator. The fluctuation of the direction of the beam due to changes in the accelerating tube makes it unnecessary to have more than estimates of order of magnitude.

The relatively numerous small angle collisions may be considered in first approximation as changing the direction of motion without chang-

ing the energy of the particle. The vector representing the velocity is changed at each collision through the addition of a small vector perpendicular to the initial direction and the probability of the occurrence of a single such change in a short path can be calculated by means of Rutherford's or Mott's scattering formula. For the first collision the change of direction occurs in a plane perpendicular to the original beam, but in later collisions it takes place in planes having slightly different directions. Since the total deflection is supposed to be small the change of orientation of the planes will be neglected. The additions to the velocity may then be considered as taking place in the same plane but each successive addition must be considered as taking place in a random direction with probabilities determined by Rutherford's formula. Instead of using the velocities one may also deal directly with vectors having absolute values equal to the angular deflections and drawn in the direction of the velocity changes. The problem is thus very similar to that of "random flights" in a plane.

A set of random radial displacements in a plane having equal magnitude α gives resultant displacements for which the Cartesian coordinates x, y, and distance, r, have $(r^2)_{Av}=(2x^2)_{Av}=(2y)^2{}_{Av}=(n\alpha^2)_{Av}$. For large n the average deviations of the squares correspond to a Gauss error distribution. It is shown in Rayleigh's *Theory of Sound*[15] that the distribution is of the Gauss error type even if one deals with the composition of a large number n of components with amplitude α, a large number n' of components with amplitude β, etc. The chance of a resultant displacement of amplitude between r and $r+dr$, is then according to Rayleigh

$$P(r)dr=2(n\alpha^2+n'\beta^2+\cdots)^{-1}r \times\exp\left[-r^2/(n\alpha^2+n'\beta^2+\cdots)\right]dr.$$

The number of deflections taking place in an infinitesimal angular range is, of course, not infinite and it is not justifiable to apply this formula since the numbers n, n', $\cdots$ are not infinite. It may, nevertheless, be expected to give the result approximately because the angular range may be divided into finite rather than infinitesimal intervals and because the validity of

$$(r^2)_{Av}=n\alpha^2+n'\beta^2+\cdots$$

does not depend on n, n', $\cdots$ having large values. In the remainder of the discussion $(r^2)_{Av}=(\theta^2)_{Av}$ (θ=angular deflection) will be calculated and it will be assumed that the distribution is not far from that given by Rayleigh's formula. Since the latter drops off steeply at and beyond $[(\theta^2)_{Av}]^{\frac{1}{2}}$, the values of this quantity will be used as estimates of the probable angular spread.

For scattering from a heavy nucleus such as that of argon Rutherford's formula applies. It will be supposed that the scattering by an atom of argon becomes zero when the impact parameter (distance from nucleus to orbital asymptote at ∞) is greater than some suitably chosen distance p of the order of nuclear dimensions. Corresponding to this distance there is an angle of minimum deflection ω which, when small, is given by

$$\omega=ZZ'e^2/Ep, \tag{6}$$

where Ze, $Z'e$ are the charges of the colliding nuclei and E is the kinetic energy of the scattered particle. The chance that one small angle collision should take place into an angular range θ, $\theta+d\theta$ on going through a thickness l of gas having n atoms per cm^3 is

$$K\theta^{-3}d\theta,$$

where

$$K=2\pi nl(ZZ'e^2/E)^2. \tag{6.1}$$

For large angles this is not true. The number of large angle collisions is, however, quite small and they will be neglected in studying the spreading of the beam. One has then

$$((\Sigma\theta)^2)_{Av}=K\int_{\omega}^{\theta_{\max}}\theta^{-3}\theta^2d\theta=K\ln(\theta_{\max}/\omega), \tag{6.2}$$

where $\theta_{\max}$, is a suitably chosen upper limit for elementary deflections that need to be taken into account. For an argon pressure of 60 mm of oil having a density 0.866 one has a pressure equal to that of 3.83 mm of mercury so that $n=2.70\times10^{19}\times3.84/760=1.36\times10^{17}$. For $E=2mc^2$ one has then $K=1.21\times10^{-4}$ for a path length $l=22$

[15] Lord Rayleigh, *Theory of Sound*, second edition (Macmillan Co., 1894), Vol. I, p. 41; G. N. Watson, *Bessel Functions* (Cambridge University Press, 1922), p. 419 for references.

cm. Assuming p = Bohr radius $= 0.528\times10^{-8}$ cm, one has at an energy of $2mc^2$ the value $\omega = 18e^2/2mc^2a_H = 9(e^2/\hbar c)^2 = 4.79\times10^{-4}$. The number of single deflections into $\Delta\omega$ is $\sim K\omega^{-3}\Delta\omega = 500\Delta\omega/\omega$. Thus practically every proton suffers several small angle collisions. Using $\theta_{max}=\pi/2$ one has $\ln(\theta_{max}/\omega)=8.1$ and using $\theta_{max}=1°$ $=1/57.3$ one has $\ln(\theta_{max}/\omega)=3.6$. The result is seen to be insensitive to the choice of θ_{max}. Using $\theta_{max}=\pi/2$ one obtains Table Xa. In the last row is given the quantity $2l\Delta\theta/3$. This is an approximate estimate of the linear spread of the beam. The root mean deviation $\Delta\theta$ is assumed here to give sufficiently well the direction of motion of the root mean deviation of the linear displacement Δx so that,

$$\Delta x = \Delta\theta\int_0^l (y/l)^{\frac{1}{2}}dy = 2l\Delta\theta/3.$$

This assumption is crude, but should be good enough for estimates of order of magnitude. The values in Table Xa are probably too high since $\theta_{max}=\pi/2$ is an overestimate. With $\theta_{max}=2°$ $=0.0349$ values given in Table Xb are obtained. These may still be somewhat too high because for this θ_{max} at $E=2mc^2$ one has $K\theta_{max}^{-2}=1.2\times10^{-4}/(0.035)^2=0.10$. There is, therefore, only a chance of 1/10 that a proton will be scattered into a 2° range at the rate at which scattering occurs at 2°. However, this chance increases rapidly towards smaller deflections.

In order to obtain the same spread at $E=4mc^2$ as at $E=2mc^2$, the pressure must be increased nearly four times so as to compensate by means of n the change in E and to obtain the same K. For $\theta_{max}=0.0349$ the factor $\ln_e(\theta_{max}/\omega)$ increases from 4.30 at $E=2mc^2$ to 5.00 at $E=4mc^2$. Hence the pressure should be increased in this case not quite by the factor four but by $4\times4.30/5.00$ $=3.4$. If $\theta_{max}=\pi/2$, the increase in pressure required to produce the same spread at $4mc^2$ at a higher pressure as at $2mc^2$ at a lower pressure is $4\times8.1/8.8=3.7$. The accidental fluctuations of the direction of the proton beam and the impossibility of knowing precisely its width make it difficult to determine just how the loss of some of the incident protons through multiple small angle scattering will affect the measurements at a given energy as the pressure is varied. A better test of the origin of the observed deviations is to vary the energy and the pressure in such a way as to obtain the same apparent deviation from Rutherford's scattering. Then according to the estimates just made the same deviations should be obtained at two Mev at a pressure of about $3.4p$ as at one Mev at a pressure p. These preliminary estimates will be improved presently by using Eq. (6.6).

In hydrogen at the pressures used the spread of the beam due to multiple small angle scattering should be much smaller than in argon because the large scattering anomaly at $\Theta=45°$ makes it unnecessary to have as large a small angle scattering in hydrogen. In this case the chance that one small angle collision should take place into an angle between Θ and $\Theta+d\Theta$ on going through a thickness l of gas having n atoms per cm³ is

$$K_H\Theta^{-3}d\Theta,$$

where

$$K_H = 2\pi nl(e^2/E)^2. \qquad (6.3)$$

For $E=2mc^2$ and a path length $l=22$ cm through hydrogen gas at 12 mm Hg pressure one has $n=8.5\times10^{17}$, $K_H=2.34\times10^{-6}$, $\omega=2.66\times10^{-5}$. The probable angular spread must be less than $[K\ln\pi/4\omega]^{\frac{1}{2}}=0.0049=0.28°$. The probable linear

TABLE IX. *Percentage by which apparent $\mathfrak{R}$ is higher than value calculated from apparent phase shift K_0 determined at $\Theta=45°$ if the voltage measurements are too high by one percent and if the anomaly is due only to S scattering. Quantity tabulated is $(b_\Theta - b_{\pi/4})/a_\Theta$. Values of K_0 correspond to $r_0=e^2/mc^2$, $D=10.5$ Mev.*

$\Theta=15°$	20°	25°	30°	35°	40°	42.5°	E (KEV)	K_0
2.09	1.72	0.95	0.34	0.090	0.017	0.003	880	30.0°
1.9	1.04	.33	.064	.004	−.002	−.002	1210	36.2°
1.7	0.74	.17	.014	−.009	−.003	−.001	1400	39.0°
1.5	.52	.085	−.013	−.015	−.005	−.001	1600	41.4°
1.3	.34	.021	−.029	−.020	−.006	−.001	1830	43.8°
1.1	.25	−.005	−.036	−.021	−.006	−.002	2000	45.1°
1.0	.21	−.018	−.039	−.020	−.006	−.001	2100	45.7°
0.84	.11	−.042	−.043	−.021	−.004	−.002	2400	47.6°

TABLE X*a*. *Estimate of linear spread of proton beam with θ_{max} assumed to be $\pi/2$.*

$E=1mc^2$	$2mc^2$	$3mc^2$	$4mc^2$
$[((\Sigma\theta)^2)_{Av}]^{\frac{1}{2}}=3.4°$	1.8°	1.2°	0.93°
$\Delta x=2l\Delta\theta/3=0.88$ cm	0.46 cm	0.31 cm	0.24 cm

displacement must be less than 0.07 cm. According to Table X*b* this linear displacement corresponds to a pressure of $(0.07/0.33)^2\times 60$ mm $=3$ mm of argon at an energy of $2mc^2$. According to Fig. 10 of the paper of HKPP a pressure of 3 mm of argon at 860 kev shows no definite difference from Rutherford's scattering and may be in agreement with it. Although the evidence for this is not very definite it would be surprising if this error could be serious for hydrogen since there is good agreement of absolute yields in the overlap region between HHT and HKPP.

The above estimates are too crude for a comparison of argon and krypton scattering since screening is taken account of too roughly. An idea of the effect of screening can be obtained using the Thomas-Fermi field. The effective nuclear charge for force as a function of the distance r will be called $Z_e(r)$. For small deflections

$$\theta=(e^2/pE)\int_0^{\pi/2} Z_e(p/\cos\varphi)\cos\varphi d\varphi$$

and

$$\int nl\theta^2\sigma d\Omega$$

$$=K\int_{p(\min)}^{\infty}\left\{\int_0^{\pi/2} Z_e(p/\cos\varphi)\cos\varphi d\varphi\right\}^2 p^{-1}dp.$$

On account of the inapplicability of the formula for θ at large θ the integration over the distance of closest approach is cut off at a suitable $p_{\min}$. The Fermi-Thomas field gives $Z_e=Zf(\xi)$ with $\xi=Z^{\frac{1}{3}}r/(0.885a_H)$. The function $f(\xi)$ starts at $f=1$ for $\xi=0$, decreases roughly linearly up to $\xi=2$ and approaches $f=0$ asymptotically for large ξ. At $\xi=8$ it is ~ 0.1. The function will be approximated by

$$f(\xi)=A-B\xi \qquad (A, B>0)$$

through the region in which the above expression gives positive values. For larger ξ it will be supposed that $f=0$. This is admittedly an approximation. The integrations give

$$\int nl\theta^2\sigma d\Omega=KA^2\left[\frac{1}{2}\zeta_m^2\sin^2\zeta_m-\frac{5}{4}\sin^2\zeta_m+\frac{3}{2}\zeta_m\sin\zeta_m\cos\zeta_m-\frac{3}{4}\zeta_m^2-\ln\cos\zeta_m\right], \quad (6.4)$$

where

$$\tan\zeta_m-\zeta_m=0.885a_HZ^{-4/3}(E/e^2)\theta_{\max}/B,$$
$$\cos\zeta_m=(B/A)Z^{\frac{1}{3}}p(\min)/(0.885a_H). \quad (6.5)$$

The last equation determines ζ_m in terms of $p(\min)$ which is the smallest impact parameter admitted by the requirement of using a formula for θ valid only for small θ. The equation before last similarly determines ζ_m in terms of $\theta_{\max}$. The large value of $a_H/(e^2/E)$ makes the right side of Eq. (6.5) of the order of 100 which makes $\zeta_m\sim\pi/2$. Setting

$$\zeta_m=\pi/2-\epsilon$$

one has

$$1/\epsilon=0.885a_HZ^{-4/3}(E/e^2)\theta_{\max}/B+\pi/2+\cdots, \quad (6.5')$$

$$((\Sigma\theta)^2)_{Av}=KA^2[-5/4-\pi^2/16+\ln(1/\epsilon)+\pi\epsilon+\cdots] \quad (6.6)$$

where K is given by Eq. (6.1). The result in the form of Eq. (6.6) is similar to Eq. (6.2). It is more suitable for the purpose of comparing krypton with argon because the screening is made to vary with Z in accordance with the Fermi-Thomas distribution. Using $\theta_{\max}=\frac{1}{10}$, $B=\frac{1}{5}$, $A=1$ one has at 860 kev $1/\epsilon\cong 1.40\times 10^4Z^{-4/3}$ which gives for the coefficient of KA^2 in Eq. (6.6) the values 2.92 for krypton and 3.83 for argon. The number of argon atoms n_A that would be expected to give the same effect as n_K krypton atoms should be therefore $n_A=4(2.92/3.83)n_{Kr}=3.0n_{Kr}$. The experimental ratio of the argon pressure to that of krypton for the same percentage difference from Rutherford is approxi-

TABLE X*b*. *Estimate of linear spread of proton beam with θ_{max} assumed to be 2°.*

$E=1mc^2$	$2mc^2$	$3mc^2$	$4mc^2$
$[((\Sigma\theta)^2)_{Av}]^{\frac{1}{2}}=2.4°$	1.3°	0.91°	0.70°
$2l\Delta\theta/3=0.61$ cm	0.33 cm	0.23 cm	0.18 cm

mately 2.3. The discrepancy between these two numbers can be reduced by using a larger B. There is some justification for using a larger B because most of the contributions to $((\Sigma\theta)^2)_{Av}$ come from small p and the values of ξ that correspond to p_{min} are, with the above constants, 0.04 for krypton and 0.02 for argon. The values of $\xi_p = Z^{\frac{1}{3}}p/(0.885a_H)$ that make important contributions are <0.4 and one may therefore use the initial rectilinear portion of the $f(\xi)$ curve. For this $A=1$, $B=\frac{1}{3}$ are fair values. Also $\theta_{max}=1/20$ corresponds better to Table Xb than $\theta_{max}=\frac{1}{10}$. Making these changes one obtains $n_A = 4(1.71/2.62)n_{Kr} = 2.6n_{Kr}$. This is not far from the experimental value $2.3n_{Kr}$. The coefficient of K in Eq. (6.6) is smaller than in the computation of Table Xb. The difference is less than a factor 2 and does not affect seriously the linear spreads.

The scattering in argon at 860 kev can be compared with that at 1830 kev. Comparing the pressures giving 16 percent difference from Rutherford's formula one has a ratio 3.1. The ratio of energies is 2.13. The ratio of pressures expected on account of the variation of K with energy is therefore $4.5=(2.13)^2$. The ratio $4.5/3.1=1.5$ must be accounted for by the change in the bracket in Eq. (6.6). Here again it is favorable to assume a large B and a small θ_{max}. With $B=\frac{1}{3}$ and $\theta_{max}=1/20$, the bracket is 2.62 for 860 kev and $2.62+\ln_e 2.13=3.38$ for 1830 kev. The corrected expectation for the ratio of pressures is $(2.13)^2(2.62/3.38)=3.5$. This is in fair agreement with the experimental 3.1. Here, as in the comparison with krypton, the coefficient of K does not change quite as rapidly as experiment requires. It appears from the above comparisons that the large scattering observed at high pressures is due to the spreading of the beam. On the other hand, the agreement between expectation and experiment is sufficiently imperfect to allow at least partly another explanation.

Double scattering in which the first deflection is greater than 5° will be seen to contribute little. The percentage difference caused by it should vary as nZ^2/E^2. Experimentally n must be varied more slowly than Z^2/E^2 in order to give the same percentage difference. This speaks against attributing a large part of the effect to double scattering in which the first deflection is $>5°$. The chance that a proton will be scattered into a cone between θ_1 and θ_2 is $(K/8)(1/\sin^2\theta_1/2 - 1/\sin^2\theta_2/2)$. For a path of 10 cm at 860 kev through argon at 60 mm oil pressure $K/8=10^{-5}$. The total number of protons scattered beyond 5° is according to this 0.5 percent of the number of incident protons. The change in the proton energy due to argon recoil is negligible for such a small fraction of the whole number. The effect of the change in direction can be estimated from a formula for second-order corrections caused by the divergence of the beam which is considered at the end of the section on "Geometrical Corrections." According to this the fractional increase in the scattering due to spreading the proton beam uniformly on the surface of a cone is $25\theta^2/4\Theta^2$ where Θ is the angle between the axis of the cone and the central line of the analyzing system while θ is the scattering angle for the first deflection. It is assumed that the angle θ is small. The chance of θ being between θ and $\theta+d\theta$ is $Kd\theta/\theta^3$. The fractional increase in scattering is

$$(25K/4\Theta^2)\ln(\theta_{max}/\theta_{min}).$$

For $\theta_{max}=\pi/2$, $\theta_{min}=5°$, $\Theta=20°$ this gives for argon at 860 kev, with path length $l=10$ cm, at a pressure of 60 mm of oil an effect of 1.1 percent. Decreasing θ_{min} to 2.5° increases this to only 1.4 percent. This effect is seen to be not serious since the total deviation from Rutherford's formula is ~ 25 percent. There should be an additional smaller effect due to having a large deflection first and a small one afterwards. This effect is expected to be smaller because the distance from the analyzing slit to the beam is ~ 3 cm. Since for larger Θ these corrections decrease as Θ^{-2} they account for only a small part of the whole.

For double scattering in which the first deflection is of the order of 1° or less it ceases to have meaning to consider only double scattering because the spread of the beam due to multiple scattering is of this order of magnitude. It is also incorrect to use the expression $(25K/4\Theta^2)\ln(\theta_{max}/\theta_{min})$ for too small values of θ_{min} because it was supposed, in deriving it, that the major part of the beam suffered no deflection comparable with θ_{min}. The contributions due to

double scattering in which the first angle is very small will be considered, therefore, as part of the effect of multiple scattering at small angles followed by a large deflection. The fractional effect due to this cause is $(25/4)((\Sigma\theta)^2)_{Av}/\Theta^2$. For a path of 10 cm in argon at 60 mm oil pressure at 860 kev for $\Theta=20°$ the above expression gives 1.0 percent. This effect should have the same value for a given value of the expression (6.6) and the estimates of the way n varies with Z and E made for the effect of missing the Faraday cylinder apply to this effect also. Double scattering through larger angles as well as multiple scattering through small angles followed by a large angle deflection give, with the approximation used here, fractional increases which vary directly with the pressure. It is surprising that the experimental curve gives also a linear variation with pressure for the fractional increase, but it is difficult to predict the law of increase with pressure without knowing more about the structure of the beam. There appears to be no objection so far, therefore, to attributing the pressure effects in argon and krypton primarily to the spreading of the beam and the too low value for the number of incident protons.

5. Values of phase shift derived from experiment

Explanation of tables.—In Table XI are given values of the ratio to Mott $\mathfrak{R}$ as obtained from experiment by Herb, Kerst, Parkinson and Plain. These represent the mean of several observations at energies close to the value listed in the first column. Where necessary corrections have been applied by them for the rate of change of yield with voltage in reducing the values to a common energy. The table consists of six sections each section of which refers to one energy. The first line of each section gives the value of $\mathfrak{R}$ tabulated by HKPP in their Table I. The second line gives the corrections which have been applied to this $\mathfrak{R}$. The corrections are expressed in percentage of $\mathfrak{R}$ and are in each case a sum of corrections for temperature of oil used in the manometer and a correction for fundamental units. The latter was made so as to reduce the values to Eq. (3.4). It amounts to a uniform increase of all values by 0.381 percent. The corrections for oil temperature are listed by HKPP in their Table I(a) and have been added to the correction for fundamental units. The final corrected value of $\mathfrak{R}$ is listed in the third row. The fourth and fifth rows give values of $\mathfrak{R}$ for two values of K_0 differing by 1° and representing approximately the experimental values. The object in listing these numbers is to show the sensitivity of $\mathfrak{R}$ to K_0. In the sixth row are given values of K_0 obtained from each scattering angle on the assumption of a pure s anomaly. The arithmetic mean of the values so obtained from $\Theta=30°$, 35°, 40°, 45° stands in the sixth row and last column. The values of K_0 obtained for smaller scattering angles were not used in taking the mean because the accuracy in the determination of K_0 is expected to be poorer for them. It is satisfactory to note, however, that for $\Theta=25°$ the experimental mean K_0 and the derived K_0 agree quite well and that the only large deviations for $\Theta=20°$ are 0.6° for 1200 kev and 0.4° at 2105 kev. For $\Theta=15°$ the deviations from the mean are large and are probably due to the poor sensitivity caused by the predominance of Rutherford scattering and by the presence of a slight systematic error caused by the variation of the scattering yield within the scattering angle. The seventh line contains values of $\mathfrak{R}$ computed for the mean K_0 on the assumption of absence of higher phase shifts and the eighth gives the percentage difference of the observed (line 3) and computed $\mathfrak{R}$. This last line contains information regarding the presence of higher phase shifts.

The experimental values used above correspond to the calibration of the ballistic galvanometer for current measurement by the "current time method." In addition Herb *et al.* have used a calibration by the "air condenser method." The latter gives values of $\mathfrak{R}$ greater than the "current time" values by 0.76 percent. Reasons for considering the current time method as more reliable are given in the paper of HKPP. The effect of using the air condenser values is, therefore, not tabulated. An alternative interpretation of the data would consist in increasing all experimental values of HKPP by 0.38 percent. According to Table VII the percentage difference between the observed and computed $\mathfrak{R}$ (eighth row of each section in Table XI) will be affected at the higher energies by negligible amounts except at $\Theta=15°$ where ~ 0.2 percent would have to be added. The uncertainties in geometrical

TABLE XI. *Phase shift analysis of data of Herb, Kerst, Parkinson and Plain.*

	Θ=15°	20°	25°	30°	35°	40°	45°
				E=860 kev			
$\mathfrak{R}$ from HKPP	0.750	0.672	0.811	1.317	2.229	3.38	3.90
Corrections	.327%	.327%	.327%	0.327%	0.327%	0.327%	0.327%
Final $\mathfrak{R}$	.752	.674	.814	1.321	2.236	3.39	3.91
$\mathfrak{R}$ (K_0=29°)	.724	.670	.811	1.288	2.184	3.278	3.821
$\mathfrak{R}$ (K=30°)	.721	.679	.853	1.394	2.395	3.608	4.211
K_0 from $\mathfrak{R}$		29.45	29.07	29.31	29.25	29.34	29.23
Mean K_0 from Θ=30°, 35°, 40°, 45°=29.28°							
$\mathfrak{R}$ (K_0=29.28°)	0.723	0.673	0.823	1.318	2.243	3.370	3.930
Diff. obs. and comp. $\mathfrak{R}$	4.0%	0.1%	−1.1%	0.2%	0.3%	0.6%	−0.5%

	Θ=15°	20°	25°	30°	35°	40°	45°
				E=1200 kev			
$\mathfrak{R}$ from HKPP	0.743	0.901	1.590	3.20	5.90	8.93	10.32
Corrections	.525%	.525%	0.525%	0.525%	0.525%	0.525%	0.525%
Final $\mathfrak{R}$	.747	.906	1.598	3.22	5.93	8.98	10.37
$\mathfrak{R}$ (K_0=35°)	.715	.860	1.516	3.004	5.511	8.43	9.87
$\mathfrak{R}$ (K_0=36°)	.718	.888	1.605	3.209	5.897	9.02	10.56
K_0 from $\mathfrak{R}$		36.60	35.92	36.05	36.08	35.93	35.72
Mean K_0 from Θ=30°, 35°, 40°, 45°=35.94°							
$\mathfrak{R}$ (K_0=35.94°)	.718	0.886	1.600	3.197	5.874	8.98	10.52
Diff. obs. and comp. $\mathfrak{R}$	4.0%	2.3%	−0.1%	0.7%	0.96%	0.0%	−1.4%

	Θ=15°	20°	25°	30°	35°	40°	45°
				E=1390 kev			
$\mathfrak{R}$ from HKPP	0.777	1.080	2.196	4.59	8.23	12.74	14.88
Corrections	.436%	0.436%	0.436%	0.436%	0.436%	0.436%	0.436%
Final $\mathfrak{R}$	.780	1.085	2.206	4.61	8.27	12.80	14.94
$\mathfrak{R}$ (K_0=38°)	.740	1.046	2.098	4.34	8.019	12.28	14.35
$\mathfrak{R}$ (K_0=39°)	.747	1.086	2.214	4.602	8.506	13.01	15.21
K_0 from $\mathfrak{R}$		38.97°	38.93°	39.03°	38.51°	38.71°	38.69°
Mean K_0 from Θ=30°, 35°, 40°, 45°=38.76°							
$\mathfrak{R}$ (K_0=38.76°)	.745	1.076	2.186	4.539	8.389	12.83	15.00
Diff. obs. and comp. $\mathfrak{R}$	4.7%	0.8%	0.9%	1.6%	−1.4%	−0.2%	−0.4%

	Θ=15°	20°	25°	30°	35°	40°	45°
				E=1830 kev			
$\mathfrak{R}$ from HKPP	0.884	1.661	3.862	8.24	15.04	23.12	27.28
Corrections	.491%	0.460%	0.460%	0.491%	0.460%	0.491%	0.460%
Final $\mathfrak{R}$	.888	1.669	3.880	8.28	15.11	23.23	27.41
$\mathfrak{R}$ (K_0=43°)	.851	1.598	3.676	7.86	14.53	22.18	25.91
$\mathfrak{R}$ (K_0=44°)	.868	1.665	3.854	8.24	15.26	23.25	27.14
K_0 from $\mathfrak{R}$		44.06°	44.14°	44.10°	43.79°	43.98°	44.22°
Mean K_0 from Θ=30°, 35°, 40°, 45°=44.02°							
$\mathfrak{R}$ (K_0=44.02°)	0.868	1.666	3.858	8.25	15.27	23.27	27.16
Diff. obs. and comp. $\mathfrak{R}$	2.3%	0.2%	0.6%	0.4%	−1.0%	−0.2%	0.9%

	Θ=15°	20°	25°	30°	35°	40°	45°
				E=2105 kev			
$\mathfrak{R}$ from HKPP	0.993	2.098	4.95	10.54	19.98	29.1	35.0
Corrections	.601%	0.601%	0.601%	0.601%	0.601%	0.601%	0.601%
Final $\mathfrak{R}$	.999	2.110	4.98	10.60	20.10	29.3	35.2
$\mathfrak{R}$ (K_0=46°)	.963	2.058	4.926	10.584	19.562	29.75	34.72
$\mathfrak{R}$ (K_0=47°)	.986	2.142	5.144	11.046	20.403	31.02	36.18
K_0 from $\mathfrak{R}$		46.62°	46.25°	46.03°	46.64°	45.64°	46.40°
Mean K_0 from Θ=30°, 35°, 40°, 45°=46.18°							
$\mathfrak{R}$ (K_0=46.18°)	.967	2.073	4.965	10.667	19.714	29.98	34.98
Diff. obs. and comp. $\mathfrak{R}$	3.3%	1.7%	0.3%	−0.6%	2.0%	−2.3%	0.9%

	Θ=15°	20°	25°	30°	35°	40°	45°
				E=2392 kev			
$\mathfrak{R}$ from HKPP	1.124	2.51	6.17	13.31	24.4	37.4	42.9
Corrections	0.604%	0.604%	0.604%	0.511%	0.511%	0.511%	0.604%
Final $\mathfrak{R}$	1.131	2.52	6.21	13.38	24.5	37.6	43.2
$\mathfrak{R}$ (K_0=47°)	1.055	2.428	5.924	12.76	23.54	35.77	41.71
$\mathfrak{R}$ (K_0=48°)	1.083	2.524	6.173	13.29	24.51	37.21	43.37
K_0 from $\mathfrak{R}$		47.96°	48.15°	48.17°	47.99°	48.27°	47.90°
Mean K_0 from Θ=30°, 35°, 40°, 45°=48.08°							
$\mathfrak{R}$ (K_0=48.08°)	1.085	2.532	6.193	13.33	24.59	37.33	43.50
Diff. obs. and comp. $\mathfrak{R}$	4.2%	−0.47%	0.44%	0.37%	−0.37%	0.72%	−0.69%

corrections at this angle are greater than this amount and the evidence regarding higher phase shifts at these energies is thus unaffected. At 880 kev somewhat larger effects are produced. But even here they are practically negligible giving 0.3 percent at 20°, 0.17 percent at 25°, 0.06 percent at 30°. Inasmuch as one expects the effects of higher phase shifts to increase with energy, these effects at 880 kev have little interest. According to Table VI the values of the "Mean K_0" would increase by ~0.04° at 860 kev, ~0.08° at 1830 kev and ~0.10° at 2400 kev. Such changes will affect the magnitude of the interaction by ~0.01 Mev for a "square well" of depth 10.5 Mev or ~0.1 percent and will shorten the range of force by an amount corresponding to an increase of α in $Ae^{-\alpha r^2}$ by less than 0.2. The fit to the data by a fixed potential cannot be made consistently to this degree of precision and such a small effect in the range is of little interest. The difference between the values obtained by the "current time" and "air condenser" methods is seen to be insignificant and the values obtained by the latter will be disregarded from now on.

In Table XII the data of Heydenburg, Tuve and Hafstad are analyzed. The arrangement is similar to that used in Table XI. The table has three sections for 670, 776 and 867 kev, respectively. The observations of HHT have been made at scattering angles differing by 2.5° from Θ=20° to Θ=45°. The observed values of $\mathfrak{R}$ have been plotted by HHT on a large scale and smooth curves against scattering angle have been drawn by them. The numbers in the first row for each voltage in Table XII have been obtained from

these curves. These numbers are then increased by 0.43 percent so as to reduce the units to those used in Eq. (3.4). Since the acceleration of gravity is different in Washington from that in Madison the 0.43 percent takes into account this difference also. The value of the mean phase shift in Table XII was computed as the arithmetic mean of the values calculated from $\Theta=30°$, 35°, 40°, 42.5°, 45°. In other respects this table is just like Table XI. The percentage difference of observed and computed $\mathfrak{R}$ will be discussed after a consideration of the geometrical corrections.

Corrections due to geometry of apparatus.—It is seen that in all cases the experimental value of $\mathfrak{R}$ for $\Theta=15°$ is higher than the computed number by two percent or more. If the scattering yield into the infinitesimal angular range is $f(\Theta)d\Theta$ and if the actual spread is $\Delta\Theta$ then

$$\int_{\Theta_0-\Delta\Theta/2}^{\Theta_0+\Delta\Theta/2} f(\Theta)d\Theta/f(\Theta_0)\Delta\Theta \cong 1+(\Delta\Theta)^2 f''(\Theta_0)/24f(\Theta_0)$$

gives the ratio of the yield which should be observed to that which would be expected from the scattering at the average angle Θ_0 through the scattering range $\Delta\Theta$. If $f(\Theta)$ is approximated by const/Θ^5 we may expect the experimental values of $f(\Theta_0)$, omitting the correction for f'', to be too high by the factor

$$1+(5/4)(\Delta\Theta/\Theta)^2.$$

In order to account for the systematic deviations from expectation at $\Theta=15°$ without using higher phase shifts this factor must be 1.033 which calls for $\Delta\Theta=2.4°$. For a defining slit of the analyzing system 1.07 mm wide (slit A, Fig. 3 of paper by Herb, Kerst, Parkinson and Plain) placed 28.2 mm from the hole of the counter each point of the hole receives protons through an angular range of 2.2° which is of the correct order of magnitude to account for the observed effect. Since the average scattering angle is different for different points in the hole the correction may be expected to be larger than the above amount. On the other hand, some of the scattering angles responsible for the protons received have the same values for different points of the diaphragm.

The geometrical corrections have been worked out approximately on the assumption that the velocities of all the protons in the incident beam are parallel to each other and perpendicular to the edge of the slit of the analyzing system. This assumption does not correspond to fact com-

TABLE XII. *Phase shift analysis of data of Heydenburg, Hafstad and Tuve.*

	$\Theta=20°$	25°	30°	35°	40°	42.5°	45°
				$E=670$ kev			
$\mathfrak{R}$ from HHT	0.654	0.600	0.730	0.980	1.330	1.482	1.545
Corrections	.43%	.43%	.43%	.43%	0.43%	0.43%	0.43%
Final $\mathfrak{R}$	.657	.603	.733	.984	1.336	1.488	1.552
$\mathfrak{R}$ (K_0=24°)	.653	.600	.669	.899	1.223	1.347	1.393
$\mathfrak{R}$ (K_0=25°)	.652	.615	.721	1.010	1.406	1.555	1.611
K_0 from $\mathfrak{R}$		24.20°	25.21°	24.77°	24.62°	24.68°	24.73°
Mean K_0 from Θ=30°, 35°, 40°, 42.5°, 45°=24.80°							
$\mathfrak{R}$ (K_0=24.80°)	.652	0.612	0.711	0.988	1.369	1.513	1.567
Diff. obs. and comp. $\mathfrak{R}$	0.8%	−1.5%	+3.1%	−0.4%	−2.4%	−1.7%	−1.0%

	$\Theta=20°$	25°	30°	35°	40°	42.5°	45°
				$E=776$ kev			
$\mathfrak{R}$ from HHT	0.705	0.738	1.078	1.584	2.284	2.580	2.722
Corrections	.43%	.43%	0.43%	0.43%	0.43%	0.43%	0.43%
Final $\mathfrak{R}$	.708	.741	1.083	1.591	2.294	2.591	2.734
$\mathfrak{R}$ (K_0=27°)	.653	.698	0.976	1.550	2.275	2.542	2.641
$\mathfrak{R}$ (K_0=28°)	.657	.727	1.058	1.717	2.540	2.842	2.954
K_0 from $\mathfrak{R}$		28.44°	28.30°	27.25°	27.07°	27.16°	27.30°
Mean K_0 from Θ=30°, 35°, 40°, 42.5°, 45°=27.42°							
$\mathfrak{R}$(K_0=27.42°)	.651	0.710	1.010	1.620	2.386	2.668	2.773
Diff. obs. and comp. $\mathfrak{R}$	8.8%	4.4%	7.2%	−1.8%	−3.8%	−2.9%	−1.4%

	$\Theta=20°$	25°	30°	35°	40°	42.5°	45°
				$E=867$ kev			
$\mathfrak{R}$ from HHT	0.738	0.852	1.360	2.324	3.360	3.808	4.008
Corrections	.43%	.43%	0.43%	0.43%	0.43%	0.43%	0.43%
Final $\mathfrak{R}$	.741	.856	1.366	2.334	3.374	3.824	4.025
$\mathfrak{R}$ (K_0=29°)	.671	.816	1.300	2.209	3.315	3.717	3.866
$\mathfrak{R}$ (K_0=30°)	.680	.857	1.407	2.422	3.650	4.093	4.259
K_0 from $\mathfrak{R}$		29.98°	29.62°	29.59°	29.18°	29.40°	29.40°
Mean K_0 from Θ=30°, 35°, 40°, 42.5°, 45°=29.41°							
$\mathfrak{R}$ (K_0=29.41°)	.675	0.833	1.344	2.296	3.452	3.871	4.027
Diff. obs. and comp. $\mathfrak{R}$	9.8%	2.8%	1.6%	1.7%	−2.3%	−1.2%	0.05%

pletely but the divergence of the beam is difficult to estimate. The corrections for a very narrow proton beam will be considered first and the effect of the width of the beam will be taken into account later. In Fig. 1 the hole in front of the ionization chamber (hole c of paper by Herb *et al.*) is in the plane OXY. The plane OXZ is perpendicular to the slit face and goes midway between the slit edges. The Y axis is made parallel to the slit edges and the Z axis is made to intersect the beam. The element dS receives from the element dB

$$Nn\sigma(\Theta)R^{-2}\cos\chi dSdB = Nn\sigma(\Theta)\cos\chi dSd\Theta/R\sin\Theta \quad (7)$$

protons, where N is the number of protons that passed in the beam, n is the number of protons per unit volume in the scattering gas, $\sigma(\Theta)$ is the scattering cross section per unit solid angle, R is the distance between dS and dB and χ is the angle between the normal to dS and R. The $d\Theta$ is the change in Θ for fixed dS which corresponds to the change dB. The scattering angle for the point $P(B=0)$ is called Θ_0 and the distance $PO=R_0$. The slit width will be called $2b$. In the figure scattered protons pass just under the upper slit edge. One has

$$\begin{aligned}\cos\chi &= (R_0-B\cos\Theta_0)/R,\\ R^2 &= (R_0-B\cos\Theta_0)^2+y^2\\ &\quad +(x-B\sin\Theta_0)^2,\\ R^2\sin^2\Theta &= (R_0\sin\Theta_0-x\cos\Theta_0)^2+y^2, \qquad (7.1)\\ B &= R_0\cos\Theta_0+x\sin\Theta_0\\ &\quad -(\cos\Theta/\sin\Theta)[(R_0\sin\Theta_0\\ &\quad -x\cos\Theta_0)^2+y^2]^{\frac{1}{2}},\end{aligned}$$

where (x, y) are the coordinates of dS. The limits of integration for B are given by

$$\frac{x-B\sin\Theta_0}{R_0-B\cos\Theta_0}=\frac{x\mp b}{\mathfrak{h}}.$$

Letting

$$\xi=\Theta-\Theta_0, \quad \mathfrak{c}_0=\cos\Theta_0, \quad \mathfrak{s}_0=\sin\Theta_0$$

one finds the approximate expansions valid to second-order quantities in x, y, ξ

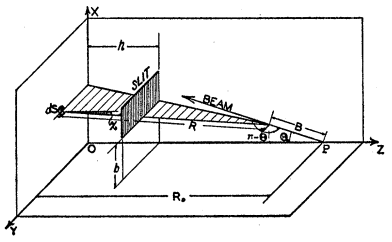

FIG. 1. Geometrical relations for the analyzing system. The slit is slit A of Fig. 3 of paper of HKPP. Element of area dS is in the plane of the round hole in front of ionization chamber. The direction of scattered protons is shown for special case of just missing the slit edge. Angle χ is formed by normal to dS and distance R.

$$B=\frac{x}{\mathfrak{s}_0}-\frac{y^2\mathfrak{c}_0}{2R_0\mathfrak{s}_0}+\xi\left(\frac{R_0}{\mathfrak{s}_0}-\frac{x\mathfrak{c}_0}{\mathfrak{s}_0^2}\right)-\frac{\xi^2 R_0\mathfrak{c}_0}{\mathfrak{s}_0^2},$$

$$\frac{R_0-B\cos\Theta_0}{R^2\sin\Theta}=\frac{1}{R_0\mathfrak{s}_0}\left(1+\frac{x\mathfrak{c}_0}{R_0\mathfrak{s}_0}+\frac{x^2\mathfrak{c}_0^2}{R_0^2\mathfrak{s}_0^2}+\frac{\mathfrak{c}_0^2-2}{2R_0^2\mathfrak{s}_0^2}y^2-\frac{\xi^2}{2}\right),$$

and for the limits of ξ corresponding to the slit edges

$$\xi=\frac{-x\pm b}{\mathfrak{h}}+\frac{\mathfrak{c}_0 y^2}{2R_0^2\mathfrak{s}_0}.$$

In these expansions, powers of ξ, x, y higher than the second are neglected. Expanding σ in powers of ξ and integrating over dS one obtains for the number of protons received

$$\begin{aligned}&\frac{Nn}{R_0\mathfrak{s}}A\sigma(\Theta_0)\frac{2b}{\mathfrak{h}}\Big\{1+\frac{\mathfrak{c}_0 x_{Av}}{\mathfrak{s}_0R_0}+\frac{\mathfrak{c}_0^2(x^2)_{Av}}{\mathfrak{s}_0^2R_0^2}\\ &+\frac{\mathfrak{c}_0^2-2}{2R_0^2\mathfrak{s}_0^2}(y^2)_{Av}-\frac{b^2}{6\mathfrak{h}^2}+\frac{(x^2)_{Av}}{2\mathfrak{h}^2}\\ &+\frac{\sigma'(\Theta_0)}{\sigma(\Theta_0)}\left[-\frac{x_{Av}}{\mathfrak{h}}+\frac{\mathfrak{c}_0(y^2)_{Av}}{2\mathfrak{s}_0R_0^2}-\frac{\mathfrak{c}_0(x^2)_{Av}}{\mathfrak{s}_0R_0\mathfrak{h}}\right]\\ &+\frac{\sigma''(\Theta_0)}{\sigma(\Theta_0)}\left(\frac{b^2}{6\mathfrak{h}^2}+\frac{(x^2)_{Av}}{2\mathfrak{h}^2}\right)\Big\}. \qquad (7.2)\end{aligned}$$

For a circular hole of radius a, $(x^2)_{Av}=(y^2)_{Av}=a^2/4$. The terms in x_{Av} can be eliminated by setting the counting system in symmetric positions with respect to the incident beam and using the mean of the counts so obtained. In the experiments of

Herb *et al.* the mean direction of the beam was determined by finding by trial the two positions or orientations of the collector system with $\Theta=15°$ for which the scattering is the same. Protons scattered symmetrically with respect to this direction were counted and their mean was used. This procedure admits of simultaneous errors due to slightly incorrect Θ_0 and due to the presence of x_{Av}. Since counts to both sides of the beam have been used the first-order effects of these errors disappear. If we write

$$\sigma(\Theta_0)\{1+\cdots\}=\boldsymbol{\sigma}(\Theta_0)+f(\Theta_0)x_{Av}+g(\Theta_0)$$

the error ϵ in the determination of the beam direction for 15° scattering is found from

$$\boldsymbol{\sigma}(\Theta_0+\epsilon)+f(\Theta_0+\epsilon)x_{Av}=\boldsymbol{\sigma}(\Theta_0-\epsilon)-f(\Theta_0-\epsilon)x_{Av}.$$

Denoting the argument Θ_0 by subscript zero this gives sufficiently accurately

$$\epsilon=-x_{Av}f_0/\boldsymbol{\sigma}_0',$$

where differentiation is denoted by the prime. For low Θ_0 Rutherford's formula can be used and one has approximately

$$\epsilon=(x_{Av}/\mathfrak{h})(1+\mathfrak{h}/4R_0),$$

so that with the dimensions of the apparatus used by Herb *et al.*, $\epsilon\leqq-0.23°$ for $x_{Av}=0.1$ mm. The mean of the counts for settings $\Theta_1\pm\epsilon$ is to within second-order quantities

$$\boldsymbol{\sigma}_1+g_1+\tfrac{1}{2}\boldsymbol{\sigma}_1''\epsilon^2+x_{Av}f_1\epsilon.$$

The fractional error introduced by x_{Av} and ϵ is thus

$$\delta=\frac{f_0^2}{\boldsymbol{\sigma}_0'^2}x_{Av}^2\left[\frac{\boldsymbol{\sigma}_1''}{2\boldsymbol{\sigma}_1}-\frac{\boldsymbol{\sigma}_0'f_1'}{\boldsymbol{\sigma}_1f_0}\right]$$

with

$$f=\boldsymbol{\sigma}\mathbf{c}/R_0\mathbf{s}-\boldsymbol{\sigma}'/\mathfrak{h}.$$

Substituting this into the expression for δ one obtains

$$\delta=\frac{x_{Av}^2}{\mathfrak{h}^2}\left(\frac{\boldsymbol{\sigma}_0\mathbf{c}_0\mathfrak{h}}{\boldsymbol{\sigma}_0'\mathbf{s}_0R_0}-1\right)^2\left\{\frac{\boldsymbol{\sigma}_1''}{2\boldsymbol{\sigma}_1}-\left[\frac{\mathfrak{h}}{R_0}\left(\frac{\boldsymbol{\sigma}_1'\mathbf{c}_1}{\boldsymbol{\sigma}_1\mathbf{s}_1}-\frac{1}{\mathbf{s}_1^2}\right)-\frac{\boldsymbol{\sigma}_1''}{\boldsymbol{\sigma}_1}\right]\Big/\left(\frac{\boldsymbol{\sigma}_0\mathbf{c}_0\mathfrak{h}}{\boldsymbol{\sigma}_0'\mathbf{s}_0R_0}-1\right)\right\}. \quad (7.3)$$

The value used in the experiments is $\Theta_0=15°$. On account of the smallness of this angle the approximations $\boldsymbol{\sigma}_0'/\boldsymbol{\sigma}_0=-4/\Theta_0$, $\mathbf{c}_0/\mathbf{s}_0=1/\Theta_0$ are good enough. One then has

$$1-\boldsymbol{\sigma}_0\mathbf{c}_0\mathfrak{h}/\boldsymbol{\sigma}_0'\mathbf{s}_0R_0=1+\mathfrak{h}/4R_0.$$

If, in addition, the angle Θ_1 is also sufficiently small to make the scattering approximately Rutherfordian and to have $\mathbf{c}_1/\mathbf{s}_1=1/\Theta_1$, then one has

$$\delta=-10(x_{Av})^2\mathfrak{h}^{-2}(1+\mathfrak{h}/4R_0)^2\Theta_1^{-2}. \quad (7.4)$$

For $\Theta_1=15°$, $x_{Av}=1$ mm, $\mathfrak{h}=28.2$ mm this formula gives $\delta=-0.23$ percent. If x_{Av} is ~0.1 mm the experimental values must be raised, therefore, by about 0.2 percent and by about 0.1 percent at $\Theta_1=20°$ at the lower energies for which scattering at this angle is still roughly following Rutherford's formula. For angles close to 45° the scattering is approximately spherically symmetric and is very nearly so at higher energies. In this region the cross section can be approximated by

$$\boldsymbol{\sigma}=K\mathbf{c},$$

where K is independent of the angle. With this approximation the general formula for δ gives for the large scattering angles

$$\delta=\frac{(x_{Av})^2}{\mathfrak{h}^2}\left(1+\frac{\mathfrak{h}}{4R_0}\right)^2\times\left\{-\frac{1}{2}+\left[1-\frac{\mathfrak{h}}{R_0}\left(1+\frac{1}{\mathbf{s}_1^2}\right)\right]\Big/\left(1+\frac{\mathfrak{h}}{4R_0}\right)\right\}. \quad (7.5)$$

For $\Theta_1=45°$, $x_{Av}=0.1$ mm one obtains on substitution the quite negligible error $-0.001(5)$ percent. This estimate is not very accurate because the approximation $\boldsymbol{\sigma}=K\mathbf{c}$ is not very good for the calculation of $\boldsymbol{\sigma}''/\boldsymbol{\sigma}$. Graphs of $\boldsymbol{\sigma}$ as a function of Θ indicate that it is correct as to order of magnitude. Checks on the mechanical construction made by Herb *et al.* after the scattering measurements showed that $x_{Av}\sim0.01$ mm which decreases this error by 1/100.

Most of the quadratic terms in Eq. (7.2) have negligible values for the experimental arrangement. With $R_0=56$ mm, $\mathfrak{h}=28.2$ mm, $a=0.365$ mm, $b=0.536$ mm $\Theta_0=15°$ the values of the terms are in order of occurrence in Eq. (7.2)

$$\mathbf{c}_0^2a^2/4\mathbf{s}_0^2R_0^2=0.000148=0.015 \text{ percent};$$

$$a^2(\mathbf{c}_0^2-2)/8R_0^2\mathbf{s}_0^2=-0.008 \text{ percent};$$

$$-b^2/6\mathfrak{h}^2=-0.006 \text{ percent};$$

$$-a^2/8\mathfrak{h}^2=-0.002 \text{ percent}.$$

Approximating $\boldsymbol{\sigma}_0'/\boldsymbol{\sigma}_0$ by $-4/\Theta_0$ and $\boldsymbol{\sigma}_0''/\boldsymbol{\sigma}_0$ by $20/\Theta_0^2$ one has also

$$\frac{\boldsymbol{\sigma}_0'\mathbf{c}_0}{\boldsymbol{\sigma}_0\mathbf{s}_0}\left(\frac{a^2}{8R_0^2}-\frac{a^2}{4R_0\mathfrak{h}}\right)=0.090 \text{ percent};$$

$$\frac{\boldsymbol{\sigma}_0''}{\boldsymbol{\sigma}_0}\left(\frac{b^2}{6\mathfrak{h}^2}+\frac{a^2}{8\mathfrak{h}^2}\right)=2.35 \text{ percent}.$$

The last correction is the largest. It represents the effect of the curvature of the plot of $\boldsymbol{\sigma}$ against Θ which was discussed qualitatively by means of the approximate formula

$$1+(5/4)(\Delta\Theta/\Theta)^2.$$

The sum of the above corrections is 2.4 percent. The observed scattering may be expected to be too high by this amount for the geometry used at $\Theta=15°$ if the incident proton beam is very narrow and if the correction δ due to a possible dissymmetry of the counter hole and counter slit is negligible. For small scattering angles at low energies this error is approximately proportional to the inverse square of the scattering angle. For high energies the scattering differs markedly from Rutherford's even at $\Theta=20°$ and the correction term $(\boldsymbol{\sigma}_0''/\boldsymbol{\sigma}_0)(b^2/6\mathfrak{h}^2+a^2/8\mathfrak{h}^2)$ is then much smaller than at $\Theta=15°$. If $\boldsymbol{\sigma}$ is plotted against Θ for $K_0=47.95°$ at 2392 kev, $K_0=43.92°$ at 1830 kev, $K_0=29.25°$ at 860 kev and $\boldsymbol{\sigma}''/\boldsymbol{\sigma}$ is estimated graphically at $\Theta=20°$ the correction term $(\boldsymbol{\sigma}_0''/\boldsymbol{\sigma}_0)(b^2/6\mathfrak{h}^2+a^2/8\mathfrak{h}^2)$ is estimated to be at this angle 0.2 percent at 2392 kev, 0.6 percent at 1830 kev, 1.4 percent at 860 kev.

On account of the finite width of the beam there are additional corrections which will now be estimated. Fixed coordinates X, Y will be used in the plane of the hole with origin at the foot of the perpendicular from the center of the beam as shown in Fig. 2. The filaments in the beam will be specified by coordinates α, β with β parallel to Y and α in the direction shown in the figure. The distance from the hole to the center of the beam will be called $\check{r}$. The distance from the point P to the hole will be called R_0. The point P is the intersection of the beam filament with the plane perpendicular to the slit face and passing midway between the slit jaws. The central filament of the beam is AB. The filament over which averaging is performed is PQ. Eq. (7.2) will be averaged over different positions of PQ by letting

$$x=X, \quad y=Y-\beta, \quad R_0=\check{r}+\alpha/\sin\Theta_0.$$

The averaging will be carried out on the assumption that the center of the beam is in line with the center of the hole. The effect of lack of such alignment is partially taken care of in the discussion of δ. The cross section of the beam will be supposed to be circular of radius $\dot{\rho}$ and the proton density will be supposed to be uniform within this cross section. One has

$$(1/R_0)_{\text{Av}}=1/\check{r}+(\alpha^2)_{\text{Av}}/(\check{r}^3\sin^2\Theta_0)$$
$$=1/\check{r}+\dot{\rho}^2/(4\check{r}^3\sin^2\Theta_0).$$

This introduces the fractional error

$$\dot{\rho}^2/(4\check{r}^2\sin^2\Theta_0).$$

For $\dot{\rho}=1.25$ mm, $\check{r}=56$ mm at $\Theta_0=15°$ it is $0.00184=0.18$ percent but for $\dot{\rho}=2.50$ mm it is 0.72 percent. In addition corrections arise from an increase in the averaged $(y^2)_{\text{Av}}$. One has

$$(y^2)_{\text{Av}}=(Y^2)_{\text{Av}}+(\beta^2)_{\text{Av}}=(a^2+\dot{\rho}^2)/4.$$

On account of the extra term in $\dot{\rho}^2/4$ there is the additional fractional error

$$\frac{\mathbf{c}_0^2-2}{8r^2\mathbf{s}_0^2}\dot{\rho}^2+\frac{\boldsymbol{\sigma}_0'\mathbf{c}_0\dot{\rho}^2}{8\boldsymbol{\sigma}_0\mathbf{s}_0\check{r}^2}.$$

With the above values of $\dot{\rho}$, $\check{r}$, Θ_0 the first term is -0.10 percent for $\dot{\rho}=1.25$ mm, -0.40 percent for $\dot{\rho}=2.50$ mm; the second term using the approximation $\boldsymbol{\sigma}_0'/\boldsymbol{\sigma}_0=-4/\Theta_0$ is -0.4 percent for $\dot{\rho}=1.25$ mm and -1.4 percent for $\dot{\rho}=2.50$ mm. For the larger of these beam widths the total error at $\Theta_0=15°$ due to beam width is -0.90 percent and for the smaller beam width it is -0.28 percent. Since the beam width is not accurately known it is impossible to set close limits on this error.

The major part of the negative error caused by beam width is due to the term in $\boldsymbol{\sigma}_0'/\boldsymbol{\sigma}_0$. It is

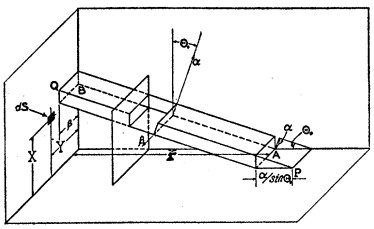

FIG. 2. Geometrical relations used for estimating effect of width of incident beam. Coordinate system α, β is used for designating different filaments of the beam. Coordinate system X, Y describes position of dS.

a result of the increase in the average scattering angle caused by the lateral extension of the proton stream. For high energies σ_0'/σ_0 at $\Theta_0=20°$ is much less than it would be on Rutherford's formula and this part of the error is correspondingly smaller. The value of σ_0'/σ_0 was estimated graphically. One obtains in this way the values given in Table XIII.

The numbers in the column under "sum" should be compared with values of $(\sigma_0''/\sigma_0)\times(b^2/6\hbar^2+a^2/8\hbar^2)$ which are 0.2 percent at 2392 kev, 0.6 percent at 1830 kev, 1.4 percent at 860 kev for $\Theta=20°$ and 2.3 percent for $\Theta=15°$. The net expected error due to the above causes may be thus expected to be between one percent and two percent for $\Theta=15°$.

The divergence of the incident proton beam also introduces an error the order of magnitude of which will now be estimated. The finiteness of the angular opening of the analyzing system will be neglected and the beam will be supposed to be very narrow. The angle made by the direction of protons which are being counted with the mean direction before scattering will be called Θ_0. The angle between the mean direction of the beam and the line of motion of the proton before scattering will be called θ. One finds discarding effects of higher order than the second in θ for an axially symmetric beam that

$$(\sigma/\mathbf{s})_{Av}=(\sigma_0/\mathbf{s}_0)+((\theta^2)_{Av}/4)\times[(\mathbf{c}_0/\mathbf{s}_0)(\sigma/\mathbf{s})_0'+(\sigma/\mathbf{s})''].$$

If the foil in front of the first hole of the collimating system acts as a source of protons then the chance of protons leaving an element of area in the foil and passing through an element of area of the last hole of the collimating system is nearly proportional to the product of these elements of area. Introducing rectangular coordinates $(x_1, y_1)(x_2, y_2)$ in the foil and in the last hole with origins on the axis of symmetry one has

$$\theta^2=[(x_1-x_2)^2+(y_1-y_2)^2]/L^2,$$

where L is the distance between the foil and the last hole. By averaging this expression over the two circles it is seen that

$$(\theta^2)_{Av}=(\theta_1^2+\theta_2^2)/2,$$

where

$$\theta_1=a_1/L, \quad \theta_2=a_2/L$$

with a_1, a_2 standing for the radii of first and last hole of the collimating system. The angle θ_1 is subtended by the radius of one hole at a point in the other hole. For small scattering angles one obtains thus approximating σ by const./Θ^4

$$(\sigma/\mathbf{s})_{Av}/(\sigma/\mathbf{s})_0=1+25(\theta_1^2+\theta_2^2)/8\Theta^2.$$

TABLE XIII. *Errors due to beam width.*

ρ	Θ_0	$\frac{\rho^2}{4r^2\mathbf{s}_0^2}$	$\frac{\mathbf{c}_0^2-2}{8r^2\mathbf{s}_0^2}\rho^2$	$\frac{\sigma_0'\mathbf{c}_0\rho^2}{8\sigma_0\mathbf{s}_0r^2}$	SUM	E (KEV)
1.25 mm	15°	0.18%	−0.10%	−0.36%	−0.28%	2392 1830 860
2.50 mm	15°	.72%	− .40%	−1.42%	−1.1%	2392 1830 860
1.25 mm	20°	.11%	− .06%	−0.02% − .05% − .17%	0.03% .00% − .12%	2392 1830 860
2.50 mm	20°	.42%	− .24%	− .09% − .20% − .69%	.09% − .02% − .51%	2392 1830 860

With $a_1=1.08$ mm, $a_2=1.40$ mm, $L=15$ cm, the measurements should be too high, because of the divergence of the beam, according to the above formula by 0.6(3) percent at $\Theta=15°$. It may be, however, that the original direction of the beam is partly preserved. If so, the above estimate is an upper limit to the error.

It should finally be mentioned that deviations of the incident beam from the plane of the scattering chamber may increase the scattering angle and decrease the yield. Professor Herb has estimated the magnitude of this error and finds it to be negligible.

It is a pleasure to acknowledge our indebtedness to Professor Herb for discussions concerning the construction and operation of the apparatus which have helped in the work of this section. Dr. S. S. Share has kindly checked the geometrical relations and other formulas.

Possible presence of p and d wave anomalies. Upper limits for their effect on K_0.—The geometrical corrections just discussed appear to be sufficiently large to account for the consistently too high values at $\Theta=15°$. For $K_1=-0.04=-2.29°$ one expects the following contributions to $\mathfrak{R}$ listed in Table XIV. The largest effects in $\mathfrak{R}$ are seen to be for $\Theta=30°$. It appears fair to claim that at 2392 kev the observations indicate a scattering agreeing within two percent with prediction in the vicinity of $\Theta=25°$ when only an s wave anomaly is used. This sets a provisional upper limit of $(0.123/1.03)2.29°=0.27°$ on $|K_1|$ at 2400 kev. At 1830 kev an upper limit of two percent in scattering at $\Theta=25°$ gives $(0.0772/0.87)2.29°=0.20°$ as the upper limit of $|K_1|$. At 860 kev it appears safer to claim three percent which gives $(0.0243/0.55)2.29°=0.10°$ for the upper limit. The data of HHT shown in Table XII indicate the possible presence of an excess of actual scattering from $\Theta=20°$ to $\Theta=30°$ over that expected for a pure s anomaly. The order of magnitude of the excess in $\mathfrak{R}$ at this angle at 800 kev is from Table XII, 0.050 which corresponds roughly to $K_1=-0.2°$. It appears to be premature, however, to conclude that this is a real effect because at $\Theta=40°$ the experimental values are below the values expected using only K_0. Since no such effect is apparent in the data of HKPP and since its theoretical explanation would require a somewhat complicated superposition of effects due to p and d waves it appears simplest at present to reserve judgment as to its origin. It is planned to analyze the data of HHT using observed counts rather than graphically interpolated values and to eliminate in this way personal judgment present in the above analysis. The geometrical effects are more difficult to estimate in the apparatus of HHT since settings at $\pm\Theta$ were not taken for each point so that first-order effects in x_{Av} could remain. It should be noted that it is not easy to distinguish with the present experimental accuracy the effects of K_1 from those of K_2 and that the effects of K_2 can be very important for the final conclusions about the range of force if K_2 is large enough. In Table XV is shown the effect of K_2 at 2400 kev. In the first row (I) are listed the values of the change in the ratio to Mott $(\Delta\mathfrak{R})_2=(\Delta\mathbf{P})_2/\mathbf{P}_M$ due to $K_2=1°$ for $K_0=48°$. In the second row (II) are listed the values of $1+(\Delta\mathbf{P})_0/(\Delta\mathbf{P}_M)=\mathfrak{R}_0$ which would be the ratios to Mott if this K_2 were absent. The sum of the numbers in rows I and II is the expected ratio to Mott for $K_0=48°$, $K_2=1°$. The third row contains values of the ratio to Mott for $K_0=45.349°$, $K_2=0$. This value of K_0 was taken so as to give a value of $\mathfrak{R}$ for $\Theta=45°$ equal to that for $K_0=48°$, $K_2=1°$. The angular distribution of $\mathfrak{R}$ expected for $K_0=45.349°$ differs relatively little from that for $K_0=48°$, $K_2=1°$. The difference between the values of $\mathfrak{R}$ that would hold for $K_0=48°$, $K_2=1°$ and those for $K_0=45.349°$, $K_2=0$ is recorded in the last row of the table. Comparison of these numbers with those in the second row of Table XIV shows that deviations from the angular distribution expected for s scattering are rather similar for small K_1 and K_2. Allowing for a deviation of two percent from scattering expected for a pure s anomaly for $\Theta=25°$ at 2400 kev one would set an upper limit on $|K_2|$ of $(0.123/0.81)°=0.15°$ which according to line I of Table XV would

TABLE XIV. *Contributions to* $\mathfrak{R}=\mathbf{P}/\mathbf{P}_M$ *due to phase shift* $K_1=-2.29°$.

E (KEV)	$\Theta=15°$	20°	25°	30°	35°	40°	45°
2400	0.45	0.77	1.03	1.10	0.82	0.30	0
1830	0.39	0.65	0.87	0.92	0.69	0.25	0
800	0.25	0.41	0.53	0.55	0.41	0.15	0

limit the error in $1+(\Delta\mathfrak{R})_0$ at $\Theta=45°$ to $\pm0.6(7)$ or ±1.5 percent in scattering. According to Table VI the value of K_0 would be in error by $\pm0.4°$. Such an error would not affect seriously conclusions about the comparison of the proton-proton and proton-neutron interaction that are made below and it would only affect slightly conclusions about the range of force if this K_2 were present at 2400 kev but not at 860 kev. One expects K_2 to vary at least as fast as $E^{5/2}$. At 1000 kev the upper limit for $|K_2|$ is thus presumably $0.15°/(2.4)^{5/2}=0.017°$. At this energy $K_2=1°$ produces an effect of $-1.2(K_0=32°$, $K_2=1°)$ on the ratio to Mott at $\Theta=45°$ so that the expected error is $\sim\pm0.022$ in $\mathfrak{R}$ which $\sim\pm0.2$ percent in the scattering and causes a negligible error in this energy range.

In the above discussion Table XV was used. The effect of a finite change in $K_2(=1°)$ was computed for it. The changes in K_2 which have been considered for the discussion of experimental data are much smaller than 1°. The linear interpolation used may, therefore, be questioned. A calculation of

$$\left[\frac{\partial\mathfrak{R}}{\partial K_2}-\left(\frac{\partial\mathfrak{R}/\partial K_2}{\partial\mathfrak{R}/\partial K_0}\right)_{\Theta=45°}\frac{\partial\mathfrak{R}}{\partial K_0}\right]\delta K_2$$

shows that the last row of the table can be used for linear interpolation to obtain the effect of a very small K_2 to within a few percent. The last number (-4.41) in the first row is then taken place of by $(\partial\mathfrak{R}_0/\partial K_2)_{45°}/57.3=-4.53$ and is sufficiently accurate. At small scattering angles the above formula gives values about ten percent higher than the numbers in the first row. These, however, are not needed in the above discussion since the determination of K_0 relies on the scattering angles from 30° to 45°. Theoretical estimates of K_2 from the Gauss or exponential type of potential indicate that it is of the order of 0.01° at 2400 kev, i.e., roughly 0.1 of the value used above. If such estimates apply when constant potentials are used one may expect the effect on K_0 to be $\sim0.03°$ which is negligible in the applications made below.

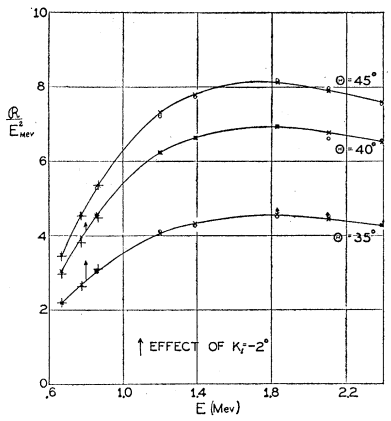

FIG. 3. Observed and computed scattering on assumption of pure s scattering anomaly for $\Theta=45°$, 40°, 35°. Ordinates give ratio to Mott divided by the square of the energy. Abscissae give the energy. Observations of HKPP are represented by circles; those of HHT by large upright crosses. The diagonal circles give values computed using the mean K_0 of Tables XI and XII. The effect of $K_1=-2°$ is roughly indicated by the length of the arrows.

In Figs. 3, 4 and 5 the agreement between expectation from a pure s scattering anomaly and observations can be seen in a different way. The curves are drawn for $\mathfrak{R}/E_{\text{Mev}}^2$ as ordinate and E_{Mev} as abscissae. The ordinate varies in nearly the same way with energy as the observed scattering. The curves are drawn through the diagonal crosses for which values of $\mathfrak{R}$ have been computed with the "mean K_0" derived from experiment and tabulated in the last column of Tables XI, XII. The circles represent the experimental points of Herb *et al.* and the upright large crosses are the experimental points of Tuve *et al.* There is a surprising absence of systematic deviations of the experimental points from the curves as one goes to higher energies indicating the probable correctness of the interpretation using a pure s scattering anomaly. In Fig. 3 the effect of $K_1=-2°$ is roughly indicated by the

TABLE XV. *Effect of K_2 at 2400 kev.*

K_0	K_2	$\Theta=15°$	20°	25°	30°	35°	40°	45°	
48°	1°	$(\Delta\mathfrak{R})_2=0.054$	0.165	0.148	−0.34	−1.63	−3.45	−4.41	I
48°	0	$\mathfrak{R}_0=1.085$	2.534	6.20	13.34	24.59	37.35	43.52	II
45.349°	0	$\mathfrak{R}_0=1.014$	2.279	5.54	11.94	22.06	33.56	39.11	III
		0.12	0.42	0.81	1.06	0.9	0.34	0.00	I+II−III

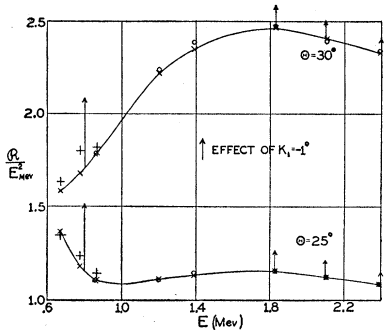

FIG. 4. Observed and computed scattering on assumption of pure s scattering anomaly for $\Theta=30°$, 25°. Notation is the same as in Fig. 3. The effect of $K_1=-1°$ is roughly indicated by the length of the arrows.

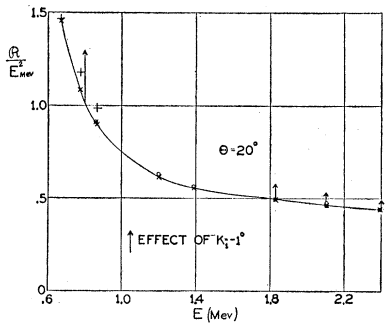

FIG. 5. Observed and computed scattering on assumption of pure s scattering anomaly for $\Theta=20°$. Notation is the same as in Fig. 3. The effect of $K_1=-1°$ is roughly indicated by the length of the arrows.

length of the arrow and in Figs. 4 and 5 the same is done for one-half of the effect of $K_1=-2°$ which is roughly the effect of $K_1=-1°$. The agreement between the two groups of experimenters is seen to be very good for the scattering angles 45°, 40°, 35° but at 30°, 25°, 20° the observations made in Washington give higher values than those in Madison. The practice of averaging observations made at $+\Theta$ and $-\Theta$ which was followed by Herb *et al.* is an argument for assigning more weight to their measurements at the smaller angles. This leads to the cancellation of first-order errors as has been discussed under "geometrical corrections." The origin of the discrepancy is not known, however, and it would be desirable to have further observations on this point. The apparent absence of K_1 at the higher energies will be discussed again in the "Concluding Remarks."

III. Calculation of the Potentials

1. The proton-neutron interaction

The scattering cross section of slow neutrons by protons determines the interaction potential for the antiparallel spin orientation (^1S state) when account is taken of the scattering in the ^3S condition. The experimental material is complicated by the effect of chemical binding of the protons to other atoms in hydrogen containing substances. The Fermi correction[16] for this binding has been discussed by several authors and will not be gone into critically here. Even though its complete quantitative justification is doubtful, there is some experimental evidence for its approximate validity through measurements of the scattering cross section for neutrons having several volts energy. Thus Carroll and Dunning[17] obtain 6.59×10^{-24} cm^2 as the lower limit for the collision cross section of neutrons having zero energy while unpublished measurements of V. W. Cohen and H. H. Goldsmith[17] indicate that the collision cross section for the Rh band neutrons is 20×10^{-24} cm^2 which would change Carroll and Dunning's figure to 80×10^{-24} cm^2 if Fermi's factor four were applicable. The difference between 65.9 and 80×10^{-24} cm^2 is not of primary importance for the determination of the ^1S interaction and allowance will be made for such variations in the experimental results.

The scattering cross section of a zero energy neutron having a statistical spin orientation with a free proton will be called $\sigma_{\pi p}$. One has

$$4\sigma_{\pi p}=12\pi a_3^2+4\pi a_1^2. \tag{8}$$

Here the quantity a is the intercept on the axis of r of the tangent to the graph of F against r, where r is the distance between proton and neutron. The tangent is taken at a sufficiently large distance to make the interaction negligible. The radial function is F/r and the a's will be positive if the tangent cuts the axis to the left of the origin. The values of a for triplet and singlet states, respectively, are $a_3<0$, $a_1>0$. For

[16] E. Fermi, Ricerca Scient. **7**, II, 13 (1936); H. A. Bethe, Rev. Mod. Phys. **9**, 71 (1937); N. Arley, Proc. Danish Academy **16**, 1 (1938). We are indebted to Prof. Wigner for discussions concerning these questions.

[17] H. Carroll and J. R. Dunning, Phys. Rev. **54**, 541 (1938); V. W. Cohen and H. H. Goldsmith, Phys. Rev. **55**, 597(A) (1939).

$r>r_0$ the graph of F against r is a straight line so that r can be increased indefinitely without ambiguity in the meaning of a. One has

$$(Fdr/dF)_{r_0}=a+r_0. \tag{8.1}$$

Square wells.—For "square wells" the potential energy has the constant amount $-D$ for $r<r_0$ and is zero for $r>r_0$. For the triplet state one obtains

$$\begin{aligned}-\frac{D_3}{E_3}&=\frac{\pi^2}{4\chi^2}+\frac{2}{\chi}+1-\frac{4}{\pi^2}+\left(\frac{32}{\pi^4}-\frac{8}{3\pi^2}\right)\chi+\left(-\frac{320}{\pi^6}+\frac{32}{\pi^4}\right)\chi^2+\cdots\\&=\frac{2.4674}{\chi^2}+\frac{2}{\chi}+0.59472+0.05832\chi-0.00434\chi^2+\cdots,\end{aligned} \tag{8.2}$$

where

$$\chi=(-ME_3/\hbar^2)^{\frac{1}{2}}r_0, \tag{8.3}$$

which gives with the fundamental constants chosen

$$\chi=0.3126(r_0mc^2/e^2)(-E_3/mc^2)^{\frac{1}{2}}=0.4370(r_0mc^2/e^2)(-E_3/\text{Mev})^{\frac{1}{2}}.$$

The energy of the deuteron is denoted by $E_3(=-2.17$ Mev). For this value $\chi=0.643_8\, r_0mc^2/e^2$. The series of Eq. (8.2) is sufficiently accurate for the calculation of D_3 with known E_3 and assumed r_0 for values of $r_0\sim 2.8\times 10^{-13}$ cm. The intercept a_3 can be expressed as

$$a_3=-r_0[1+(\chi+c_2\chi^2+c_3\chi^3+\cdots)^{-1}]$$

with

$$c_2=\tfrac{1}{2},\quad c_3=\frac{2}{\pi^2}=0.20264,\quad c_4=-\frac{16}{\pi^4}+\frac{5}{2\pi^2}=0.08905;\quad c_5=0.0419.$$

This formula is good to about 0.2 percent for $r_0\sim e^2/mc^2$. One obtains

$$\begin{aligned}12\pi a_3^2&=12\pi(-\hbar^2/ME_3)[1+\chi+(3/4-2c_3)\chi^2+(c_3-2c_4)\chi^3+\cdots]\\&=3.058\times 10^{-23}(-mc^2/E_3)[1+\chi+0.34472\chi^2+0.02454\chi^3-0.0117\chi^4+\cdots]\ \text{cm}^2.\end{aligned} \tag{8.4}$$

The first two terms in the brackets have been given by Wigner.[18] For $r_0=e^2/mc^2$ the last two terms give nine percent of the first two. The terms omitted in the above formula for $12\pi a_3^2$ decrease its value by about 0.1 percent for $r_0\sim e^2/mc^2$ as is found from exact solutions.

For the singlet state one has to determine the depth D_1 from a knowledge of a_1 which results from the experimental $\sigma_{\pi\nu}$ and the computed $12\pi a_3^2$. With

$$\chi_1=r_0/(a_1+r_0) \tag{8.5}$$

one finds

$$z_1^2=\frac{M}{\hbar^2}D_1r_0^2=\frac{\pi^2}{4}-2\chi_1-\frac{4}{\pi^2}\chi_1^2+\left(\frac{8}{3\pi^2}-\frac{32}{\pi^4}\right)\chi_1^3+\left(-\frac{320}{\pi^6}+\frac{32}{\pi^4}\right)\chi_1^6+\cdots, \tag{8.6}$$

which becomes with the adopted choice of fundamental units

$$\begin{aligned}D_1&=5.233z_1^2(e^2/r_0mc^2)^2\ \text{Mev}\\&=5.233(2.4674-2\chi_1-0.40528\chi_1^2-0.05832\chi_1^3-0.00434\chi_1^4-\cdots)(e^2/r_0mc^2)^2\ \text{Mev}.\end{aligned} \tag{8.6'}$$

[18] E. Wigner, Zeits. f. Physik **83**, 253 (1933).

This series converges rapidly, the approximate value of χ_1 being 0.1. The third term in brackets is about 0.2 percent of the whole. The series has been checked by comparing the results with solutions obtained by means of trigonometric tables. The use of the above series is simple and convenient. The quantity χ_1 is positive for a virtual level since a_1 is positive. For a real and only slightly stable level χ_1 is negative.

The calculation of the depth of the square well which corresponds to a given value of the scattering cross section by means of Eqs. (8), (8.5), (8.6) is closely related to the customary use of the virtual level. The energy of the latter may be defined as a positive energy E_1 such that if the energy of the singlet state is $-E_1$ and if F is regular at $r=0$ then

$$dF/Fdr=(ME_1/\hbar^2)^{\frac{1}{2}};\quad (E=-E_1). \tag{8.7}$$

At zero energy (thermal neutrons) one has then approximately

$$dF/Fdr=(ME_1/\hbar^2)^{\frac{1}{2}}-Mr_0E_1/(2\hbar^2)=1/(a_1+r_0)$$

since $\partial/\partial E(\partial F/F\partial r)\sim -Mr_0/2\hbar^2$ when the phase at $r_0\sim\pi/2$. Hence

$$a_1\cong\hbar(ME_1)^{-\frac{1}{2}}-r_0/2$$

and

$$4\pi a_1^2=4\pi(\hbar^2/ME_1)[1-(ME_1/\hbar^2)^{\frac{1}{2}}r_0],$$

which is the customary formula for the scattering cross section in terms of E_1. It should be noted that in order to obtain this form it was necessary to assume that Eq. (8.7) holds at $E=-E_1$ and not at the energy of the virtual level.

The quantity χ_1 is related to E_1 in the present approximation by

$$\chi_1=r_0/(a_1+r_0)=r_0(ME_1)^{\frac{1}{2}}/\hbar-r_0^2ME_1/(2\hbar^2)$$

so that the depth D_1 is given by (see Eq. (8.6))

$$D_1=\frac{\pi^2\hbar^2}{4Mr_0^2}\left(1-\frac{8}{\pi^2}\chi_1+\cdots\right)=\frac{\pi^2\hbar^2}{4Mr_0^2}-\frac{4}{\pi}(E_1D_1)^{\frac{1}{2}}, \tag{8.8}$$

the latter form being directly obtainable[19] from the definition of E_1. Eq. (8.8), useful as it is for rapid estimates, is not quite accurate enough for the calculations needed here. On the other hand, Eq. (8.6′) is sufficiently accurate and avoids the introduction of a virtual level which is seen to be artificial when the range of force is of importance in the correction for range in the cross section.

Expansion for wells of any shape.—For the Gauss error potential the wave equation was solved by numerical integration. In order to have a check on the accuracy of the numerical work the values of the logarithmic derivative of the function needed in the determination of the proton-proton and proton-neutron potentials were checked against each other also by using a power series expansion. The method consists in obtaining a power series in $\kappa-\kappa_0$, $\lambda-\lambda_0$, $\mu-\mu_0$ for $dF/Fdx=y$ where F is the solution, regular at $x=0$, for

$$d^2F/dx^2+[\kappa+\lambda\varphi(x)+\mu\chi(x)]F=0. \tag{9}$$

Eliminating F one obtains the Riccati equation

$$dy/dx+y^2+\kappa+\lambda\varphi(x)+\mu\chi(x)=0.$$

[19] H. A. Bethe and R. F. Bacher, Rev. Mod. Phys. **8**, 82 (1936).

For fixed x the value of y is a function of κ, λ, μ. Partial differentiation with respect to these quantities will be designated by suffixes as follows

$$y_\lambda = \partial y/\partial\lambda, \quad y_{\lambda\mu} = \partial^2 y/\partial\lambda\partial\mu.$$

Differentiating the above differential equation successively one obtains ordinary differential equations for these derivatives:

$$dy_\kappa/dx + 2yy_\kappa + 1 = 0, \qquad dy_{\kappa\lambda}/dx + 2yy_{\kappa\lambda} + 2y_\kappa y_\lambda = 0,$$
$$dy_{\kappa\kappa}/dx + 2yy_{\kappa\kappa} + 2y_\kappa{}^2 = 0, \quad dy_{\kappa\lambda\mu}/dx + 2yy_{\kappa\lambda\mu} + 2y_\lambda y_{\mu\kappa} + 2y_\mu y_{\kappa\lambda} + 2y_\kappa y_{\lambda\mu} = 0.$$

For $x=0$ the function F should be a power series in x beginning with a term of power 1. Therefore,

$$y(0) = 1$$

independently of κ, λ, μ. Hence

$$y_\kappa(0) = y_\lambda(0) = \cdots = y_{\kappa\lambda\mu}(0) = 0.$$

The values of y_κ, etc. are, therefore, determined by the above linear differential equations and these boundary conditions. One obtains

$$y_\kappa = -F^{-2}\int_0^x F^2 dx\,; \quad y_\lambda = -F^{-2}\int_0^x F^2\varphi dx\,; \quad y_\mu = -F^{-2}\int_0^x F^2\chi dx\,;$$

$$y_{\kappa\kappa} = -2F^{-2}\int_0^x y_\kappa{}^2 F^2 dx\,; \quad y_{\kappa\lambda} = -2F^{-2}\int_0^x y_\kappa y_\lambda F^2 dx\,;$$

$$y_{\lambda\lambda\lambda} = -6F^{-2}\int_0^x y_\lambda y_{\lambda\lambda} F^2 dx\,; \quad y_{\lambda\lambda\mu} = -F^{-2}\int_0^x (4y_\lambda y_{\lambda\mu} + 2y_\lambda{}^2 y_\mu) F^2 dx\,; \tag{9.1}$$

$$y_{\kappa\lambda\mu} = -2F^{-2}\int_0^x (y_\kappa y_{\lambda\mu} + y_\lambda y_{\mu\kappa} + y_\mu y_{\kappa\lambda}) F^2 dx\,;$$

$$y_{\kappa\lambda\mu\nu} = -2F^{-2}\int_0^x (y_\kappa y_{\lambda\mu\nu} + y_\lambda y_{\mu\nu\kappa} + y_\mu y_{\nu\kappa\lambda} + y_\nu y_{\kappa\lambda\mu} + y_{\kappa\lambda} y_{\mu\nu} + y_{\kappa\mu} y_{\lambda\nu} + y_{\kappa\nu} y_{\lambda\mu}) F^2 dx.$$

The last formula applies to a differential equation including a fourth linear parameter ν. From the last formula one obtains the other derivatives of the fourth order by equating indices in $y_{\kappa\lambda\mu\nu}$. The $y_{\kappa\lambda}\ldots$ can be evaluated by means of the above formulas with numerical quadratures, and the needed values of F and y can be obtained from one numerical integration for F. The formulas for the first-order derivatives have apparently been given for the first time by BCP where they have been obtained by a slightly different method. In Wigner's Princeton lectures for 1936 the same formulas for first-order derivatives are obtained from Riccati's equation which suggested the extension to higher derivatives made here. An obvious extension to parameters entering nonlinearly can be made and is used for Eq. (12) below.

Formulas for neutron-proton potential for the Gauss error type interaction.—In the calculation of the proton-neutron potential use can be made of the simplication due to the fact that experiments are concerned with zero energy. The wave function is, therefore, practically a linear function of the distance beyond the region where the Gauss error function potential has an appreciable value. The effect on y of a change in the potential can be calculated for any distance greater than this and its effect on the collision cross section will be the same. It may be expected, therefore, that this distance can be eliminated from the calculations. In order to do this the distance will be made infinite. In

nuclear units the differential equation for the Gauss error potential and zero energy is

$$d^2F/dr^2+Ae^{-\alpha r^2}F=0. \tag{10}$$

Substituting $x=r\alpha^{\frac{1}{2}}$ one has

$$d^2F/dx^2+\lambda\varphi(x)F=0\,;\quad \varphi(x)=e^{-x^2}\,;\quad \lambda=A/\alpha, \tag{10.1}$$

which is of the form of Eq. (9). The intercept on the r axis is called a. It is connected with the collision cross section of neutrons with free protons by

$$\sigma=4\pi a^2$$

and with properties of F by $Fdr/dF=a+r$. In terms of x one has for any x beyond which φ is negligible

$$y=dF/Fdx=(x+a\alpha^{\frac{1}{2}})^{-1}. \tag{10.2}$$

It will be supposed that φ has been modified to be exactly zero beyond a certain distance. The limiting value of the result for an infinite value of this distance will be taken at the end of this calculation. To every λ there corresponds a definite value of the intercept and hence also of $a\alpha^{\frac{1}{2}}$ which by Eq. (10.2) determines y. One has thus asymptotically for large x:

$$y-y_0\sim(a_0\alpha_0^{\frac{1}{2}}-a\alpha^{\frac{1}{2}})x^{-2}, \tag{10.3}$$

where y, a correspond to λ, α and y_0, a_0 to λ_0, α_0. By the method explained for Eq. (9) one may expand $y-y_0$ as

$$y-y_0=(\lambda-\lambda_0)y_\lambda+\tfrac{1}{2}(\lambda-\lambda_0)^2y_{\lambda\lambda}+\tfrac{1}{6}(\lambda-\lambda_0)^3y_{\lambda\lambda\lambda}+\cdots,$$

where y_λ, $y_{\lambda\lambda}$, $y_{\lambda\lambda\lambda}$ are to be evaluated for $\lambda=\lambda_0$. This series can be calculated for a finite x and can be used directly in the above form as has been done in some of the calculations for interchecks between numerical integrations. The limiting form of the series will now be worked out for $x\to\infty$. For finite x outside the potential hole one has

$$y_\lambda=-I_1(x+a_0\alpha_0^{\frac{1}{2}})^{-2}\,;\quad I_1=\int_0^\infty F_0^2(x)\,\varphi(x)dx, \tag{10.4}$$

where $F_0(x)$ is the solution of Eq. (10) regular at $x=0$ evaluated for λ_0. The solution F_0 is normalized so as to have outside the potential hole:

$$F_0=x+a_0\alpha_0^{\frac{1}{2}}. \tag{10.5}$$

Similarly

$$y_{\lambda\lambda}=-2(x+a_0\alpha_0^{\frac{1}{2}})^{-2}\left[\int_0^{x_0}F_0^2y_\lambda^2dx+\int_{x_0}^{x}F_0^2I_1^2(x+a_0\alpha_0^{\frac{1}{2}})^{-4}dx\right].$$

Here $x_0<x$ and x_0 is also outside the potential hole. From Eq. (10.5) the last term can be integrated and gives

$$-I_1^2(x+a_0\alpha_0^{\frac{1}{2}})^{-1}+I_1^2(x_0+a_0\alpha_0^{\frac{1}{2}})^{-1}.$$

The sum

$$\int_0^{x_0}F_0^2y_\lambda^2dx+I_1^2(x_0+a_0\alpha_0^{\frac{1}{2}})^{-1}$$

must be independent of x_0 since $y_{\lambda\lambda}$ does not depend on it. One has thus

$$y_{\lambda\lambda}=-2(x+a_0\alpha_0^{\frac{1}{2}})^{-2}[I_2-I_1^2/(x+a_0\alpha_0^{\frac{1}{2}})],$$

where

$$I_2=\int_0^\infty F_0^2 y_\lambda^2 dx=\int_0^{x_0} F_0^2 y_\lambda^2 dx+I_1^2/(x_0+a_0\alpha_0^{\frac{1}{2}}). \tag{10.6}$$

The object of expressing I_2 as a sum is only that of having a form convenient for numerical evaluation. Proceeding similarly for $y_{\lambda\lambda\lambda}$ it is found that

$$y_{\lambda\lambda\lambda}=-6(x+a\alpha^{\frac{1}{2}})^{-2}[I_3-2I_1I_2(x+a_0\alpha_0^{\frac{1}{2}})^{-1}+I_1^3(x+a_0\alpha_0^{\frac{1}{2}})^{-2}],$$

where

$$I_3=\int_0^\infty F_0^2 y_\lambda y_{\lambda\lambda} dx=\int_0^{x_0} F_0^2 y_\lambda y_{\lambda\lambda} dx+2I_1I_2(x_0+a_0\alpha_0^{\frac{1}{2}})^{-1}-I_1^3(x_0+a_0\alpha_0^{\frac{1}{2}})^{-2}. \tag{10.7}$$

Substituting the values of y_λ, $y_{\lambda\lambda}$, $y_{\lambda\lambda\lambda}$ into the Taylor expansion and equating for large x the governing terms in x^{-2} one obtains with Eq. (10.3)

$$a\alpha^{\frac{1}{2}}-a_0\alpha_0^{\frac{1}{2}}=I_1(\lambda-\lambda_0)+I_2(\lambda-\lambda_0)^2+I_3(\lambda-\lambda_0)^3+\cdots, \tag{10.8}$$

which is convenient for the calculation of $a\alpha^{\frac{1}{2}}$ for different λ using a single numerical integration for λ_0. The above series can be inverted and gives them

$$\lambda-\lambda_0=(a\alpha^{\frac{1}{2}}-a_0\alpha_0^{\frac{1}{2}})I_1^{-1}-I_2I_1^{-3}(a\alpha^{\frac{1}{2}}-a_0\alpha_0^{\frac{1}{2}})^2+(2I_2^2-I_1I_3)I_1^{-5}(a\alpha^{\frac{1}{2}}-a_0\alpha_0^{\frac{1}{2}})^3+\cdots,$$

which determines λ through a and α. One obtains in this way for $\lambda_0=2.35$ evaluating the integrals at $x=3.5$ for the Gauss-error potential

$$A/\alpha=\lambda=2.35+0.037032(a\alpha^{\frac{1}{2}}-a_0\alpha_0^{\frac{1}{2}})-0.004102(a\alpha^{\frac{1}{2}}-a_0\alpha_0^{\frac{1}{2}})^2+0.000454(a\alpha^{\frac{1}{2}}-a_0\alpha_0^{\frac{1}{2}})^3-\cdots; \tag{10.9}$$

$$a_0\alpha_0^{\frac{1}{2}}=7.9535.$$

This formula becomes poor for large a but is convenient for the values indicated by present experimental material. The choice $\lambda_0=2.35$ was made so as to be able to start a corresponding expansion for proton-proton calculations.

It is also useful to have the following expansion for y as a power series in $\lambda-\lambda_0$ for $\lambda_0=2.35$, $x=3.5$,

$$y=0.08731-0.2059(\lambda-\lambda_0)-0.1303(\lambda-\lambda_0)^2-0.0847(\lambda-\lambda_0)^3\cdots \quad (\text{at } x=3.5),$$

which can be used with Eq. (10.2) for the calculation of a. This series has been checked against a direct numerical integration for $\lambda=2.25$ which gave $(dF/Fdx)_{x=3.5}=0.10668$. Exactly the same value is obtained by means of the series the successive terms contributing $0.08731+0.02059-0.00130+0.00008=0.10668$.

A slight error is made by extending the numerical integration to finite rather than infinite values of x. This error can be estimated using the formula for y_λ already explained. Using $x=\xi$ instead of $x=\infty$ in the calculations amounts to neglecting the part of φ in $\xi<x<\infty$. The first-order correction due to taking into account φ from ξ to η is

$$y(\eta)-y_0(\eta)=-\lambda(\eta+a_0\alpha_0^{\frac{1}{2}})^{-2}\int_\xi^\eta (x+a_0\alpha_0^{\frac{1}{2}})^2\varphi(x)dx,$$

where $a_0\alpha_0^{\frac{1}{2}}$ is the value obtained for $a\alpha^{\frac{1}{2}}$ by breaking the potential off at ξ, and $y_0(\eta)$ is the value of $y(\eta)$ obtained in the same way. On the other hand,

$$y(\eta)-y_0(\eta)=-(a\alpha^{\frac{1}{2}}-a_0\alpha_0^{\frac{1}{2}})/(\eta+a\alpha^{\frac{1}{2}})(\eta+a_0\alpha_0^{\frac{1}{2}}).$$

Comparing the two values of $y(\eta)-y_0(\eta)$ for infinite η one has the first-order correction

$$a\alpha^{\frac{1}{2}}-a_0\alpha_0^{\frac{1}{2}}=\lambda\int_\xi^\infty (x+a_0\alpha_0^{\frac{1}{2}})^2\varphi(x)dx.$$

For $\varphi(x)=e^{-x^2}$ this becomes approximately

$$a\alpha^{\frac{1}{2}}-a_0\alpha_0^{\frac{1}{2}}=(\lambda/2\xi)(\xi+a_0\alpha_0^{\frac{1}{2}})^2e^{-\xi^2}. \tag{10.91}$$

For $\lambda=2.35$, $\xi=3.5$, $a_0\alpha_0^{\frac{1}{2}}=7.95$ this estimate gives $(a\alpha^{\frac{1}{2}}-a_0\alpha_0^{\frac{1}{2}})/a_0\alpha_0^{\frac{1}{2}}=2.7\times10^{-5}$ which is negligible.

Intercomparison of numerical integrations.—In order to avoid unknown cumulative errors in numerical integrations the series solutions have been carried out in a few cases to $x=1$ and the cumulative effect of the term in δ^4F'' has been taken into account. The integration from $x=1$ to higher values has been carried out at intervals of 0.1 in x. For the numerical integrations used for proton-proton scattering the series solution usually stopped at $x\sim4$. An intercheck between the numerical integrations for proton-proton scattering for $\alpha=20$, $A=47.17$, $E=200$ kev, $r=2.00288$, $x=2.8000$ was made with the numerical integration used for proton-neutron scattering with $\lambda=2.35$. The differential equation for the proton-proton functions is

$$d^2\mathfrak{F}/dx^2+(\lambda e^{-x^2}-\beta/x+\gamma)\mathfrak{F}=0$$

and $\beta=0.06990$, $\gamma=0.009773$, $\lambda=2.3585$ have been used. With these values the direct numerical integration gave $d\mathfrak{F}/\mathfrak{F}dx=0.15250$. The first-order corrections are

$$y_\lambda\delta\lambda+y_\beta\delta_\beta+y_\gamma\delta\gamma=-0.00198+0.08258-0.01668=0.06392.$$

The second-order corrections are

$$\tfrac{1}{2}y_{\lambda\lambda}(\delta\lambda)^2+\tfrac{1}{2}y_{\beta\beta}(\delta\beta)^2+\tfrac{1}{2}y_{\gamma\gamma}(\delta\gamma)^2+y_{\lambda\beta}\delta\lambda\delta\beta+y_{\lambda\gamma}\delta\lambda\delta\gamma+y_{\beta\gamma}\delta\beta\delta\gamma=-0.000008-0.00764$$
$$-0.00020+0.00049-0.00007+0.00238=-0.00505.$$

The numbers are given in the same order as symbols. Most of the third-order corrections are negligible, only five being large enough to affect $y(x)$ in the fifth place. These are

$$\tfrac{1}{6}y_{\beta\beta\beta}(\delta\beta)^3+\tfrac{1}{2}y_{\beta\beta\gamma}(\delta\beta)^2\delta\gamma+\tfrac{1}{2}y_{\beta\beta\lambda}(\delta\beta)^2\delta\lambda+\tfrac{1}{2}y_{\beta\gamma\gamma}\delta\beta(\delta\gamma)^2+6y_{\beta\gamma\lambda}\delta\beta\delta\gamma\delta\lambda=0.00086-0.00014$$
$$-0.000045+0.000025+0.000025=0.00072.$$

Not all of the fourth-order corrections have been taken into account but the following give appreciable effects:

$$(1/24)y_{\beta\beta\beta\beta}(\delta\beta)^4+\tfrac{1}{6}y_{\beta\beta\beta\gamma}(\delta\beta)^3\delta\gamma+\tfrac{1}{6}y_{\beta\beta\beta\lambda}(\delta\beta)^3\delta\lambda=-0.000099-0.000019-0.000006=-0.00012.$$

The value of y for $\lambda=2.35$, $\beta=\gamma=0$ by numerical integration is 0.09315. The expected value of y for $\lambda=2.3585$, $\beta=0.06990$, $\gamma=0.009773$ is, therefore,

$$0.09315+0.06392-0.00505+0.00072-0.00012=0.15262.$$

This is to be compared with $y=0.15250$ obtained by numerical integration for these λ, β, γ. The

error in $xd\mathfrak{F}/\mathfrak{F}dx$ due to the remaining discrepancy is 0.00034. The corresponding error in K_0 is given by

$$\delta\left(\frac{xdF}{Fdx}\right)=-C_0^2\rho\Phi_0^2\left(\frac{xd\mathfrak{F}}{\mathfrak{F}dx}-\frac{\Phi_0^*}{\Phi_0}\right)^2\frac{\delta K_0}{\sin^2 K_0}.$$

In the present case it is $-2.6\delta K_0$. The error 0.00034 in $xd\mathfrak{F}/\mathfrak{F}dx$ produces therefore $\delta K_0=-0.00013=-0.007°$. At this energy such an error corresponds to roughly 0.2 percent error in scattering and is considerably below possible accuracy of an experiment. At higher energies the experimental accuracy is higher but here also an accuracy of 0.01° in K_0 is sufficient.

2. Coulomb effect for square wells

The depth of the square well inside of which the Coulomb repulsion between two protons is assumed to act must be somewhat greater than if this repulsion is supposed to exist only outside the well. It is necessary to take this effect into account because it amounts to about 0.8 Mev and affects, therefore, the comparison between proton-proton and proton-neutron interactions. In the work of BCP the effect of the Coulomb repulsion inside the potential hole was taken into account by two different methods. In the first method the wave functions inside the hole have been computed taking into account the Coulomb repulsion and using power series. This method is somewhat laborious. In the second method the first-order effects on the logarithmic derivative due to introducing the Coulomb repulsion and due to increasing the depth of the hole have been taken into account. This gave rise to the formula

$$\delta D=\frac{e^2z\int_0^z(\sin^2 z/z)dz}{r_0\int_0^z\sin^2 zdz}=\frac{e^2z[\ln 2z+0.5772\cdots-Ci(2z)]}{r_0(z-\sin z\cos z)},\quad Ci(x)=-\int_x^\infty\frac{\cos u}{u}du,$$
$$z=[2\mu\hbar^{-2}(D+E')]^{\frac{1}{2}},\quad r_0=0.4371(r_0mc^2/e^2)(D+E')^{\frac{1}{2}}(\text{Mev})^{-\frac{1}{2}}. \tag{11}$$

The two methods agreed to within the accuracy desired then. The requirements for precision in the calculations are higher now on account of improvements and extensions in the experiments. The second method has been extended, therefore, so as to include second- and third-order effects. The differential equation is

$$\frac{d^2\mathfrak{F}}{dr^2}+\frac{2\mu}{\hbar^2}\left(D+E'-\frac{e^2}{r}\right)\mathfrak{F}=0. \tag{11.1}$$

Here it is convenient to set

$$\beta_s=2\mu e^2/\hbar^2,\quad y_s=d\mathfrak{F}/\mathfrak{F}dr. \tag{11.11}$$

For fixed r and E' the quantity y_s is a function of D, β_s. Using the formulas previously described in connection with the Gauss error potential one obtains

$$\frac{\partial y_s}{\partial\beta_s}=\frac{C+\ln 2z-Ci(2z)}{2\sin^2 z};\quad C=0.577216\cdots;$$
$$\frac{\partial y_s}{\partial D}=-\frac{\mu(z-\sin z\cos z)}{\hbar^2\kappa_s\sin^2 z};\quad \kappa_s=(2\mu(E'+D)\hbar^{-2})^{\frac{1}{2}}. \tag{11.12}$$

The values of these derivatives correspond to $\beta_s=0$. Similarly, letting

$$I_{DD}=\int_0^z(\sin z)^{-2}(z-\sin z\cos z)^2dz,$$

$$I_{\beta D}=\int_0^z(\sin z)^{-2}[C+\ln 2z-Ci(2z)](z-\sin z\cos z)dz, \tag{11.13}$$

$$I_{\beta\beta}=\int_0^z(\sin z)^{-2}[C+\ln 2z-Ci(2z)]^2dz,$$

one has

$$\frac{\partial^2 y_s}{\partial\beta_s^2}=-\frac{I_{\beta\beta}}{2\kappa_s\sin^2 z};\quad \frac{\partial^2 y_s}{\partial\beta_s\partial D}=\frac{\mu I_{\beta D}}{\hbar^2\kappa_s^2\sin^2 z};\quad \frac{\partial^2 y_s}{\partial D^2}=-\frac{2\mu^2 I_{DD}}{\hbar^4\kappa_s^3\sin^2 z}.$$

In the present approximation δD, the increase in the depth due to the Coulomb repulsion inside the potential well, is connected with β_s by

$$\frac{\partial y_s}{\partial\beta_s}\beta_s+\frac{\partial y_s}{\partial D}\delta D+\frac{\partial^2 y_s}{2\partial\beta_s^2}\beta_s^2+\frac{\partial^2 y_s}{\partial\beta_s\partial D}\beta_s\delta D+\frac{\partial^2 y_s}{2\partial D^2}(\delta D)^2=0,$$

so that sufficiently accurately

$$\delta D=\frac{e^2z[\ln 2z+0.577216-Ci(2z)]}{r_0(z-\sin z\cos z)}f, \tag{11.2}$$

where

$$f=1+\frac{\partial^2 y_s/\partial\beta_s^2}{2\partial y_s/\partial\beta_s}\beta_s-\frac{\partial^2 y_s/\partial\beta_s\partial D}{\partial y_s/\partial D}\beta_s-\frac{\partial^2 y_s/\partial D^2}{2(\partial y_s/\partial D)^2}\frac{\partial y_s}{\partial\beta_s}\beta_s,$$

so that

$$f=1+\beta_s\epsilon/\kappa_s, \tag{11.3}$$

where

$$\frac{\beta_s}{\kappa_s}=\frac{e^2}{\hbar c}\left(\frac{Mc^2}{E'+D}\right)^{\frac{1}{2}}=\frac{0.223}{[(E'+D)/\mathrm{Mev}]^{\frac{1}{2}}}$$

and

$$\epsilon=-\frac{I_{\beta\beta}/2}{C+\ln 2z-Ci(2z)}+\frac{I_{\beta D}}{z-\sin z\cos z}-I_{DD}\frac{C+\ln 2z-Ci(2z)}{2(z-\sin z\cos z)^2}. \tag{11.4}$$

Some numerical values of ϵ and of the coefficient of e^2/r_0 in the first-order approximation for δD are given in Table XVI. The experimental values for nonvelocity dependent potentials lie close to $z=1.4$. The depth of the well is in this case 10.5 Mev so that $\beta_s/\kappa_s=0.069$ for low proton energies and is smaller than this at the higher energies. Hence $f=1-0.069\times 0.029=0.9980$. The second-order correction is thus -0.2 percent of the first-order correction. This extreme smallness of the second-order effect should not be interpreted as an indication of a similar ratio of third- and second-order terms in the series for δD because the three terms in $I_{\beta\beta}$, $I_{\beta D}$, I_{DD} approximately cancel each other. The three contributions for $z=1.2$ are $-0.257_7+0.393_9-0.159_6=-0.023$. Even though the third-order correc-

TABLE XVI. *Values of* $z[ln\ 2z+0.5772\cdots-Ci(2z)](z-sin\ z\ cos\ z)^{-1}$ *and of* ϵ.

$z=$	1.0	1.1	1.2	1.3	1.4	1.5	1.6	1.7
$z\frac{\ln 2z+0.5772-Ci(2z)}{z-\sin z\cos z}=$	1.554	1.566	1.580	1.596	1.613	1.633	1.655	1.679
$\epsilon=$	−0.019	−0.021	−0.023	−0.026	−0.029	−0.031	−0.034	−0.038

tion cannot be expected to be as small as 0.002 of the second there is no reason to expect it to be more than $(0.02)^2=0.0004$ of the first-order effect. The solution as used above can be thus expected to be good enough.

It will be noted that the first-order effect varies slowly with z. Since z itself varies slowly with E it also changes slowly with proton energy. As a good approximation, therefore, a range of force which fits experiment if the Coulomb effect is neglected inside the potential well fits it also if this effect is assumed to be present. The main change due to the Coulomb potential inside the potential hole is nearly a constant increase in the depth of the hole for a fixed range of force, energy and phase shift.

The accuracy of Eqs. (11.2), (11.3) and (11.4) for the computation of the correction to the depth of the square well due to the introduction of the Coulomb interaction inside of it has been tested using the third-order correction for the effect of the interaction on the wave function. Analogously to the formulas preceding Eq. (11.2) one obtains by the method of Eqs. (9.1) an expansion for y_s the first three terms of which give

$$\left(\frac{rd\mathfrak{F}}{\mathfrak{F}dr}\right)_{r_0}=r_0y_s=z\cot z+\frac{\beta_s[C+\ln 2z-Ci(2z)]}{2\kappa_s\sin^2 z}-\frac{\beta_s{}^2z}{4\kappa_s{}^2\sin^2 z}I_{\beta\beta}+\frac{\beta_s{}^3}{4\kappa_s{}^3\sin^2 z}I_{\beta\beta\beta},\tag{11.5}$$

where

$$I_{\beta\beta\beta}=\int_0^z[C+\ln 2z-Ci(2z)](I_{\beta\beta}/\sin^2 z)dz.\tag{11.6}$$

Here z is the internal phase defined in Eq. (11), β_s is defined in Eq. (11.11), κ_s in Eq. (11.12), $I_{\beta\beta}$ in Eq. (11.13). The expansion in Eq. (11.5) is seen to be in powers of β_s/κ_s. It converges rapidly for radii $\sim e^2/mc^2$ in the energy range tried. The last term is slightly less than 0.0001 up to 2600 kev and can be neglected in most applications. The term in $I_{\beta\beta}$ is more important and is ~-0.002.

According to Eq. (11.2) a square well of depth $D^c=D+\delta D$ with Coulomb interaction acting inside of it gives nearly the same $rd\mathfrak{F}/\mathfrak{F}dr$ as a square well of depth D without the Coulomb interaction inside of it. For the latter $rd\mathfrak{F}/\mathfrak{F}dr$ can be evaluated as $z\cot z$ using z as in Eq. (11). At the same time $rd\mathfrak{F}/\mathfrak{F}dr$ for D^c with Coulomb potential can be computed using the more accurate method of Eq. (11.5). With $D=10.500$ Mev and $r_0=e^2/mc^2$ the two ways of computing $rd\mathfrak{F}/\mathfrak{F}dr$ agree to within 0.0001 for $E=200$ kev and 0.0002 for $E=2600$ kev. This accuracy is higher than any present requirement. Eq. (11.2) may be, therefore, considered as being sufficiently accurate for the calculation of the depth of a square well taking account of the Coulomb interaction down to $r=0$.

The value of δD depends slightly on the proton energy. For $D=10.500$ Mev one finds $\delta D=0.826$, 0.830, 0.834 Mev for $E=200$, 1400, 2600 kev, respectively. The variation in $D^c=D+\delta D=11.33$ Mev is less than 0.1 percent in the above range of energies. For most purposes, therefore, one can first calculate without taking into account the Coulomb interaction inside the well and then increasing the depth by the same amount δD throughout the present energy range.

The accuracy of this procedure has been tested directly as well. The phase shift was computed for $r_0=e^2/mc^2$, $D=10.500$ Mev and with no Coulomb potential inside r_0. It was then also computed for $r_0=e^2/mc^2$, $D^c=11.3302$ Mev, and with the Coulomb potential taken into account by means of Eq. (11.5). The value of K_0 for D^c

minus its value for D varies slightly with energy changing from 0.02° at $E=200$ kev to 0.06° at $E=2600$ kev. This change is invisible on the graphs for K_0 against E.

It is useful to have the numerical values of the functions of z that occur in the expansion of $rd\mathfrak{F}/\mathfrak{F}dr$ in Eq. (11.5). The necessary quantities are given in Table XVII.

3. Adjustment of range and values of interaction constants obtained from experiment

A "square well" potential of depth $D=10.5$ Mev (no Coulomb repulsion inside well) and radius e^2/mc^2 gives values of the phase shift which agree approximately with experiment. The comparison is shown in Figs. 6 and 7. In the first of these there are three curves for radius e^2/mc^2 and another set for a radius 1.25 e^2/mc^2. In the second of these figures graphs for a radius 0.75 e^2/mc^2 are used instead of for the radius 1.25 e^2/mc^2. In both cases experiment is seen to favor the range e^2/mc^2 in preference to the other two. The measurements of HKPP speak for a range slightly smaller than e^2/mc^2 indicating perhaps 0.95 e^2/mc^2 as the better value. Combined with experiments of HHT a better average fit is obtained for a slightly larger range. The graphs show that the range 0.75 e^2/mc^2 is too small and the range 1.25 e^2/mc^2 is too large if it is desired to represent the data as a whole. It is seen from

TABLE XVII. *Table of quantities for computation of logarithmic derivative of wave function for square well and Coulomb potential by means of Eq. (11.5). The second column gives the coefficient of $\beta_s/2\kappa_s$ in Eq. (11.5). The last two columns have been computed with Simpson's rule at intervals of 0.1 in z.*

z	$\frac{C+\ln 2z-Ci(2z)}{\sin^2 z}$	$\sin^2 z$	$I_{\beta\beta}$	$I_{\beta\beta\beta}$
0.4	1.027	0.1517	0.021	0.0022
.5	1.043	.2298	.042	.0053
.6	1.063	.3188	.072	.0112
.7	1.088	.4150	.114	.0212
.8	1.118	.5146	.171	.0368
.9	1.154	.6136	.244	.0602
1.0	1.197	.7081	.335	.094
1.1	1.247	.7943	.447	.142
1.2	1.307	.8687	.583	.207
1.3	1.378	.9285	.745	.296
1.4	1.463	.9711	.937	.415
1.5	1.564	.9950	1.162	.574
1.6	1.687	.9991	1.426	.783
1.7	1.836	.9834	1.733	1.061
1.8	2.020	.9484	2.091	
1.9	2.251	.8955	2.511	
2.0	2.545	.8268	3.004	

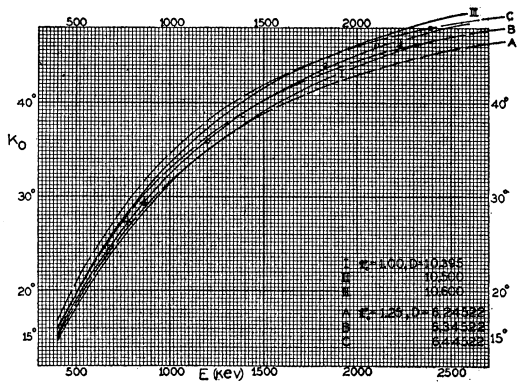

FIG. 6. Comparison of experimental and calculated phase shift for square wells of radii e^2/mc^2 and 1.25 e^2/mc^2. Circles represent observations of HKPP, upright crosses those of HHT. The depth of well is given in Mev. Coulomb interaction is supposed to take place outside the well only.

Figs. 6 and 7 that through the region 700–2400 kev a change of depth with fixed range produces a displacement of the curve by approximately a fixed amount. On the other hand, a change of range produces in addition a rotation. These relationships are only approximate but are helpful in forming an opinion regarding the range and depth of potential indicated by experiment. They are also true for the Gauss error potential which gives nearly the same shape of the (K_0, E) curve as the square well. The same percentage change in the range produces approximately the same amount of turning for the two types of potential. This relationship is true also for other potentials as long as the main part of the interaction occurs within a small distance. The effects of changes in depth and range are seen more clearly using a plot of $(\eta/C_0^2)\tan K_0$ against E. Such plots are shown in Figs. 8 and 9 the ranges for which correspond to Figs. 6, 7. The quantity plotted is chosen so as to give approximately horizontal curves through the present energy range as well as the region below 600 kev. The crowding of curves which occurs at low energies for the graphs of K_0 against E is seen to be absent for the plots of $(\eta/C_0^2)\tan K_0$. With either type of graph it is possible to adjust the two constants in the Gauss error type of potential so as to make K_0 have the desired values at two energies.

In view of the possibility of cumulative errors in the numerical integrations the range was adjusted also by means of formulas. This enables the calculation of corrections to A and α by

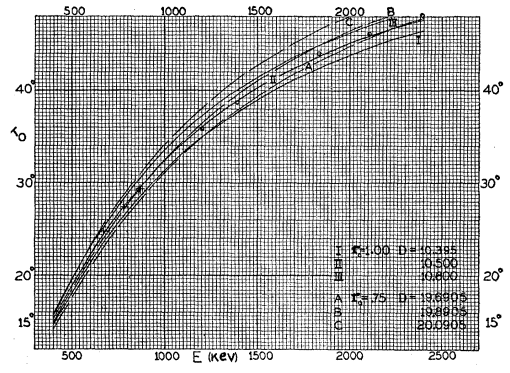

FIG. 7. Comparison of experimental and calculated phase shift for square wells of radii e^2/mc^2 and $0.75\ e^2/mc^2$. Notation and conventions are the same as for Fig. 6.

numerical integrations for values of these constants determined by rough inspection of the graphs. Several procedures have been found useful. In the first the range was fixed arbitrarily and the depth was determined at several energies so as to give the desired phase shift. If the range is too great the depth increases with energy. For small changes $\delta\alpha$, δA of depth and range the phase shift remains unchanged if

$$\frac{\delta\alpha}{\alpha}=\left[\int_0^\infty \mathfrak{F}^2 e^{-x^2}dx \Big/ \int_0^\infty \mathfrak{F}^2 x^2 e^{-x^2}dx\right]\frac{\delta A}{A}. \quad (12)$$

The integrals in this formula having been determined by numerical integration at two or more energies, one knows the ratio of the percentage changes which must be made at two energies in order that the phase shift be unchanged. Hence one can determine the value of $\delta\alpha$ which is needed for obtaining the same A at the two energies. Roughly the same results can be obtained by noting how rapidly $\delta A/A$ decreases with an increase in α and extrapolating to 0. It is helpful to note that $\delta A/A$ varies approximately linearly with energy. This crudest method will be called the "percentage method." A third way involving numerical integrations for only one set of A and α is to use the approximate linear equations

$$\left[\delta\left(\frac{r\partial\mathfrak{F}}{\mathfrak{F}\partial r}\right)\right]_1=\left[\frac{\partial}{\partial\alpha}\left(\frac{r\partial\mathfrak{F}}{\mathfrak{F}\partial r}\right)\right]_1\delta\alpha+\left[\frac{\partial}{\partial A}\left(\frac{r\partial\mathfrak{F}}{\mathfrak{F}dr}\right)\right]_2\delta A, \quad (12.1)$$

$$\left[\delta\left(\frac{r\partial\mathfrak{F}}{\mathfrak{F}\partial r}\right)\right]_2=\left[\frac{\partial}{\partial\alpha}\left(\frac{r\partial\mathfrak{F}}{\mathfrak{F}\partial r}\right)\right]_2\delta\alpha+\left[\frac{\partial}{\partial A}\left(\frac{r\partial\mathfrak{F}}{\mathfrak{F}\partial r}\right)\right]_2\delta A, \quad (12.2)$$

where

$$\frac{\partial}{\partial\alpha}\left(\frac{r\partial\mathfrak{F}}{\mathfrak{F}\partial r}\right)=\frac{xA}{\alpha^2\mathfrak{F}^2}\int_0^x x^2e^{-x^2}\mathfrak{F}^2dx, \quad (12.3)$$

$$\frac{\partial}{\partial A}\left(\frac{r\partial\mathfrak{F}}{\mathfrak{F}\partial r}\right)=-\frac{x}{\alpha\mathfrak{F}^2}\int_0^x e^{-x^2}\mathfrak{F}^2dx, \quad (12.4)$$

and suffixes 1, 2 denote values of derivatives and changes for energies E_1, E_2 at which the adjustment is to be made. Evaluating the coefficients on the right side of (12.1), (12.2) by means of (12.3), (12.4) and computing the left sides by using the relation between K_0 and $r\partial\mathfrak{F}/\mathfrak{F}\partial r$, one obtains $\delta\alpha$ and δA.

Applying Eq. (12) to numerical integrations made for $\alpha=18$, $A=42.8$ and requiring a fit with the square well $r_0=e^2/mc^2$ at $E=200$ kev and $E=2000$ kev one obtains $\alpha=20.6$, $A=48.6$. The percentage method indicates using numerical integrations for $\alpha=16$ and $\alpha=18$ at 200, 800, 1400, 2600 kev that one must take $\alpha>18$ in order to obtain a fit with the square well for any pair of these voltages and that the approximate value of α is 20.

A set of accurate numerical integrations was made for $\alpha=20$, $A=47.17$. The Gauss error potential was broken off at the distance $3\ e^2/mc^2$ and the joining of internal to external wave functions was made at this distance. As expected this range is slightly too great (r_0 is too small) to fit the square well and is, therefore, definitely too great to fit experiment. The comparison is shown in Table XVIII.

The last figure is uncertain in this table but it is seen that $\alpha=20$ is too small. In the range 800–2600 kev the phase shift curve for this potential is turned by roughly the same amount under the curve for $D=10.5$, $r_0=e^2/mc^2$ as the experimental curve is turned above it.

From the accurate integrations for $A=47.17$, $\alpha=20$ the values of A, α needed to fit the square well $D=10.500$, $r_0=e^2/mc^2$ at 1400 kev and 2600 kev are found by means of Eqs. (12.1) and (12.2)

to be $A=51.55$, $\alpha=21.70$. By fitting the square well at 800 and 2600 kev one similarly finds $A=51.76$, $\alpha=21.78$ and fitting it at 200 kev and 1400 kev one obtains $A=51.85$, $\alpha=21.83$. It is seen that in the present energy region nearly constant values of A and α are needed to give results equivalent to a square well.

The sensitivity of the value of α to changes in K_0 can be computed using Eqs. (12.1) and (12.2) together with the relation of $r\partial\mathfrak{F}/\mathfrak{F}\partial r$ to K_0. One obtains in this way the values in Table XIX. In this table the first row is labeled E_1, E_2 and gives the values of the energies at which the adjustment of range is made. In the second row are listed the changes made in K_0 at the energies E_1, E_2. Here the entry (0, 0.4°) means that no change is made at the lower energy and that the phase shift is changed by 0.4° at the higher energy. The third row gives the resultant change in α, denoted by $\delta\alpha$. The last row gives the resultant α, which is obtained by adding $\delta\alpha$ to the value of α which corresponds to the pair E_1, E_2 and fitting the Gauss error potential to the square well of radius $r_0=e^2/mc^2$ and depth $D=10.500$ Mev. The lowest α obtained in Table XIX is 19.8. To make the value so low it was necessary to raise the phase shift by 0.4° at 800 kev from the value obtained for $r_0=e^2/mc^2$, $D=10.500$ Mev. Such an adjustment of range appears to be decidedly too low for α, since at 800 kev the 776 kev, 867 kev and 860 kev-experimental points lie practically on the curve for $r_0=e^2/mc^2$, $D=10.500$ Mev and since at 1830 kev, 2105 kev and 2392 kev the experimental points lie decidedly above

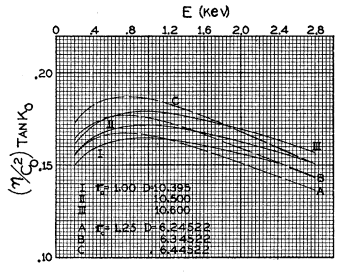

FIG. 8. Effect of change of range for square wells as shown by $(\eta/C_0^2)\tan K_0$ for the radii e^2/mc^2 and 1.25 e^2/mc^2 with depths in Mev. Note that change of range turns a curve and change of depth moves it up and down. These graphs are useful for interpolation eliminating the need for Coulomb functions at too many energies. The low energy point lies decidedly off the curve $r_0=1.00$, $D=10.500$ Mev when plotted in this way.

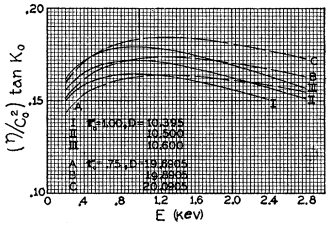

FIG. 9. Effect of change of range for square wells as shown by $(\eta/C_0^2)\tan K_0$ for the radii e^2/mc^2 and 0.75 e^2/mc^2.

this curve. It should be noted, on the other hand, that at 670 kev the experimental phase shift lies above the value expected for $r_0=e^2/mc^2$, $D=10.500$ Mev so that the correction of α towards smaller values appears to be called for from this point of view. It is probable, however, that such a correction is better represented by the last column in Table XIX where the phase shift is increased by 0.4° at 800 as well as 2400 kev. This adjustment requires according to the above calculation $\alpha=21.59$, $A=51.44$.

These values of A and α are in good agreement with the two ends of the experimental curve giving a good fit at 670 kev as well as at 1830, 2105 and 2392 kev. At intermediate voltages, however, the experimental phase shifts are consistently lower than the calculated, the larger deviations occurring at 1200 and 1390 kev where they are about 0.5°. The comparison of this curve with experiment is shown in Fig. 10. The theoretical curve is seen to be slightly bulged at intermediate voltages. The same tendency is noticed also for square wells with $r_0=e^2/mc^2$, $D=10.500$ and 10.520 Mev. It appears premature to conclude that these small deviations indicate an impossibility of representing the interaction by fixed potentials of the types discussed. It is remarkable, nevertheless, that the experimental points fall very beautifully on a smooth curve so that there appears to be some justification for requiring a better fit than has been attempted.

A better judgment regarding the validity of such conclusions can be obtained also from a direct comparison of observed and expected scattering shown in Fig. 11. This figure is to be compared with Fig. 8 of the paper of HKPP. In both of these figures the observed number of counts per microcoulomb is plotted against energy for fixed scattering angle. In Fig. 11 of the present paper the averages of the experi-

mental observations are plotted as circles from Table I of HKPP instead of results of different runs. Fig. 11 gives, therefore, an optimistic picture of the data since it does not show the scattering due to the errors in individual runs shown in Fig. 8 of HKPP. The observations of HHT have been reduced to what they would be in the apparatus of HKPP and are plotted as upright crosses. The diagonal crosses show the scattering that would be expected for a pure s anomaly with mean values of the phase shift obtained in Tables XI, XII from the experimental data. Such values are referred to here as "empirical." The empirical phase shift for Fig. 11 was obtained by plotting the experimental values of K_0 against E as in Fig. 10. There are shown besides in Fig. 11 three sets of theoretical curves. In order to avoid complicating the figure the empirical phase shift curve is not drawn. The full curves are for a square well with $r_0=e^2/mc^2$, $D=10.500$ Mev. The curve with short dashes is for a square well with $r_0=1.25$ e^2/mc^2, $D=6.34522$ Mev and the curve with long dashes is for the Gauss error potential $\alpha=21.59$, $A=51.44$. The conclusions arrived at in the comparison of computed and observed phase shift in Figs. 6, 7 and 10 are seen to be supported by Fig. 11. The comparison of Figs. 6 and 7 corresponds to the use of a mean of the curves for $\Theta=45°$, 40°, 35° and 30° and is somewhat more consistent in its indications concerning range than either of these curves. It is, nevertheless, seen also in the comparison with scattering that the range 1.25 e^2/mc^2 for a square well is decidedly too wide. The curves corresponding to it either cut across the region covered by experimental points or else they fit experiment at the lower energies but deviate from it markedly at the high energy end. The observations of HHT are seen to speak against the interpretation by $r_0=e^2/mc^2$, $D=10.500$ Mev and to favor rather $r_0=1.25\,e^2/mc^2$, $D=6.34522$ Mev or else $\alpha=21.59$, $A=51.44$. It is interesting to note that this indication is particularly marked for $\Theta=30°$. For this angle the scattering as a function of the energy should have a minimum at about 600 kev while the points of HHT lie too high and indicate that the minimum is at a lower energy. Inasmuch as the agreement of HHT and HKPP at $\Theta=25°$ is not as good as desirable and inasmuch as the agreement of the points of HHT with $r_0=e^2/mc^2$, $D=10.500$ Mev is fair at this angle a final conclusion regarding this question appears to be premature. At $\Theta=20°$ and 15°, the expected scattering is nearly independent of the potential assumed, the difference being too small in most of the region to show on the scale used. These curves have been drawn for $r_0=e^2/mc^2$, $D=10.500$ Mev. For $\Theta=15°$ the experimental points are consistently above the theoretical curve indicating the presence of geometrical corrections. This point has already been discussed in connection with Table XI.

TABLE XVIII. *Comparison of phase shift obtained for Gauss error potential $47.17e^{-20r^2}$ with square well $D=10.500$, $r_0=e^2/mc^2$.*

$E=$	200	800	1400	2000	2600 kev
$K_0(D=10.5$ Mev$)=$	6.78°	27.90°	39.00°	45.10°	48.62°
$K_0(A=47.17, \alpha=20)=$	6.80°	27.83°	38.77°	44.71°	48.16°
Difference $=$	−0.02°	0.07°	0.23°	0.39°	0.46°

TABLE XIX. *Sensitivity of range to changes in phase shift.*

$(E_1, E_2)=$	(1400,2600)	(800,2600)	(800,2600)	(800,2600 kev)
$(\delta_1 K_0, \delta_2 K_0)=$	(0, 0.4°)	(0.4°, 0)	(0, 0.4°)	(0.4°, 0.4°)
$\delta\alpha=$	2.7	−2.0	1.8	−0.2
$\alpha=$	24.4	19.8	23.6	21.6

The adjustments for range that have been considered do not take into account the finer features of the experimental phase shift-energy curve. The three energies investigated in Washington when taken by themselves would give a definitely longer range than the phase shift curve taken as a whole. Similarly, the high energy part corresponds to a shorter range than the average values arrived at. It may be hoped that further experimental work will show whether such finer deviations of phase shift from theory are real. It appears that they indicate a possibility of inferring the shape of the potential as well as the range and that it may be possible to obtain from them information concerning a possible velocity dependence of the forces such as has been first proposed by Wheeler.

It is probable that the information concerning fits with phase shift curves corresponding to the simple potentials of fixed magnitude can be obtained by extending the experiments to higher as well as to lower energies. The possibilities for this will be discussed in the last section of the paper.

4. Comparison of the proton-proton and proton-neutron interactions

The comparison of the proton-proton and proton-neutron interactions made by BCP and by BS[14] indicated that in the ^1S state the proton-neutron attraction is slightly greater than the corresponding quantity for two protons. The experimental situation has improved considerably since then. The two types of scattering are known better and scattering experiments on neutrons in ortho- and parahydrogen indicate according to Teller and Schwinger and Teller[20] that the ^1S level of the deuteron must be virtual. The newer values support the previous view regarding the relative magnitude of the two interactions. In Table XX the comparison is shown for square wells.

The value 68.8×10^{-24} cm^2 corresponds to one of the possibilities in Table I of BS and has been used here so as to make it unnecessary to go into the effect of range. According to Carroll and Dunning 65.9×10^{-24} cm^2 is the probable lower limit for σ_{th} and according to Cohen and Goldsmith the probable value of σ_{th} is $(80\pm8)\times10^{-24}$ cm^2. There appears to be no doubt, therefore, that for the square well potential the proton-neutron attraction should be taken as the stronger. It should be noted that this conclusion is not sensitive to the range assumed as is seen in Table I of BS. It is also quite insensitive to the value used for the binding energy of the deuteron because with $E=-2.17$ Mev, $12\pi a_3^2=12.9\times10^{-24}$ cm^2 which is relatively small compared with σ_{th} [See Eq. (8)]. Since a_3^2 is approximately proportional to $1/E_3$ even a ten percent change in E_3 is of no importance as is seen from Table XX.

In Table XXI a similar comparison is made for the Gauss error potential. For this table the value of $12\pi a_3^2$ was redetermined using the Gauss error potential for the ^3S state. Since $12\pi a_3^2$ need not be known very accurately the value $\alpha=20$ was used. This gives $A(^3S)=85.5$ and $12\pi a_3^2=12.6\times10^{-24}$ cm^2. The difference between this and the corresponding value for the square well is seen to be practically immaterial.

According to Table XXI the relative values of the proton-proton and proton-neutron interactions are much the same for the Gauss error potential as for the square well. It appears, therefore, very probable that as long as the potentials are assumed to have fixed magnitude and the same range for the ^1S and ^3S interactions the proton-neutron potential should be taken as having a value roughly three percent higher than the proton-proton potential. The last row in Table XX shows that in order that this conclusion be materially affected by a change in the ^3S scattering cross section it is necessary to increase $12\pi a_3^2$ by roughly 30×10^{-24} cm^2 i.e., by more than twice the value expected on the simple views used here.

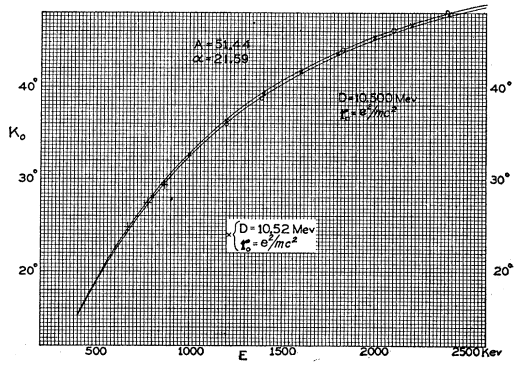

FIG. 10. The Gauss error potential with $A=51.44$, $\alpha=21.59$ compared with experiment and the square well potential $r_0=e^2/mc^2$, $D=10.500$ Mev. The effect of increasing the depth of the square well by 0.02 Mev is shown by the diagonal crosses. Circles give observations of HKPP, upright crosses those of HHT.

5. Possibilities at low and high energies and higher phase shifts

In Fig. 12 are shown graphs of a quantity proportional to the expected scattering in the region 200–600 kev. The quantity plotted is $4(\mathbf{c}/\mathbf{s})\mathfrak{M}\mathfrak{R}/E^2_{\text{Mev}}$. By means of Eq. (3.4) one can obtain from it the number of counts per microcoulomb per mm oil pressure in the standard design of apparatus. The graphs are plotted for

TABLE XX. *Comparison of proton-proton and proton-neutron interactions for the square well potential.*

σ_{th} IN 10^{-24} CM^2	$D_{\pi\nu}$ IN MEV	$D^c_{\pi\pi}$ IN MEV
80	11.75	11.35 ± 0.03
68.8	11.65	" "
52	11.4	" "

[20] E. Teller, Phys. Rev. **49**, 420 (1936); J. Schwinger and E. Teller, Phys. Rev. **52**, 286 (1937).

the square well potentials $D=10.500$ Mev, $r_0=e^2/mc^2$ and $D=19.6905$ Mev, $r_0=3e^2/4mc^2$. The scattering expected for these potentials at about 2200 kev is the same. Either of them may be looked at as representing satisfactorily the high end of the experimental region that has been investigated. It is seen from the figure that relatively large differences can be expected at about 500 kev as well as around 350 kev at scattering angles near 45°. The curves for the two ranges intersect in the vicinity of 400 kev and thus for each scattering angle there is an energy region insensitive to the range of force. At 300 kev for 45° scattering one expects a relative difference between 25 percent and 20 percent for the shorter and longer range of force. At 450 kev the condition is even more favorable the scattering for the shorter range being roughly $\frac{1}{2}$ of that for the longer. The steepness of the curves at 250 kev and lower energies presumably introduces difficulties on account of the necessity of having an accurately defined energy of the incident protons. From this point of view measurements at 500 and 600 kev are more practical.

The first set of measurements published by Tuve, Heydenburg and Hafstad includes a point at 600 kev. Relatively good agreement was obtained with the expected angular distribution as is seen in Fig. 6 of BCP. The value of K_0 so obtained was fixed at the time between 21° and 22°. Even the higher of these values would speak for a shorter range than e^2/mc^2 for a square well as is seen in Figs. 6 and 7. It partly balances the new point of HHT at 670 kev which indicates a longer range. It will doubtless be of value to have more observations in this region. The counting difficulties at 45° caused by the low proton energy can be avoided by making measurements at smaller scattering angles. Measurements at 300 kev will have the obvious additional value of extending the phase shift curve over a wider energy region. The observations of Hafstad, Heydenburg and Tuve made in this region with a point counter were intended as a test of the attractive nature of the force and are hardly quantitative enough for the determination of the range of force. A comparison of the values obtained by Heydenburg, Hafstad and Tuve for the ratio of scattering at 45° to that at 25° is shown in Fig. 13. The values are obtained from their Table II. The high sensitivity of scattering to energy apparent in Fig. 12 must have introduced errors into these measurements in addition to those due to difficulties with the point counter. Only the point at 335 kev falls appreciably off

TABLE XXI. *Comparison of proton-proton and proton-neutron potentials for the Gauss error interaction.*

σ_{th} IN 10^{-24} CM^2	α	$A_{\pi\nu}$	$A_{\pi\pi}$
80	20	48.9	47.2
80	22	54.0	52.4
65.9	20	48.3	47.2

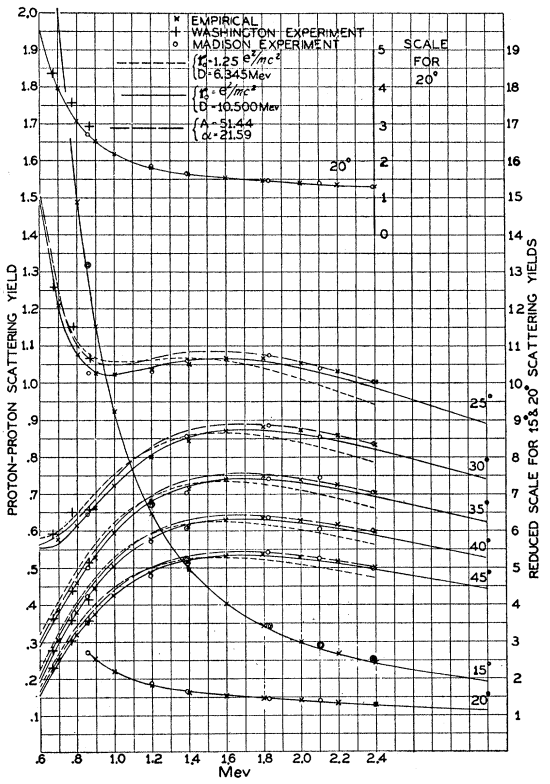

FIG. 11. Comparison of expected and observed scattering. This figure is to be compared with Fig. 8 of HKPP. Averages of their observations are plotted as circles. For scattering at 15° the observations are plotted as double circles. The upright crosses represent observations of HHT reduced to the scale of the apparatus of Herb *et al.* The diagonal crosses, designated as "empirical" are computed using the "mean K_0" of Tables XI, XII interpolating graphically for K_0, and assuming a pure s scattering anomaly. All the curves are theoretical assuming a pure s scattering anomaly. Note the definite effect of a 25 percent change in the range of force and the too high scattering expected for the Gauss potential ($A=51.44$, $\alpha=21.59$) around 1400 kev. The latter shows that the data contain more information than just about the range of force and depth of the interaction potential.

the theoretical curves. The points appear to favor even a shorter range than e^2/mc^2 for a square well but such a conclusion from this energy region should obviously be postponed until more complete information is available.

In Fig. 14 are shown graphs for the scattering expected with the potentials $D=10.500$ Mev, $r_0=e^2/mc^2$ and $D=46.78$ Mev, $r_0=e^2/2mc^2$ on the assumption of pure s scattering. The curves are drawn for $\Theta=15°$, 25°, 35°, 45° and cover the energy range up to nine Mev. It is striking that the small angle scattering shows at the higher energies pronounced effects of range. This is to be expected since the scattering anomaly is spherically symmetric in the center of gravity system and since it becomes more important at high energies than the Coulomb scattering. To some extent this is a disadvantage because a check on the absolute values using small angle scattering becomes more difficult. Measurements in which the technique is tested around two Mev would be very valuable.

The high energy region is expected to yield valuable information regarding higher phase shifts. The initial effect per $-1°$ for K_1 is given in Table XXII. The effect of K_1 is known to be simply additive to that of K_0 as is seen e.g., in Eq. (6.6) of BCP. The first row for each energy in the table gives the rate of change of the contribution to the ratio to Mott with respect to K_1 which is expressed in degrees. This rate of change is computed for very small K_1 and the effect tabulated is, therefore, the initial effect when K_1 just begins to make itself felt. In the second row for each energy the value in the first row is expressed as a percentage effect in the value expected for s scattering alone. The Mott ratio used in the denominator is that for $D=10.500$ Mev, $r_0=e^2/mc^2$ except for 1.83 Mev where the experimental values were used. For negative K_1, i.e., repulsive interaction, the effect of K_1 increases and remains positive as K_1 increases. For positive K_1, on the other hand, the initial effect of K_1 is negative, but as K_1 increases the effect becomes zero and then positive. This is analogous to the very small 45° scattering which is found at about 400 kev and represents a contest between the interference effect with the Coulomb scattering and the direct effect of the scattering anomaly represented by the term

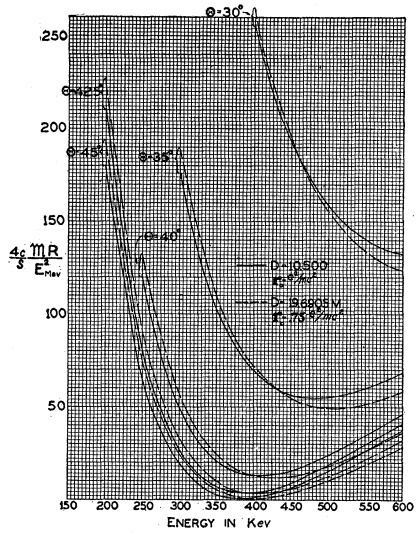

FIG. 12. The low energy region. The curves show how additional information may be obtained by observations at low energies. The quantity plotted may be used together with Eq. (3.4) to obtain proton counts per microcoulomb of incident protons.

$108\eta^{-2}P_1^2\sin^2 K_1$ in Eq. (6.6) of BCP. One expects, therefore, a qualitative difference in the behavior for repulsive and attractive p waves which should show itself for rather small values of K_1. Thus at 2400 kev for $\Theta=20°$ one expects the compensation to occur at $K_1\sim10°$ and at $\Theta=30°$ for $K_1\sim5°$. At eight Mev the compensation is expected to occur for $\Theta=20°$ at $K_1\sim5°$ and for $\Theta=30°$ at $K_1\sim3°$. If the interaction is attractive it may therefore be missed at some angles. It does not seem probable that such compensations have already occurred using the somewhat old fashioned types of theory with exchange forces. But this possibility, nevertheless, exists and should be pointed out particularly since a form of mesotron theory has been proposed by Bethe[21] in which the direct contribution of the p wave anomaly is much larger than with exchange forces. This comes about on account of a strong dependence of the phase shift on the coupling between spin and orbital momentum, the phase shift being positive for $^3P_1$ and negative for $^3P_0$ and $^3P_2$.

The value of K_1 expected for potentials involving no spin-spin interactions can be obtained by substitution into formulas which express the

[21] H. A. Bethe, Fifth Washington conference on Theoretical Physics.

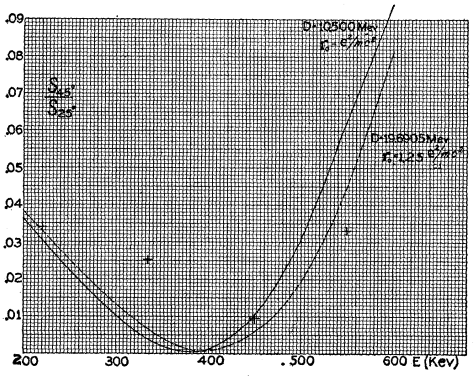

FIG. 13. Comparison with point counter experiment of Hafstad, Heydenburg and Tuve. Quantity plotted against energy is ratio of counts at 45° to that at 25° as given in their Table II. Note misprint in table assigning at 640 kev $S_{45°}/S_{20°}=0.038$ to $S_{45°}/S_{25°}$. The figure shows the possibility of using ratios of scattering at two angles for obtaining information about the range of force.

requirement of smooth joining of internal and external functions. For small phase shifts and for small effects on the wave function one can use Taylor's approximation[22] which in the present notation is

$$K_L \cong -\int (V/E')\mathfrak{F}_L{}^2 d\rho.$$

For the potential $Ae^{-\alpha r^2}$ this gives

$$|K_L| = \frac{|A|}{mc^2}\left(\frac{E'}{mc^2}\right)^{(2L+1)/2} \times C_L{}^2 \frac{\pi^{\frac{1}{2}}}{2}\frac{1}{2}\frac{3}{2}\cdots\frac{2L+1}{2}\alpha^{-(2L+3)/2}$$

and where the Coulomb function power series Φ_L is approximated by unity and the unit of length is $\hbar/(Mm)^{\frac{1}{2}}c$. For $A=38$, $\alpha=16$ calculations for 2400 kev using numerical integration and joining of wave functions gave $+0.47°$ for an attractive potential and $-0.33°$ for a repulsive one. The above approximation gives $|K_1|=0.41°$ which is just about the mean of the two values computed by numerical integration. The value of K_1 is sensitive to the extension of the potential towards the larger distances. Thus using a repulsive square well potential of absolute value 10.4 Mev through a distance e^2/mc^2 one obtains $K_1=-0.15°$. This value of K_1 is roughly $\frac{1}{2}$ of the value for the Gauss error potential while they give about the same phase shift for the s wave. For the potential $B\exp(-2r/b)$ used by Rarita and Present, Taylor's approximation is

$$K_L=(B/mc^2)C_L{}^2(E'/mc^2)^{(2L+1)/2} \times(2L+2)!/(2/b)^{2L+3},$$

the unit of length being again $\hbar/(Mm)^{\frac{1}{2}}c$. For $B=137\ mc^2$, $b=0.200$ this approximation gives $|K_1|=0.54°$. No attempt is made here to give exact values for the expected K_1 but it is intended to bring out the sensitivity of this quantity to the shape of the potential and the consequent difficulty of assigning to it a definite value.

According to Feenberg one expects from saturation inequalities the repulsive interaction in the ^3P state to be at least as great as $(1/3)72\ mc^2 e^{-16r^2}$ which leads one to expect $|K_1|>0.25°$ at 2400 kev. According to Table XXII one would expect an effect of about four percent at 15° and of about three percent at 20° for the total scattering. At 1830 kev the expected phase shift should be about 0.63 of 0.25° or 0.16°. One would expect then ~2.7 percent of total scattering at 15° and ~2.2 percent at 20° to be due to the p wave. Table XI shows no consistent evidence of the

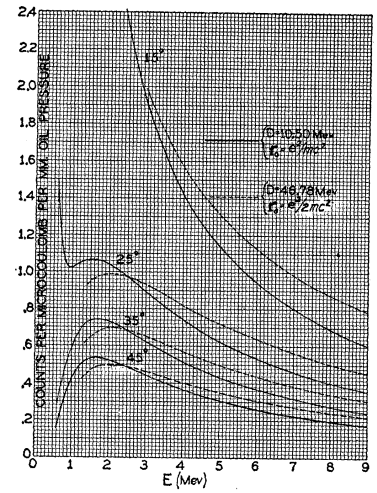

FIG. 14. High energy region. Quantity plotted against energy represents the number of counts per microcoulomb per mm oil pressure that would be expected for the scattering chamber of HKPP at energies up to nine Mev for an s scattering anomaly. Note the pronounced effect of the range of force. Also the definite divergence of the two theoretical curves at $\Theta=20°$ indicating the subordination of Rutherford scattering to the scattering anomaly.

[22] H. M. Taylor, Proc. Roy. Soc. **A134**, 103 (1931).

presence of such an effect. There is no indication of a systematic difference between 20° and 25° scattering which could be considered to be greater than the experimental error. On the other hand, the percentage of scattering expected due to the p wave at 25° should be about one-half of that at 20°. The data at 15° recorded in Table XI should be higher by a few percent than the expected values for a pure s scattering anomaly. There is thus no conclusive evidence from this scattering angle. The average percentage of the difference between observed and computed values taken for 2400, 2105, 1830 kev is 0.5 percent at 20°, 0.4 percent at 25°, 0.1 percent at 30°, 0.2 percent at 35°. From these numbers it appears surprising that the expected effect of ~ 2 percent at 20° did not appear and it may be that this should be taken as an indication against the customary saturation arguments with exchange forces. The evidence is not strong enough, however, to make a definite conclusion safe since the variations of the percentage differences at the separate energies are just about of the order of magnitude of the expected effects and since the expected effect of $|K_1|$ is sensitive to the shape and range of the potential. For $\alpha = 20$ the minimum $|K_1|$ expected from saturation arguments corresponds to a repulsive potential $(85/3)e^{-20r^2}$. The effects expected for this potential are ~ 0.67 of those used above.

IV. Concluding Remarks

It is seen from the above attempt to represent the experimental material that the range of force for the customary Gauss error type of potential cannot be taken as large as has been customary. The constant α in $Ae^{-\alpha r^2}$ cannot have the value 16 but must be taken to be about 21. This is approximately the change tried by Rarita and Present. In their work this change of range was indicated by the binding energy of H^3. Their calculations with the potential $Be^{-2r/b}$ in which a corresponding change of range was made give a too low value for the mass of He^4. Analogous but less accurate calculations made by them using the Gauss error potential give also a too low value for this mass. They pointed out that one cannot, therefore, fit the binding energies of H^3 and He^4 consistently using the simple exchange force theories. The degree to which this difficulty may be important has appeared in a different light in the calculations of Margenau and Warren and of Margenau and Tyrrell who have encountered relatively smaller difficulties in fitting the binding energy of H^3 with the Gauss error potential with $\alpha = 16$. It is seen from the above analysis that such a fit, interesting as it is, cannot be made consistently with the scattering experiments. It appears likely from their results also that one will have difficulty in fitting the mass defects of both H^3 and He^4. Particularly for the latter a too low energy is expected. It is thus impossible to use fixed interaction potentials of the types assumed in these calculations. It may be that a solution of the problem will be given by a development of the mesotron theories of nuclear interactions.

Table XXII. *Percentage effect on scattering per $K_1 = -1°$. Quantity tabulated is $-100(\Delta \mathfrak{R})_1/\mathfrak{R}\Delta K_1{}^c$. It represents the slope of $100(\Delta \mathfrak{R})_1/\mathfrak{R}$ plotted against $-K_1$ which is expressed in degrees.*

$\Theta =$	15°	20°	25°	30°	35°	E (Mev)
$-(\Delta \mathfrak{R})_1/\Delta K_1° =$	0.15	0.24	0.29	0.29	0.21	1.83
Percentage =	17	14	7.5	3.5	1.4%	1.83
$-(\Delta \mathfrak{R})_1/\Delta K_1° =$	.18	.27	.33	.33	.24	2.4
Percentage =	16	11	5.5	2.5	1.0%	2.4
$-(\Delta \mathfrak{R})_1/\Delta K_1° =$		.35	.43	.42	.30	4
Percentage =		6.9	3.4	1.5	.6%	4
$-(\Delta \mathfrak{R})_1/\Delta K_1° =$		.49	.61	.60	.43	8
Percentage =		4.5	2.2	1.0	.4%	8

It should be mentioned, however, that the behavior of phase shift with energy is sensitive to a velocity dependence of the potential. It has been pointed out by Wheller that exchange forces are special cases of a more general class of velocity dependence. It is also obvious from relativistic arguments that fixed exchange or ordinary potentials can only be a first approximation. By introducing a velocity dependence of the potential one can fit the experimental phase shift using a longer range of force. The approximate depths needed are seen in Table XXIII.

The table shows that one needs an approximately uniform increase of depth with energy and that the amount is relatively small. The adjustment is made so as to make the Gauss error potentials give the same phase shifts as the square well $r_0 = e^2/mc^2$, $D = 10.500$ Mev. The latter approximates the experimental phase shift

curve from 800 to 2400 kev. The increase in depth from 200 to 2600 kev is only 1.6 percent for $\alpha=16$ and 0.7 percent for $\alpha=18$. One can thus try to interpret the results using a range of 2.25×10^{-13} cm ($\alpha=16$) but with a progressive increase in depth of the well amounting to 1.6 percent per 1.2 Mev of the relative kinetic energy of the two protons. The change 1.2 Mev in the relative kinetic energy is ~10 percent of the kinetic energy which the two protons have inside the potential well. The velocity dependence suggested by the experiment is thus of the order of

$$\frac{1.6 \text{ percent}}{10 \text{ percent}} 100 \text{ percent} = 16 \text{ percent}$$

of the change in kinetic energy of relative motion. The depth of the square well potential 11.3 Mev would change on this basis to only roughly 9.5 Mev if the relative energy of the two protons is -10 Mev. If such a velocity dependence were speculatively supposed to show itself also in the ^3S interaction then it is imaginable that the degree of binding in such a nucleus as He^4 will be seriously affected. The sign of the effect does not appear to be immediately obvious since the distribution of relative momenta of the particles is important and this in turn depends on the structure of the nucleus which follows from the assumed interaction. The ^3S interaction may, however, be changing in a direction opposite to that of ^1S. A more careful analysis of this question would be helpful. It is clear, however, that even a relatively slow velocity dependence can affect quite fundamentally the conclusions from the binding energies of light nuclei.

If it is supposed that the ^1S interaction depends on velocity then the difference between the proton-neutron and proton-proton interactions becomes partly explicable. The relative kinetic energy of the two protons is smaller when they are close to each other on account of the Coulomb repulsion. At the boundary of a square well of radius e^2/mc^2 the difference in relative kinetic energy for a proton-neutron and a proton-proton collision of low energy is 0.51 Mev. Inside the square well the difference is larger on account of the increase in Coulomb energy. As a rough approximation one may estimate 0.83 Mev which is the correction for square well depth due to the Coulomb effect. The velocity dependence obtained from $\alpha=16$ would lead one to expect then a decrease of the interaction potential by 0.16×0.83 Mev$=0.13$ Mev. The difference to be accounted for is 0.4 Mev. The effect due to this velocity dependence appears to be too small. It may, nevertheless, be significant that it is of the right order of magnitude and in the right direction. Interactions emphasizing the effect of short distances would increase it.

TABLE XXIII. *Velocity dependence needed to account for the s phase shift.*

E	200	800	1400	2000	2600 KEV	α
A	36.8(7)	36.9(7)	37.1(8)	37.3(0)	37.4(5)	16
A	41.9(0)	41.9(7)	42.0(5)	42.1(3)	42.2(0)	18

The discrepancy between the scattering of fast and slow neutrons may also be connected with a velocity dependence of the forces of a slowly progressive type. An increase in interaction depth with velocity would decrease the scattering cross section for fast neutrons. At 2.8 Mev for incident neutrons the depth of the well could be expected to be increased by ~0.2 Mev which would produce only a very small effect in the right direction on the position of the ^3S level and hence on the scattering. The observed difference of ~17 percent needs presumably a different explanation along the lines of Schwinger's use of $(\boldsymbol{\sigma}_1\mathbf{r})(\boldsymbol{\sigma}_2\mathbf{r})$ types of coupling. These terms are now necessary in view of the experimentally established quadrupole moment of the deuteron and the proton-proton scattering experiments do not appear as yet to throw much light on interactions of this type on account of the predominance of the s wave anomaly.

The s wave anomaly is dissociated from the other phase shifts. The interactions of the $(\boldsymbol{\sigma}_1\mathbf{r})(\boldsymbol{\sigma}_2\mathbf{r})$ type do not couple the ^1S wave to other types of waves. This is a fortunate circumstance for the simplification of the analysis of experimental material but it also has made it impossible so far to relate the proton-proton experiments to the noncentral nature of nuclear forces.

With fixed interaction potentials it is possible in theory to distinguish between wells of different shapes. Shapes of potential wells having considerable extension to larger distances give a relatively small slope for the K_0, E curve at large energies. The curves have as a result a bulge in the central energy range (1400 kev) and cannot be fitted to this range if they are made to agree with experiment at 2400 kev and 800 kev. The relatively good agreement of the square well potential with experiment is presumably due, from this point of view, to the fact that it has no extensions to high energies. The mesotron type of potential appears hopeful in this connection. It will be reported on in another publication.

Summarizing the main results it has been found that: (*a*) There is no consistent evidence for p or d scattering above experimental error. The absence of the p wave is surprising from the point of view of Feenberg's lower limit for the ^3P repulsion but the experimental error is too large to make a definite conclusion safe. (*b*) The s phase shift depends on the energy so rapidly as to indicate a shorter range of force than has been customary to use in calculations with the Gauss error potential. This conclusion holds only if the potential is independent of velocity. A velocity dependence amounting to one-sixth of the change in relative kinetic energy would bring the range of force back to its old value. (*c*) The proton-proton interaction determined from the experiments is definitely smaller than the proton-neutron interaction in the ^1S state. The difference is approximately the same as that obtained by Breit, Condon and Present and by Breit and Stehn using the older observations of Tuve, Heydenburg and Hafstad. The difference is roughly three percent of the whole. This conclusion, however, is subject to modification in case the contribution due to ^3S scattering to the

Appendix

Table of Coulomb functions. The table gives the quantities needed for Eq. (7.8) of BCP.

E IN KEV	Φ_0^*/Φ_0	$\Phi_0\Theta_0$	$C_0^2\rho\Phi_0^2$	Φ_0^*/Φ_0	$\Phi_0\Theta_0$	$C_0^2\rho\Phi_0^2$	Φ_0^*/Φ_0	$\Phi_0\Theta_0$	$C_0^2\rho\Phi_0^2$	Φ_0^*/Φ_0	$\Phi_0\Theta_0$	$C_0^2\rho\Phi_0^2$
	$r=0.5e^2/mc^2$			$r=0.75e^2/mc^2$			$r=e^2/mc^2$			$r=1.25e^2/mc^2$		
200	1.0227	0.9034	0.01957	1.0327	0.8793	0.02997	1.0419	0.8606	0.0409	1.0502	0.8452	0.0522
400	1.0212	.9148	.04215	1.0292	.8946	.06453	1.0356	.8786	.0877	1.0403	.8649	.1115
600	1.0193	.9212	.06158	1.0259	.9017	.0940	1.0293	.8855	.1274	1.0307	.8702	.1614
800	1.0180	.9247	.07865	1.0221	.9053	.1199	1.0231	.8872	.1620	1.0209	.8690	.2045
1000	1.0164	.9269	.0940	1.0186	.9065	.1431	1.0168	.8861	.1927	1.0111	.8641	.2425
1200	1.0148	.9282	.1081	1.0150	.9063	.1642	1.0105	.8829	.2206	1.0012	.8567	.2765
1400	1.0133	.9288	.1211	1.0114	.9051	.1837	1.0040	.8787	.2461	0.9914	.8478	.3074
1600	1.0117	.9290	.13335	1.0080	.9031	.2017	0.9979	.8732	.2695	.9814	.8376	.3355
1800	1.0100	.9288	.1448	1.0044	.9007	.2187	.9914	.8672	.2914	.9714	.8267	.3614
2000	1.0086	.9282	.1557	1.0007	.8978	.2347	.9850	.8606	.3119	.9614	.8151	.3853
2200	1.0068	.9275	.1661	0.9972	.8945	.2497	.9787	.8534	.3309	.9513	.8030	.4074
2400	1.0054	.9265	.1759	.9937	.8909	.2640	.9724	.8459	.3489	.9413	.7904	.4280
2600	1.0037	.9255	.1853	.9900	.8871	.2777	.9659	.8381	.3659	.9312	.7777	.4472
2800	1.0022	.9242	.1944	.9864	.8831	.2907	.9595	.8299	.3820	.9210	.7646	.4652
	$r=1.5e^2/mc^2$			$r=2e^2/mc^2$			$r=2.5e^2/mc^2$			$r=3e^2/mc^2$		
200	1.0578	0.8323	0.0638	1.0702	0.8113	0.0883	1.0796	0.7942	0.1142	1.0858	0.7791	0.1412
400	1.0438	.8522	.1358	1.0456	.8283	.1859	1.0413	.8034	.2369	1.0307	.7757	.2881
600	1.0298	.8547	.1958	1.0207	.8212	.2651	1.0023	.7817	.3333	0.9742	.7350	.3984
800	1.0157	.8493	.2471	0.9956	.8032	.3308	0.9627	.7468	.4100	.9166	.6798	.4817
1000	1.0014	.8392	.2917	.9702	.7796	.3863	.9224	.7058	.4719	.8575	.6187	.5444
1200	0.9871	.8265	.3312	.9444	.7526	.4337	.8815	.6613	.5222	.7970	.5556	.5917
1400	.9728	.8117	.3666	.9184	.7237	.4748	.8405	.6156	.5626	.7352	.4931	.6259
1600	.9584	.7958	.3984	.8925	.6933	.5099	.7978	.5698	.5960	.6714	.4320	.6504
1800	.9440	.7786	.4271	.8659	.6626	.5406	.7550	.5240	.6223	.6066	.3731	.6661
2000	.9293	.7613	.4534	.8391	.6313	.5673	.7113	.4792	.6430	.5396	.3170	.6748
2200	.9146	.7433	.4774	.8121	.6004	.5903	.6667	.4355	.6589	.4712	.2638	.6774
2400	.8998	.7251	.4993	.7849	.5692	.6101	.6214	.3928	.6704	.4007	.2139	.6752
2600	.8849	.7065	.5194	.7574	.5386	.6273	.5755	.3518	.6780	.3280	.1673	.6688
2800	.8702	.6879	.5377	.7293	.5085	.6419	.5282	.3123	.6826	.2520	.1237	.6585

slow neutron scattering cross section is strongly affected by the interaction of ^3S with ^3D as has been pointed out by Schwinger. For a given range the data determine the proton-proton interaction probably to within better than 0.3 percent.

We would like to acknowledge our indebtedness to the two groups of experimenters for their whole hearted cooperation and to Messrs. Share, Hoisington and Kittel for occasional help. We are especially indebted to Professor Herb and Dr. Tuve for many discussions which have helped to clarify the interpretation. Grateful acknowledgment is made also of the financial assistance received from the Wisconsin Alumni Research Foundation, the Carnegie Institution of Washington and the WPA project in natural sciences at the University of Wisconsin.

Note in proof.—According to Lennart Simons [Phys. Rev. **55**, 792 (1939)] $\sigma_{\pi p}=14.8\times10^{-24}$ cm^2 so that $\sigma_{th}=59\times10^{-24}$ cm^2 and $D_{\pi p}=11.5(2)$ Mev. This differs by only 1.5 percent from $D_{\pi\pi^c}=11.35$ Mev. Potentials such as the meson potential which are more concentrated at small r may reduce this difference to zero.

JUNE 1, 1939 PHYSICAL REVIEW VOLUME 55

Reflectivities of Evaporated Metal Films in the Near and Far Ultraviolet

GEORGE B. SABINE*
Department of Physics, Cornell University, Ithaca, New York
(Received April 10, 1939)

The reflectivities of evaporated metal films from the visible to 450A have been determined for the following metals: Aluminum, antimony, beryllium, bismuth, cadmium, chromium, copper, gold, iron, lead, magnesium, manganese, molybdenum, nickel, palladium, platinum, silver, tellurium, titanium, zinc and zirconium. Photographic methods were used. From the visible to 2400A, a quartz mercury arc with calibrated wire screens and a quartz prism spectrograph were employed. From 2400A to 450A it was necessary to use a vacuum spectrograph with grating, a discharge tube, and oiled photographic film. The accuracy of the work in the near ultraviolet is of the order of three percent and in the far ultraviolet not better than five percent. Curves of reflectivity against wave-length for these metals are included.

1. INTRODUCTION

THE purpose of this paper is to extend the available information on the reflectivities of evaporated metal films. Most previous work has been confined to the determination of the reflectivities of metals in bulk or of sputtered and electrolytically deposited films. The reflectivities reported here are those which would normally be expected under ordinary laboratory conditions where the mirrors are exposed to air. They do not necessarily give the true reflectivity of the metallic surfaces before contamination by vapors and gases.

2. APPARATUS AND PROCEDURE

The method of evaporation and the equipment used are similar to that described by Williams and Sabine.[1] The metal to be evaporated was placed in a conical helix of fifteen-mil tungsten wire which could be heated by an electric current. In some cases, it was found to be advantageous to wrap two or three inches of the metal to be evaporated, if it were obtainable in wire form, around a short length of twenty-five-mil tungsten wire. This proved to be particularly useful in the case of metals which attack tungsten when molten or which evaporate only at very high temperatures.

The films were deposited on special scratch-free plate glass which had been washed with a strong solution of potassium hydroxide, then with hydrochloric acid, and finally dried in front of a fan with ethyl alcohol. Rubber gloves were worn on the hands and the glass was held

* Now at the Kodak Research Laboratories.

[1] R. C. Williams and G. B. Sabine, Astrophys. J. **77**, 316 (1933).